

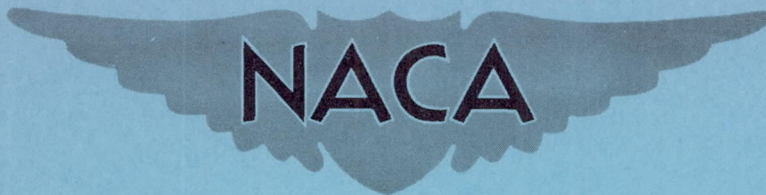
SECURITY INFORMATION

CONFIDENTIAL

Copy 337

RM A53E06

NACA RM A53E06



# RESEARCH MEMORANDUM

THE USE OF AREA SUCTION FOR THE PURPOSE OF IMPROVING  
TRAILING-EDGE FLAP EFFECTIVENESS ON  
A 35° SWEEPBACK WING

By Woodrow L. Cook, Curt A. Holzhauser,  
and Mark W. Kelly

Ames Aeronautical Laboratory  
Moffett Field, Calif.

CLASSIFICATION CHANGED TO UNCLASSIFIED  
AUTHORITY: NACA RESEARCH ABSTRACT NO. 109  
EFFECTIVE DATE: NOVEMBER 14, 1956  
WHL

CLASSIFIED DOCUMENT

This material contains information affecting the National Defense of the United States within the meaning of the espionage laws, Title 18, U.S.C., Secs. 793 and 794, the transmission or revelation of which in any manner to an unauthorized person is prohibited by law.

## NATIONAL ADVISORY COMMITTEE FOR AERONAUTICS

WASHINGTON

July 2, 1953

CONFIDENTIAL



CONFIDENTIAL

ERRATA NO. 1

NACA RM A53E06

THE USE OF AREA SUCTION FOR THE PURPOSE OF IMPROVING  
TRAILING-EDGE FLAP EFFECTIVENESS ON A  
35° SWEEP-BACK WING

By Woodrow L. Cook, Curt A. Holzhauser, and Mark W. Kelly

July 2, 1953

---

Page 3 In notation change  $C_l$  to  $c_l$

Page 55 Change figure 16 ordinate from  $\frac{P}{P_{p_f}}$  to  $\frac{P_{p_f}}{P}$ .

Correct title of figure 16 is "Variation with wing lift coefficient of the ratio of plenum-chamber pressure coefficient to the peak pressure coefficient over the flap hinge radius,  $\delta_f = 55^\circ$ "

Page 74 Abscissa of figure 28(b) is "Suction-air velocity  $w_0$ , feet per second"

## NATIONAL ADVISORY COMMITTEE FOR AERONAUTICS

RESEARCH MEMORANDUMTHE USE OF AREA SUCTION FOR THE PURPOSE OF IMPROVING  
TRAILING-EDGE FLAP EFFECTIVENESS ON  
A 35° SWEEPBACK WINGBy Woodrow L. Cook, Curt A. Holzhauser,  
and Mark W. Kelly

## SUMMARY

An investigation was conducted to determine the effectiveness of suction applied through a porous area at the leading edge of the flap, on a 35° sweptback wing. Several chordwise extents and positions of area suction were tested for the suction flap deflected 55° and 70°. The effectiveness of the flap was determined in conjunction with three types of leading-edge devices: (1) a leading-edge slat, (2) a modified leading edge incorporating camber and an increased leading-edge radius, and (3) a porous leading edge with area suction applied. Measurements were made of the static longitudinal characteristics and, in some cases, measurements were made of wing-surface pressure distributions. Measurements were also made of the suction requirements for the application of area suction on the flap alone and in conjunction with area suction applied at the wing leading edge.

The results indicated that large increases in flap lift increment can be made by applying suction with very small flow quantities to an area near the leading edge of a flap. It was determined that with area suction the flap effectiveness predicted by inviscid theory could be realized. It was determined that irrespective of angle of attack, the flap lift increment could be maintained almost constant to the angle of maximum lift of the wing. The wing maximum lift appeared to be governed by leading-edge separation in all cases, including those where leading-edge-separation control devices were used. The maximum lift increment obtained by the use of area suction on the flap was not critical as to location of the porous area, but the suction requirements to maintain this flap lift did vary with the location of the porous area.

The results indicated that with the use of a partial-span extent of leading-edge area suction from 0.45 semispan to 0.96 semispan,



there was no indication of longitudinal instability beyond maximum lift; whereas for all the other configurations of leading edges tested longitudinal instability was indicated at attitudes above that for maximum lift.

An approximate design procedure is discussed to demonstrate how the results of tests of a suction flap on a  $35^\circ$  sweptback wing can be used to determine the suction-power requirements and the lift attainable with suction flaps on wings having other sweepback.

## INTRODUCTION

The trend of aircraft-wing design toward thinner sections, lower aspect ratios, and more sweepback has necessitated a search for more effective high-lift devices for low-speed flight. The investigations of references 1 through 5 have shown various means of delaying the occurrence of air-flow separation and thus improving the low-speed characteristics of swept wings. The devices - leading-edge slats, modified leading edges incorporating camber and an increased leading-edge radius, and leading-edge area suction - were all used for the purpose of delaying the occurrence of leading-edge air-flow separation. The effect of these devices was to extend the linear portions of the lift and pitching-moment curves to higher lift and angles of attack. In many cases, depending on the sweep and aspect ratio, the angles of attack at which these improvements in lift were made are considerably higher than those used by present-day aircraft in landing, take-off, or maneuvering.

The investigations of references 1, 2, and 4 through 7 show the effect of single- or double-slotted flaps in reducing the angle of attack for a given lift coefficient for swept wings of various aspect ratios and taper ratios. The degree of effectiveness obtained from such flaps was considerably less than has been anticipated to be necessary in future wing designs.

Several investigations have shown that flap effectiveness can be increased, especially at high deflections, by application of a form of boundary-layer control more effective than that achieved by such common designs as single- or double-slotted flaps. Two types of boundary-layer control, sucking or blowing air through slots at the forward edge of the flap, as reported in references 8 through 12, showed this increased effectiveness. The results of reference 1 indicated that much less power is required to obtain boundary-layer control at a wing leading edge with suction through a porous area than through a slot. It was reasoned that similar gains could be realized in the case of boundary-layer control at the forward edge of a flap.

Because of these possible gains, an investigation was conducted on a  $35^\circ$  sweptback wing with area suction applied through various



chordwise extents and positions of porous surface on a partial-span flap. Since it was anticipated that maximum lift would be established by leading-edge separation, the investigation also included the use of the suction flap in combination with several wing leading-edge devices; (1) a leading-edge slat, (2) a modified leading edge having camber and an increased leading-edge radius, and (3) partial and full-span extents of area suction at the wing leading edge.

In analyzing the data from the investigation of the 35° sweptback wing, it appeared that the results could be of immediate interest in the design of flaps for wings of other plan forms. In order to provide the background for the design of flaps with area suction, the discussion has been extended to cover qualitatively the physical phenomena involved. In addition, the design procedure used to estimate the characteristics and suction requirements for an example application is included in Appendix A.

The investigation was conducted in the Ames 40- by 80-foot wind tunnel. The results of the tests are presented herein.

#### NOTATION

- b wing span, ft
- c chord, measured parallel to the plane of symmetry, ft
- $\bar{c}$  mean aerodynamic chord,  $\frac{2}{S} \int_0^{b/2} c^2 dy$ , ft
- $C_L$  section lift coefficient,  $\frac{1}{c} \int_0^c P dx \cos \alpha - 1/c \int_0^t P dz \sin \alpha$
- $C_D$  drag coefficient,  $\frac{\text{drag}}{q_0 S}$
- $C_L$  lift coefficient,  $\frac{\text{lift}}{q_0 S}$
- $C_m$  pitching-moment coefficient computed about the quarter-chord point of the mean aerodynamic chord,  $\frac{\text{pitching moment}}{q_0 S \bar{c}}$
- $C_Q$  flow coefficient,  $\frac{Q}{U_0 S}$
- d chordwise extent of porous surface, measured in chord plane, ft

- $l$  length of porous surface, measured along surface normal to leading edge, in.
- $p_0$  free-stream static pressure, lb/sq ft
- $p_l$  local-surface static pressure, lb/sq ft
- $P$  airfoil pressure coefficient,  $\frac{p_l - p_0}{q_0}$
- $P_d$  average duct pressure coefficient,  $\frac{P_d - p_0}{q_0}$
- $P_p$  plenum-chamber pressure coefficient,  $\frac{p_p - p_0}{q_0}$
- $q_0$  free-stream dynamic pressure, lb/sq ft
- $Q$  volume of air removed through porous surface, cu ft/sec, based on standard density
- $R$  Reynolds number,  $\frac{U_0 \bar{c}}{\nu}$
- $S$  wing area, sq ft
- $t$  thickness of porous material, in.
- $U_0$  free-stream velocity, ft/sec
- $w_0$  suction-air velocity, ft/sec
- $W$  assumed weight of airplane,  $C_L q_0 S$
- $x$  distance along airfoil chord, referenced to the leading edge of the unmodified sections, ft
- $y$  spanwise distance, measured perpendicular from fuselage center line, ft
- $z$  height above wing reference plane defined by the wing quarter-chord line and the chord of the unmodified section at  $0.663 b/2$
- $\Lambda$  sweep angle, deg
- $\alpha$  angle of attack of fuselage center line, deg
- $\delta_f$  flap deflections measured in plane normal to the hinge line, deg



- $\Delta p$  pressure drop across porous material, lb/sq ft  
 $\nu$  kinematic viscosity, ft<sup>2</sup>/sec

## Subscripts

- f trailing-edge flap  
L leading edge  
crit critical  
R reference conditions

## CORRECTIONS

The standard tunnel-wall corrections for a straight wing of the same area and span as the sweptback wing were applied to the angle of attack, pitching-moment, and drag-coefficient data. This procedure was followed since an analysis indicated that tunnel-wall corrections were approximately the same for straight and swept wings of the size under consideration. The following increments were added:

$$\Delta\alpha = 0.61 C_L$$

$$\Delta C_D = 0.0107 C_L^2$$

$$C_{mT} = 0.008 C_L \text{ (tail-on data only)}$$

No corrections were made for strut interference. All flow coefficients were corrected to standard sea-level conditions. The effect of the thrust of the exhaust jets was found to be negligible.

## MODEL AND APPARATUS

A general view of the model is shown in figure 1. Except for the flaps, the model is the same as was used in the investigation of reference 1 where it is described completely. The geometric characteristics of the model are shown in figures 2 and 3. The wing panels and horizontal tail are from an F-86A airplane. The horizontal tail is in the same position relative to the wing as on the airplane. The coordinates for the airfoil section at two spanwise sections are given in table I.

### Suction Flaps

The original trailing-edge flaps on the wing described in reference 1 were removed and replaced with suction flaps that could be deflected to  $55^\circ$  and  $70^\circ$  (fig. 4(a)). The flaps had a constant chord and extended from 0.135 semispan to 0.495 semispan. The flaps were constructed with a porous surface on the upper surface over the axis of rotation as shown in figures 4(b) and 5. The porous surface extended from a point  $1/2$  inch aft of the reference line to 8 inches aft of the reference line measured along the surface normal to the reference line. The reference line, shown in figure 4, is a line on the upper surface of the wing in a vertical plane with the hinge line. The chordwise extent and position of porous surface was controlled with a nonporous tape of about 0.003-inch thickness. The various extents and positions of porous areas tested are listed in table II. The dimensions given are normal to the reference line and are measured along the curved porous surface. The chordwise extent of the porous surface for all configurations was constant across the span of the flap.

The porous material used for the flap was the same type as used in the investigation of reference 1. The material was composed of an electroplated metal mesh sheet backed with  $1/16$ -inch-thick white wool felt. The metal mesh sheet had 4225 holes per square inch, was 11-percent porous, and was 0.008 inch thick. The wool felt had a weight of 4 pounds per square yard for  $1/2$ -inch-thick material. The flow resistance characteristics for the porous material are shown in figure 6 for  $1/2$ -inch-thick wool felt. For other thicknesses of wool felt, the pressure drop across the porous material for a given suction velocity is directly proportional to the thickness of the wool felt.

### Wing Leading Edges

The various leading-edge configurations used in the tests are listed in table III. Some tests were made with the F-86A airplane leading edge, configuration A, with the slat in the closed position as shown in figure 7. In these tests the slits between the four segments of the slats were taped as in reference 2 to prevent flow of air from the bottom surface to the top. The majority of the tests with an unmodified F-86A wing leading-edge contour were made with the porous leading edge taped with a nonporous tape, configuration B. Three leading-edge devices were used to attain higher maximum lift coefficient: (1), the modified leading edge of reference 2 which had camber added to the forward portion of the chord and an increased leading-edge radius, as shown in figure 7(a) and table IV; (2) the F-86A leading-edge slat, shown in figure 7(b), extending from 0.245 semispan to 0.94 semispan; (3) the porous leading



edge used in the investigation of reference 1. The various spanwise extents of leading-edge area suction used and the one spanwise variation of the chordwise extent (configuration B of ref. 1) used for all spanwise extents are shown in figure 8 and table III. Figure 9 shows the variation of the thickness of porous wool felt backing material at various spanwise sections. The flow resistance of the porous material for the leading edge is shown in figure 6. As indicated in the figure, this porous material has approximately twice the density for a given thickness of material as the porous material used at the flap.

### Suction Apparatus

Two completely separate suction systems were employed; one for the leading edge and one for the flap. Each system consisted of a centrifugal compressor driven by an electric motor mounted in a plenum chamber in the fuselage. The air was drawn from the wing surface, into wing ducts, through the plenum chamber and the compressor and out the exit ducts at the bottom of the fuselage. The quantity of air removed for each suction system was measured by survey rakes located at the exit of the system. The rakes were calibrated with standard ASME orifice meters. Plenum-chamber and duct pressures were measured with static pressure orifices and can be assumed to be equal to the total pressure since the suction-air velocities in the duct and plenum chamber were low. The spanwise location of the surface pressure orifices are shown in figure 2, and the chordwise positions are listed in table V. The total suction power was measured with a wattmeter and included pump losses, duct losses, and the suction requirements.

### TESTS

The primary purpose of the investigation was to determine the relation between the lift increments realized from the flap and the suction power and flow quantities required. Three-component force data were obtained at zero sideslip for all flap and wing configurations. For some conditions, pressure distributions over the wing were obtained. In addition, tests were made of three wing and flap arrangements with the horizontal tail removed to show the effects on longitudinal stability. Table VI lists the various configurations that were investigated.

Initial tests showed that as suction was increased, the lift increment first increased rapidly, then, quite abruptly, the rate of increase fell off to a very low value. The test procedure followed, therefore, was to determine for each model arrangement and angle of attack the power and suction quantities required to reach the point where further increases in these quantities gave little increase in lift increment.

This was done by holding the angle of attack and free-stream velocity constant and obtaining data as the suction quantity was varied.

For the model with the unmodified wing leading-edge profile, an extensive investigation was made, for both  $55^\circ$  and  $70^\circ$  of flap deflection, of the effect of position and extent of the porous area. Table II presents a summary of the porous area arrangements tested. Data were obtained at Reynolds numbers of 7.5 and  $9.6 \times 10^6$ . For the model with wing leading-edge modifications, only one flap deflection,  $55^\circ$ , and only one arrangement of porous area on the flap were tested (see table VI). For the full-span leading-edge suction, suction quantities required at the wing leading edge were determined for each angle of attack as those which, by observation of pressure distribution, just prevented separation of flow from the wing leading edge.

## RESULTS AND DISCUSSION

### Model With Suction Flap and Unmodified Leading Edge

The lift, drag, and pitching-moment data are shown in figure 10 with the trailing-edge flap deflected  $55^\circ$  and  $70^\circ$ . The results are shown with and without suction applied on the flap and are compared with a slotted flap deflected  $38^\circ$  having essentially the same span and chord (ref. 2).

Lift.— Figure 11 shows the variation of the flap lift increment with flow coefficient. These data were obtained at one wing angle of attack,  $0.5^\circ$ , and for one location and extent of porous area for each flap (configuration 4 for the flap deflection of  $55^\circ$  and configuration 18 for the flap deflection of  $70^\circ$ ). Similar data were obtained at other angles of attack and for other configurations of porous area. Examination of all these data showed the following important facts which are applicable to each condition of flap deflection:

1. The variation of lift increment with flow coefficient was qualitatively the same for any configuration of porous area in that, as flow coefficient was increased, an initial slow rise in lift was followed by an abrupt rise to a particular value which could be increased only slightly by further large increases in flow coefficient.

2. For any one configuration of porous area, the variation of lift increment with flow coefficient showed almost no variance with angle of attack, provided the angle of attack was less than that at which separation of flow appeared at the wing leading edge.



3. For all configurations of porous area, the same total increase in lift occurred as the flow coefficient was increased, but the abruptness of the rise and the flow coefficient at which it occurred were modified by the chordwise extent and location of the porous area.

The data shown in figure 10 represent, for either flap deflection, the condition wherein the flow coefficient at each angle of attack was sufficient to be in the range where a negligible increase in lift could be realized from increased flow coefficient. The data therefore are applicable to any configuration of porous area for each flap deflection that is noted in table II.

The existence, for each flap deflection, of a particular value of lift increment which could be exceeded only slightly by large increases in flow coefficient suggests that as soon as there is sufficient area suction to permit attaining nearly linear flap effectiveness, no further gains in lift could be expected. This can be indicated by comparing measured flap lift increments and total-wing lifts with those predicted by the method of reference 13, wherein linear flap effectiveness to these deflections can be assumed. In making such a comparison, it is first necessary to make a choice of the experimental  $\Delta C_L$  increment gained by the use of suction. For instance (fig. 11) with  $55^\circ$  of flap deflection, the  $\Delta C_L$  increases from 0.75 to 0.78 as the flow coefficient increases from 0.00048 to 0.002. This lift increase was considered of small interest in view of the increase in flow coefficient required; hence, the choice was arbitrarily made to direct attention to that value of  $\Delta C_L$  reached when the linear increase with flow coefficient begins (see fig. 11). It should be noted that often this is not a sharply defined point and, therefore, the choice of the value of flow coefficient associated with it is somewhat arbitrary; an attempt will be made to make apparent the degree of interpretation as results are discussed. Herein, the lift increments corresponding to this value are denoted as  $\Delta C_{L_{crit}}$ , the associated total-wing lift coefficients are  $C_{L_{crit}}$ , and the associated flow coefficient is  $C_{q_{crit}}$ .

Good agreement between theory and experiment was obtained for the  $55^\circ$  flap-deflection case ( $0.78 = \Delta C_{L_{crit}}$  from tail-off experimental data and  $0.80 = \Delta C_L$  from theory); poorer agreement existed in the  $70^\circ$  flap-deflection case ( $0.87 = \Delta C_{L_{crit}}$  estimated from tail-on experimental data and  $0.99 = \Delta C_{L_{crit}}$  from theory), and it is not clear whether this is a limitation of the theory or a failure of the area suction to totally eliminate separation, although tuft studies and pressure-distribution measurements indicated that the latter was a contributing factor to the disagreement.

It will be noticed from figure 10 that  $\Delta C_{L_{crit}}$  was maintained almost without loss up to  $C_{L_{max}}$ . For these cases,  $C_{L_{max}}$  appeared to

be limited by separation of flow from the wing leading edge which was indicated by the pressure distributions and will be discussed later. Thus, application of suction to the flap gave a major increase in  $C_{L_{max}}$  with only a slight change (reduction) in stall angle. Installation of the smooth F-86A leading edge in place of the taped-over porous leading edge (ref. 1) enabled an increase in  $C_{L_{max}}$  from 1.48 to 1.68; even in this latter case, there is apparently no important reduction in  $\Delta C_{L_{crit}}$  with angle of attack.

The majority of tests were made with no discontinuity existing where the upper wing surface joined the surface formed by the flap deflection. Recognizing that such would not be possible in practice, since a discontinuity must exist to enable flap retraction, a limited study was made of the effect of such a discontinuity in the form of an abrupt 3/16-inch drop in contour along the flap just forward of the porous area. No change in flap effectiveness was measured, although a slight increase in flow coefficient was required to obtain  $\Delta C_{L_{crit}}$ .

Pitching moment.— Suppression of separation on the flap caused no particular change in the variation of pitching moment with lift coefficient, except that the linear range was extended to higher lift coefficients. A point worthy of note is that in the tail-on case, the increase in flap effectiveness was not accompanied by a pronounced change in pitching moment (fig. 10(a)). It can be seen by comparing the data of figures 10(a) and 10(b) that in a large measure, the self-trimming effect results from the particular location of the tail in the downwash field since an increase in flap lift is accompanied by an increase in the negative value of the tail-off pitching moment. However, it can be shown from figure 10(b) that the pitching moment per unit of flap lift is less for the flap with area suction (a value of 0.155) than for the flap without suction (a value of 0.18). Presumably, this results from a forward shift in local center of pressure as separation is suppressed on the flap. This fact may be of importance if greater flap lift increments than shown herein are desired and maximum lift of the horizontal tail is approached.

Suction requirements - effect of position of porous area.— It was noted in the previous section that figure 11 shows a typical variation of lift increment with suction, and that a value of lift noted as  $\Delta C_{L_{crit}}$  was chosen to represent the most interesting case wherein the flow coefficient was limited to that required to just suppress separation and maintain nearly linear flap effectiveness. It was also noted that while all porous area configurations achieved this end,  $C_{Q_{crit}}$  varied for each configuration of porous area. Figures 12 and 13 have been prepared to show this variation for the  $55^\circ$  and  $70^\circ$  flap deflections, respectively. The effects of two variables are shown in each



figure, first, the effect of position of two extents of porous area, and, second, the effect of the extent of porous opening with the forward edge at a fixed point.

The results shown in figures 12(a) and 13(a) indicate that there is a particular position for the forward edge of the porous opening which results in minimum  $C_{Q_{crit}}$  and that this position is not greatly affected by the extent of opening - at least within the range tested. Figures 12(b) and 13(b) indicate that with the forward edge at the position for minimum  $C_{Q_{crit}}$ , for either of the two extents, there is also a particular extent required to realize minimum  $C_{Q_{crit}}$ .

While figures 12 and 13 serve to show trends, it would appear reasonable to assume they are not quantitatively applicable to other wing-flap arrangements. Evidence of this is the differences in the variation for the two flap angles (figs. 12 and 13). If the reasons for these differences were known, the usefulness of the data would obviously be greatly increased. In the following paragraphs, the extent to which they are understood will be discussed.

It has been shown previously, in connection with application of area suction to control separation of flow from the leading edge of a wing, that area suction is most effective when the forward edge of the porous area coincides with the point of maximum negative pressure. That this is also true in the case of the flap is indicated by the relative positions of the maximum negative pressure measured over the flap and the position of the forward edge of the porous area for minimum flow-coefficient requirement. Suction forward of this point results in needlessly withdrawing air in the region of a favorable pressure gradient. Moving the leading edge of the area suction progressively aft results in not only increased flow requirements but, as found during this investigation, instability of the flow and, finally, inability to maintain attached flow. It seems safe to conclude that the optimum location for the forward edge of the porous area will, for any plain flap, be at or very close to the point of maximum negative pressure.

Conclusions similar to the foregoing but with regard to the extent of the porous area are not so readily reached. It can be conjectured from figures 12(b) and 13(b) that the position of the aft edge of the porous area for the minimum flow coefficient is at the point where the boundary layer is just sufficiently stable to withstand the subsequent pressure recovery without aid. If the porous area is not carried to this point, then the boundary layer must be made more stable than in the case just mentioned, requiring larger flow coefficients, in order to suppress flow separation beyond the region of porous area. If the porous area is carried beyond the optimum point, then needless control is being applied. As yet, however, no theory is available analogous to that shown in reference 14 for predicting the required extent of porous area

in the case of the flap. Fortunately, it appears that estimates made in the direction of establishing too great an extent do not result in excessive flow coefficients. Further investigation of this problem is indicated.

Suction requirements - effect of lift coefficient and free-stream velocity.- Choice of a porous area which appeared, at least within the range of configurations studied, to be that one requiring minimum flow coefficient to maintain  $\Delta C_{L_{crit}}$  enabled limited studies of the variation of  $C_{Q_{crit}}$  with free-stream velocity and with total lift coefficient. Typical data obtained during these studies are shown in figures 14 and 15.

It is evident from figure 14 that if differences in lift coefficient of about 3 percent can be ignored, then the effect of free-stream velocity on  $C_{Q_{crit}}$  can be considered inconsequential within the range of free-stream velocities tested in this investigation. When these results are considered in the light of the limited amount of data available, it is concluded that any attempt to demonstrate a variation of flow coefficient for  $\Delta C_{L_{crit}}$  with free-stream velocity is unjustified; until more detailed studies can be made, the flow coefficient for  $\Delta C_{L_{crit}}$  (within  $\pm 3$  percent) must be considered independent of free-stream velocity.

A condition similar to the foregoing exists when an attempt is made to ascertain the variation of  $C_{Q_{crit}}$  with total-wing lift coefficient (see fig. 15). At the lowest free-stream velocity,  $C_{Q_{crit}}$  for  $\Delta C_{L_{crit}}$  ( $\pm 1$  percent) shows a slight increase with  $C_L$ , while at the higher velocity, it shows a slight decrease with  $C_L$ ; however, if a 3-percent drop in  $\Delta C_{L_{crit}}$  is accepted, then, the tests made at the higher velocity also show a slight increase in  $C_{Q_{crit}}$ . As a result of this, it is concluded that existing data are incapable of demonstrating any significant variation of  $C_{Q_{crit}}$  with  $C_L$ ; until more detailed studies are made, the flow coefficient for  $\Delta C_{L_{crit}}$  ( $\pm 3$ -percent) must be considered independent of total wing lift. For the tests reported herein, the smallest value of  $C_{Q_{crit}}$  was 0.0005 for  $55^\circ$  of flap deflection and 0.0009 for  $70^\circ$  of flap deflection.

All the conclusions reached in the foregoing examinations of data are contrary to what would be expected. As discussed briefly in reference 3, any one configuration of porous area should give minimum  $C_{Q_{crit}}$  at only one velocity and, hence,  $C_{Q_{crit}}$  should vary with velocity. Further, it is reasonable to expect the stability of the boundary layer approaching the flap to decrease as the wing lift increased (and the adverse pressure gradient traversed by the boundary layer at the wing



leading edge also increased); as a consequence, minimum  $C_{Q_{crit}}$  should increase with wing lift since more stability must be imparted to the boundary layer at the flap. These apparent contradictions are probably evidence that the so-called minimum values of  $C_{Q_{crit}}$  found in this investigation are, in reality, so far from a true minimum that the effects of the factors under consideration are totally masked. It is believed that a large percentage reduction in minimum  $C_{Q_{crit}}$  may be realized (Appendix B) by controlling the chordwise distribution of inflow velocities. In view of the moderate values of  $C_{Q_{crit}}$  measured in the subject investigation, a large percentage reduction is, in fact, a small absolute value, and the value of its realization may be open to questions in the range of lift conditions and flight speeds considered of current interest. It must be pointed out, however, that the reduction of flow coefficients may become of great importance in cases where duct space is limited.

Plenum-chamber pressure coefficients - relation to external peak-pressure coefficient.- The total power required is directly a function of the plenum-chamber pressure coefficients as well as the flow coefficient. The plenum-chamber pressure coefficient,  $P_{p_f}$ , must have a sufficiently negative value to overcome duct losses and pressure drop through the porous material at the required flow rate and, also, to overcome the external negative pressures. In the general case, duct losses and the pressure drop through the porous material are readily calculable within the accuracy required, and it would be anticipated they would be small. In the subject investigation, these losses were negligible; hence, required values of  $P_{p_f}$  are almost entirely a result of external pressures.

The variation of the ratio of plenum-chamber pressure to peak external pressure with lift coefficient is shown in figure 16. A surprising feature indicated by these results is that the ratio is definitely less than 1.0. For all the cases shown, the forward edge of the porous area was at the location for minimum  $C_{Q_{crit}}$  required to reach  $\Delta C_{L_{crit}}$ ; as noted earlier, this location is very close to the peak negative pressure. It can only be concluded from this that some outflow of air occurred through the porous surface near its forward edge. Such an occurrence does not seem favorable to any form of boundary-layer control, and it is probable that the outflow in these cases was possible only because excess air was being withdrawn through a major portion of the porous area. It is apparent the latter would be the result when the external pressure over the porous surface varied in a chordwise direction, while the internal pressure was a constant and the porosity of the material was a constant. It is believed that the value of  $C_{Q_{crit}}$  could be substantially reduced, and that the required internal duct pressure would become at least equal to the maximum negative external pressure if the chordwise porosity variation were adjusted to maintain nearly constant

suction velocities. Some discussion of this problem of controlling the chordwise variation of suction velocities at a wing leading edge is given in references 3 and 15; detailed research, however, is yet required before a quantitative evaluation of its effects can be made in the case of the flap. Until such research can be completed, it is concluded that a conservative estimate of the required duct pressures would be that they must equal the maximum negative external pressure.

Plenum-chamber pressure coefficients - effect of free-stream velocity and lift coefficient.- It was found experimentally that the plenum-chamber pressure coefficient for any one configuration and angle of attack was essentially independent of free-stream velocity within the range tested. As indicated in the subsequent tables, the value of  $P_{pf}$  is primarily controlled by the external pressure coefficient; this showed negligible variation over the Reynolds number range and Mach number range of the investigation. Loss through the porous material and duct losses, which secondarily control the value of  $P_{pf}$  required, were changing with the variations in  $C_{Q_{crit}}$ , but the effects remained a negligible part of the total.

A significant effect of lift coefficient on the required value of  $P_{pf}$  was found (see fig. 17). Again, this was due almost entirely to the variation in the peak negative external pressure coefficient which dropped appreciably with an increase in lift coefficient. Such a drop is not compatible with potential theory; it would be expected that, provided theoretical flap effectiveness were realized, a slight rise in external peak negative pressure would be experienced. It may be concluded that 100-percent flap effectiveness was not realized.

Pressure distributions.- Chordwise pressure distributions and section lift-curve slopes obtained with the flap deflected  $55^\circ$  and with and without suction are shown in figures 18 and 19. Two points are of particular interest; first, the marked change in pressure distributions as a result of application of suction and, second, evidence of separation of flow first appearing at the leading edge of the wing with suction applied to the flap.

It can be seen that the effect of applying suction to the flap is to change the pressure distribution from one indicating separation of flow over the flap to one closely resembling the type predicted by the airfoil theory where no separation of flow is considered. These results substantiate two comments made earlier: That the expected lift increment from such a flap is predictable from thin-airfoil theory, and that the pitching moment for a given flap lift increment is less for this type of flap than for other types because of the amount of lift induced on the forward part of the wing.



Examination of figure 18 shows that with suction applied to the flap, leading-edge separation (as evidenced by the collapse of the peak negative pressure at the leading edge) occurred between  $10.9^\circ$  and  $12.8^\circ$  angle of attack. This, as was noted earlier, limits the maximum lift. Partial collapse of lift on the flap occurred at the same time; however, this was believed to be the result of air-flow separation at the wing leading edge. The investigation was therefore continued by examining the effect of several devices designed to delay separation of flow from the leading edge.

Typical power requirements.— The actual power requirements for an airplane should be specified in terms of the wing loading and landing speed. In order to determine such values which were free from the uncertainties of estimating flow coefficient and pressure coefficient, data were obtained under conditions corresponding to level flight at wing loadings of 40 and 60 pounds per square foot.

The following table shows measured minimum suction horsepower required to obtain  $\Delta C_{L_{crit}}$ . The powers shown are those required to drive the pump and thus include duct losses, system leakage, and the effect of pump efficiency. For the conditions quoted in the table, the first two items caused a small increase in power; for all conditions the pump efficiency was about 65 percent, thus, a substantial reduction in power could be achieved by improved pump characteristics.

W/S, 40 lb/sq ft										
Flap deflection, $55^\circ$						Flap deflection, $70^\circ$				
Angle of attack	$C_L$	$U_o$ ft/sec	$C_{Q_f}$	$P_{p_f}$	Measured suction hp	$C_L$	$U_o$ ft/sec	$C_{Q_f}$	$P_{p_f}$	Measured suction hp
0.5	0.79	206	0.00047	-4.4	23.0	0.91	192	0.00088	-7.8	59.2
4.6	1.06	178	.00050	-4.2	15.7	1.14	172	.00090	-7.6	40.0
10.9	1.45	152.5	.00062	-3.5	10.1	1.50	149	.00072	-6.4	15.1
15.1 <sup>a</sup>	1.68	141.5	.00065	-3.0	6.7					
W/S, 60 lb/sq ft										
0.5	0.77	256	0.00049	-4.5	43.7	0.90	237	0.00098	-8.0	107
4.6	1.04	220	.00052	-4.2	28.5	1.13	216	.001	-7.4	70.5
10.9	1.43	187.6	.00056	-3.8	16.9	1.44	187	.00086	-6.6	36.0

<sup>a</sup>Suction requirements for  $15.1^\circ$  angle of attack were obtained with unmodified leading-edge configuration A; others were obtained with unmodified leading-edge configuration B.

It is interesting to note that the power required varies roughly as the cube of the velocity ratios. In any attempt to extrapolate these results to much different conditions (e.g., higher wing loadings, higher lift coefficients) by this variation, due consideration should be given the compensating effects which make the extrapolation fit the range of test conditions given here.

It is apparent that forward speed has a large effect on powers required. An attempt to reach  $\Delta C_{L_{crit}}$  at high forward speeds can require very high powers. This does not appear to be of particular importance, however, because it has been demonstrated that area suction will cause reattachment of flow when applied where separation exists. Therefore, it would be necessary to supply only the power required to cause reattachment of flow at a desired low forward speed; as this speed was approached from some higher speed, an increase in flap effectiveness due to the attachment of flow to the flap would be felt, similar to an increase in deflection of a conventional flap. The increased forward speeds resulting from even higher wing loadings than considered here may, however, result in undesirably high power requirements. It is believed that in these cases, the required power can be reduced by control of the chordwise distribution of normal velocities through the porous surface.

#### Model with Suction Flap and Leading-Edge Devices

Three types of leading-edge devices designed to delay separation of flow at the leading edge were readily available. To limit the number of variables under study, only one suction flap configuration was used during these tests. This was configuration 4 which gave minimum  $C_{Q_{crit}}$  with  $55^\circ$  of flap deflection. The primary purpose of this phase of the study was to ascertain the effect of higher wing lift coefficients on the characteristics of the suction flap and to ascertain if any major changes were made in these characteristics by the type of device used to delay leading-edge separation in order to achieve the higher wing lifts. It is believed that any significant changes found for this flap configuration would also exist for any other.

Lift.— The effect of the three leading-edge modifications on the lift characteristics is shown in figure 20. Considering first the modified leading edge and the area-suction leading edge, it was apparent that the major portion of the flap effectiveness was maintained to very high angles of attack with the control of leading-edge separation. There is a gradual reduction in lift-curve slope above a lift coefficient of about 1.4; as will be noted later, there is slight evidence that this was due to a loss in flap effectiveness. However, for all points tested,



there was a well-defined value of  $\Delta C_{L_{crit}}$  that could be chosen similar to that shown in figure 11. It can be concluded, therefore, that an increase in over-all wing lift will have no pronounced effect upon the lift contributed by the suction flap.

The case of the partial-span leading-edge slat is somewhat different. At an angle of attack of about  $6^\circ$ , a marked loss in flap effectiveness occurred. This was traced to the rough air flow which came from the inboard end of the slat. This restricted area of rough air flow succeeded in separating the flow from that area of the flap lying directly behind the inboard end of the slat. It was not possible to attain as high a value of lift increment as was attained with other leading edges with the amounts of suction tried in the tests.

Pitching-moment characteristics.— No particular effect was found in the pitching-moment characteristics with the possible exception that the partial-span slats could not provide nose-down moments at stall with the suction flap, although they could with the normal F-86A slotted flap. The tail-off moments shown in figure 20(b) are included simply to show that there were no sudden changes in wing moments that were obscured by the tail contribution.

All the model configurations considered to this point showed instability beyond maximum lift. Although the undesirability of this is open to question (ref. 16), some tests were made to see if it could be overcome by limiting the spanwise extent of area suction. This is similar to the procedure used in reference 1. As is evident in figure 21, it was possible to alter the pitching moment at stall although a substantial reduction in maximum lift resulted. It is not meant to be implied by these tests that only spanwise control of area suction at the leading edge will give nose-down moments at stall. The significant point is that the suction flap does not eliminate the effectiveness of this type of control.

Suction requirements.— As noted earlier, a primary point of interest in these tests was to determine whether various leading-edge modifications would significantly affect the flap suction requirements. Subject to the qualifications made previously with regard to fixing an exact minimum value of  $C_{Q_{crit}}$ , it can be stated that, except where partial-span leading-edge stall occurred with the partial-span slat, no differences in suction requirements greater than 10 percent were found. It should be emphasized, however, that a more detailed study will be required to determine whether there are any such effects.

Up to the highest lift coefficients attainable with the various leading-edge modifications, subject to the limitations previously discussed,  $C_{Q_{crit}}$  was independent of lift coefficient and velocity. Also, the comments previously made regarding plenum-chamber pressure coefficient were found to be applicable at the higher lift coefficients.

Pressure distributions.— Chordwise-pressure-distribution data and section-lift-curve slopes obtained with area suction applied at both the leading edge of the wing and on the flap are shown in figures 22 and 23. Below the first appearance of separation, there existed characteristics very similar to those already discussed. The initial location of separation, however, is not so readily definable as in the previous case.

Comparison of figures 22(c) and 22(d) shows that at the 0.45  $2y/b$  station, the leading-edge peak pressure has nearly ceased to rise and the peak pressure over the flap has practically collapsed (although no pronounced effect of separation is apparent). It cannot be ascertained which of these flow changes is cause and which is effect but it is suspected that, at least for this configuration of area suction on the flap, the limit of control of the area suction on the flap is being approached.

Typical power requirements.— The following table has been prepared to demonstrate the order of magnitude of powers required at the high lift coefficients made possible by use of leading-edge devices. In addition to the powers required at the flap, powers required for area suction at the wing leading edge are given for comparison with those of reference 1. As in the previous table, two values of wing loading were examined for the F-86A model, 40 and 60 pounds. As noted previously, tests were made with velocity and attitudes corresponding to those of flight for these wing loadings. For the case of area suction at the wing leading edge, the measured suction power includes the duct losses and pump losses which are listed in table VII and are subtracted to obtain the values of suction power.

Flap deflection, 55°, W/S, 40 lb/sq ft								
Flap, configuration 4					Leading-edge, configuration B-B			
$C_L$	$U_o$ ft/sec	$C_{Q_f}$	$P_{P_f}$	Measured suction hp	$C_{Q_L}$	$P_{P_L}$	Measured suction hp	Suction hp
1.6	145	0.00042	-3.3	7.8	0.00039	-12.7	18.8	12.4
1.82	136	.00040	-3.0	6.0	.00051	-19.4	36.4	23.7
1.95	131.5	.00040	-2.7	4.1	.00063	-23.0	43.7	28.0
2.07	127.5	.00034	-2.8	3.8	.00081	-30.0	63.3	36.0
2.17	124.5	.00033	-2.8	2.8	.00101	-38.0	97.6	44.4
Flap deflection 55°, W/S, 60 lb/sq ft								
1.6	179.5	0.00058	-3.4	14.0	0.00044	-14.4	37.6	23.0
1.82	166.5	.00057	-3.2	9.4	.00061	-19.8	77.9	43.1
1.95	161	.00059	-3.0	8.3	.00072	-24.7	98.2	54.7
2.07	153	.00058	-2.8	6.8	.00088	-31.4	171.0	92.0



When these powers and flow coefficients required to control separation of flow at the leading edge are compared with those quoted in reference 1 for corresponding conditions, it will be evident that a reduction in both power and flow coefficient have occurred. That such is the case, despite the fact that the same leading edge was used for each test, is worthy of some consideration. A comparison on the basis of equal  $C_L$ 's produces such a result largely because the increased flap effectiveness reduces the leading-edge pressure peaks required to reach a given wing  $C_L$ . A more valid comparison on the basis of equal wing loading and equal angles of attack, where the leading-edge pressure peaks should be very similar, also shows a substantial reduction in power and flow coefficient, particularly at the lower lift coefficients. This is partially due to a decrease in velocity for level flight brought about by the increase in lift due to greater flap effectiveness. Even when this is accounted for, however, a reduction remains. It is thought to be due to a change in the span loading and chordwise loading, induced by the more effective flaps, which resulted in a more favorable spanwise distribution of suction velocities at the leading edge. This is partly supported by the fact that the differences tend to disappear as the flap effectiveness diminishes slightly at the higher  $C_L$ 's. Insufficient data exist to evaluate quantitatively these effects, but it is important to note they exist.

#### CONCLUDING REMARKS

The results of the wind-tunnel investigation of a  $35^\circ$  sweptback wing indicated that large increases in flap lift increment can be made by applying area suction with very small suction flow quantities to an area near the leading edge of a flap. It was determined that the area suction served to prevent air-flow separation and, hence, flap effectiveness agreeing closely with inviscid flow theory could be realized. It was determined that the flap lift increment could be maintained almost without loss to maximum lift of the wing which appeared to be governed by leading-edge separation in all cases, including those where leading-edge-separation control devices were used. The effectiveness of the area suction was not too critical as to location of the porous area but the suction requirements did vary with the location of the porous area.

For the particular model under investigation, a flap lift increment of 0.78 was realized for a flap deflection of  $55^\circ$  with a flow coefficient of 0.0005 and a lift increment of 0.87 for a flap deflection of  $70^\circ$  with a flow coefficient of 0.0009; both flap deflections gave a lift increment of about 0.5 without area suction. Study of the results indicated that substantial reduction in the values of flow coefficient can be made by further refinements (see Appendix B). Examination of

the power requirements for this type of boundary-layer control for a typical fighter-type airplane showed values of the order of 17 horsepower.

It was found possible, from the results available, to develop a procedure which enabled estimates to be made of the flap lift increments and power requirements for wings other than the one tested.

Ames Aeronautical Laboratory  
National Advisory Committee for Aeronautics  
Moffett Field, Calif.



## APPENDIX A

## A FIRST APPROXIMATION OF A DESIGN PROCEDURE

## FOR APPLYING AREA SUCTION TO A FLAP ON

A WING HAVING  $45^\circ$  OF SWEEPBACK

From the results presented in this report for the suction flaps on a  $35^\circ$  sweptback wing, an approximate design procedure was devised to enable estimation of the suction requirements for suction flaps on wings having other angles of sweepback. The design procedure will be discussed for flaps on a wing having  $45^\circ$  of sweepback, an aspect ratio of 3.5, a taper ratio of 0.5, and a wing area of 300 square feet. The flap will be of constant 30-percent chord (measured along the streamwise chord), extending from 0.17 semispan to 0.72 semispan. The procedure will be directed toward, first, calculating the increment of lift to be obtained from the flap; second, selecting the chordwise extent and position of the porous area; third, estimating the pressure coefficient necessary for pumping; and fourth, estimating the flow coefficient and the suction power required.

Calculation of flap increment of lift.- The results of the investigation on the  $35^\circ$  sweptback wing and the results of some unpublished small-scale two-dimensional tests (2-foot-chord model) indicate that applying area suction to a trailing-edge flap simply allows the flap to be deflected to high angles without allowing air-flow separation to occur on the flap. With no air-flow separation on the flap, a nearly linear variation of flap lift increment with flap deflection angle is maintained to very high angles of flap deflection. Therefore, the first step of the design procedure, to calculate the increment of flap lift attainable with a given flap on a  $45^\circ$  sweptback wing, can be made with the use of the theory of reference 13. The validity of the step has been indicated by comparison of experiment and theory for the tests on the  $35^\circ$  sweptback wing reported herein.

The small-scale two-dimensional tests indicated that the linear variation of lift increment with flap deflection could be maintained to flap deflections of  $65^\circ$ . In this discussion, the assumption will be made that  $55^\circ$  and  $65^\circ$  of flap deflection with area suction will have unseparated air flow. The theory was used to calculate the increment of flap lift with these flap deflections measured in the plane normal to the flap hinge line. The calculations indicate that an increment of flap lift of 0.89 should be obtained with  $55^\circ$  deflection and an increment of lift of 1.05 with  $65^\circ$  deflection. These lift increments, as in the case of the  $35^\circ$  sweptback wings, should be of nearly constant value at all angles of attack below the angle where leading-edge separation occurs on the wing.

Position and chordwise extent of area suction.- From the tests on the  $35^\circ$  sweptback wing, it can be established that the leading edge of the porous area should be placed within a distance of  $\pm 1$ -percent normal chord (chord normal to the hinge line) from the peak negative pressure on the flaps. The peak negative pressure on the flap occurs quite near the midpoint of the radius of curvature but it can be located more accurately from airfoil-section theory. The chordwise extent of porous area can be from 1.5 to 3 percent of the normal chord for  $55^\circ$  flap deflection and 3.5 to 5.0 percent of the chord for  $65^\circ$  flap deflection. The use of any positions and chordwise extents of suction given in this range will give approximately the calculated increments of flap lift with suction power requirements of the same order of magnitude as possible minimum values.

Suction pressure coefficient.- The suction pressure is the sum of the external surface pressure, the pressure drop through the porous surface, and the pressure drop through the ducts. In this discussion, no calculations will be made of the pressure drop due to duct losses, for they are dependent entirely on the specific design of the ducts.

The external surface pressure coefficient can be calculated theoretically with the flap deflected. However, for simplicity in this case, the external surface pressure coefficient will be estimated from the values measured over the flap for the  $35^\circ$  sweptback wing. At  $55^\circ$  deflection, the maximum negative pressure coefficient over the flap was about  $-4.5$  (fig. 18). The angle of sweepback of the hinge line is approximately  $29^\circ$  compared to a value of approximately  $40^\circ$  for the 30-percent-chord flap on the example  $45^\circ$  sweptback wing. If simple sweep theory is used and it is assumed that the pressure coefficient based on the normal velocity is constant, the value of this pressure coefficient based on the free-stream velocity will vary as the square of the cosine of the sweep angle. On this basis the maximum negative pressure coefficient is  $-3.6$  on the flap surface for the  $45^\circ$  sweptback wing. It is realized that section thickness and chordwise extent of flap will have an effect on the magnitude of the radius of curvature over the hinge line and, hence, the pressure coefficient, but these effects will be neglected for this analysis. The value of pressure coefficient for the  $65^\circ$  flap deflection is estimated from the value of  $-8.2$  measured on the two-dimensional model. When this value is corrected by simple-sweep theory, the pressure coefficient on the  $45^\circ$  sweptback wing flap would be  $-4.8$ . This value compares quite closely to the value which would be obtained using a linear variation between  $55^\circ$  and  $70^\circ$  on the flap for the  $35^\circ$  sweptback wing and correcting for angle of sweep as shown in figure 24.

A rough approximation can be made for the pressure drop through the porous surface. This is sufficient since the pressure drop through the surface will be a small part of the total pumping pressure. In the tests of this investigation at a free-stream velocity of 183 feet per second



and a flap deflection of  $55^\circ$ , the suction-air velocity had an average value of about 5 percent of free-stream velocity. This resulted in a pressure drop of about 8 pounds per square foot through the 1/16-inch-thick porous material, giving a pressure coefficient of -0.2, based on the free-stream dynamic pressure. However, as was discussed previously, the suction-inflow velocities varied from a small value near the leading edge of the porous area, where the maximum peak negative external pressures existed, to a very large excess value at the aft edge of the porous area. It is believed that for any porous material for which the surface porosity or permeability is kept constant across the chordwise extent, a conservative value for the inflow velocities at the forward edge of 1 to 2 percent of the free-stream velocity will assure prevention of air-flow separation on the flap. For other porous materials, the pressure drop can be calculated by knowing the flow characteristics of the material and assuming an inflow velocity. For an installation on an aircraft, a porous stainless-steel surface could be used. The flow characteristics which might be obtained for porous stainless steel are shown in figure 25. The pressure coefficient necessary to draw the air through this type of porous surface would be about -0.2 for  $55^\circ$  deflection and about -0.3 for  $65^\circ$  deflection, based on an assumed inflow velocity at the leading edge of 1 percent of free-stream velocity. Therefore, the total pumping pressure coefficient, neglecting duct losses, would be -3.8 for  $55^\circ$  deflection and -5.1 for  $65^\circ$  deflection.

Suction flow coefficient and power.- The suction-flow-coefficient variation with angle of flap deflection is shown in figure 26 for the flap on the  $35^\circ$  sweptback-wing panels for  $0.5^\circ$  angle of attack and a free-stream velocity of 183 feet per second. The flow coefficients, based on the total-wing area and the free-stream velocity, are 0.0005 for a flap deflection of  $55^\circ$  and are estimated from figure 26 to be 0.0008 for  $65^\circ$  of flap deflection. For wings of other plan forms having flaps of other spans, the flow coefficients must be adjusted to a similar reference area and velocity. The reference area taken will be the area of the wing over which the flap extends, which is 39 percent of the wing area for the  $35^\circ$  sweptback wing and 50 percent of the wing area for the  $45^\circ$  sweptback wing. The reference velocity will be the component of the free-stream velocity normal to the flap. The flow coefficients required for the  $35^\circ$  sweptback wing, based on these references, are 0.0015 for  $55^\circ$  flap deflection and 0.0025 for the  $65^\circ$  flap deflection. These values of flow coefficient, based on the new reference area and velocity, can be used directly on the  $45^\circ$  sweptback wing flap to determine the quantity of air flow necessary for boundary-layer control. By this method, it was determined that 30.5 cubic feet of air per second would have to be removed with  $55^\circ$  of flap deflection and 53.2 cubic feet per second with  $65^\circ$ .

With the knowledge of the flow quantity and the pressure ratio, the suction horsepower necessary for the example wing was calculated, assuming

isentropic compression. The calculations indicate that 13.3 horsepower would be required for  $55^\circ$  flap deflection and 28.1 for  $65^\circ$  flap deflection. These power calculations do not include duct losses or the pump loss. It is believed, based on the results of the investigation on the  $35^\circ$  sweptback wings, that these losses would only require from 20- to 30-percent additional power, depending on the efficiency of the pump. Therefore, an increment of flap lift of 0.89 can be obtained with a suction flap deflection of  $55^\circ$  and approximately 16.7 horsepower and an increment of lift of 1.05 with  $65^\circ$  deflection and 35 horsepower. These values would result in a wing lift coefficient of approximately 1.4 and 1.5, respectively, for  $55^\circ$  and  $65^\circ$  deflection at a wing angle of attack of  $10^\circ$ .



## APPENDIX B

## ADDITIONAL INVESTIGATIONS OF SUCTION FLAP

Subsequent to the preparation of the text material, additional data were obtained on the reduction of suction flow coefficients and on an intermediate flap setting of  $64^\circ$ . The results of these tests substantiate much of the discussion presented in the report.

The results indicated that large reductions in the value of flow coefficient were obtainable with control of the chordwise distribution of suction-air velocities. This control can be obtained by two methods: First, by using a porous surface of constant thickness having higher pressure-drop characteristics than that used in the original tests; and, second, by using a porous surface having varying chordwise pressure-drop characteristics, as described in references 1, 3, and 15 for the case of wing leading-edge suction. The chordwise distribution of suction velocities required to attain equal values of  $\Delta C_{L_{crit}}$  for three porous materials are shown in figure 27 for the 25-percent spanwise station with chordwise extent of area suction, configuration 4, on the flap deflected  $55^\circ$ . The distributions shown were obtained at an angle of attack of  $0.5^\circ$  and a free-stream velocity of 183 feet per second. The chordwise distribution of suction velocities, curve (a) figure 27, is for the original 1/16-inch-thick porous material (flow characteristics of this material, grade 1, are shown in fig. 28). To obtain this distribution of suction-air velocities, a pumping pressure coefficient of -4.5 was required, resulting in a total flow coefficient of 0.00049. For the same flap deflection with a constant 1/16-inch-thick porous material having approximately twice the pressure-drop characteristics (porous material, grade 2, in fig. 28) the chordwise distribution required to prevent air-flow separation on the flap is shown by curve (b) in figure 27. As can be seen by comparing curves (a) and (b), a large reduction in suction-air velocities was obtained at the aft edge of the porous surface. To obtain this distribution of suction-air velocities with this porous surface, a pumping pressure coefficient of -4.9 was required, resulting in a total flow coefficient of 0.00036 or about a 27-percent reduction in flow. A further reduction of suction velocity and flow coefficient was obtained by using a tapered porous material. The change in thickness of the material, shown in figure 28(a), varied as the external surface pressure varied chordwise on the flap with the thinnest section at the forward edge near the peak negative pressure and the thick section at the aft edge where the external surface pressure was less negative. With the tapered porous surface, the chordwise distribution of suction-air velocities required to prevent air-flow separation is shown by curve (c) in figure 27. A pumping pressure coefficient of -5.3 was required to obtain this distribution, resulting in a flow coefficient of 0.00022 or a 55-percent reduction of total flow from the case with the constant-thickness high-porosity material.

Shown in figure 29 is the variation of flow coefficient required with flap deflection angle for the various types of porous materials used. It can be concluded that with the proper distribution of suction-air velocities, large reductions in flow coefficient are obtainable. As pointed out previously in the text of this report, there is probably an ideal chordwise distribution that will give the absolute minimum flow coefficient, which these tests have only approached. However, the ideal distribution will not give a very large reduction in flow coefficient below that of distribution (c) of figure 27. Also, as the chordwise distribution of velocities approach the ideal, the value of pumping pressure required increases because of the larger values of inflow required at the forward edge of the porous area. Therefore, the reduction in suction power that can be made below that of distribution (c) will be very small unless the ducting is such that the duct losses are a large part of the pressure losses in the system and then, small reductions in flow quantity will give large reductions in duct losses.

Additional tests were made with the suction flap deflected  $64^\circ$ . The force characteristics with this flap deflection are shown in figure 30. As shown by the data in figure 31, the increment of flap lift with flap deflection angle is nearly linear through  $0^\circ$  from  $64^\circ$ . These tests were made with the same two grades of 1/16-inch constant-thickness porous material investigated with  $55^\circ$  deflection. The chordwise extent of suction that gave the minimum suction requirements was an extent from 2 inches aft of the hinge reference line (fig. 4) to 5 inches aft of the reference line. The flow coefficient required with the material of greater porosity (fig. 28) was 0.0008 and, with the material of lower porosity, a value of 0.00054 was required. This reduction in flow coefficient is due again to better chordwise distribution of suction-air velocities.

The following table shows the measured minimum requirements to obtain  $\Delta C_{Lcrit}$  with the horizontal tail off:

W/S, 40 lb/sq ft										
Flap deflection, $55^\circ$						Flap deflection, $64^\circ$				
Angle of attack	$C_L$	$U_o$ ft/sec	$C_{Q_f}$	$P_{p_f}$	Measured suction hp	$C_L$	$U_o$ ft/sec	$C_{Q_f}$	$P_{p_f}$	Measured suction hp
0.5	0.83	202	0.00022	-5.3	12.5	0.92	191	0.00054	-6.8	28.0
6.6	---	---	---	---	---	1.28	162	.00050	-6.3	15.8
10.9	1.46	151.5	.00035	-4.8	8.3	1.52	148.5	.00050	-6.0	12.4

The powers shown include pump and duct losses. Values are given for the porous surface having a tapered material with the flap deflected  $55^\circ$



and for the 1/16-inch constant-thickness felt (grade 2) with the flap deflected  $64^{\circ}$ . These suction requirements were measured at conditions corresponding to level flight at various angles of attack at a wing loading of 40 pounds per square foot.

## REFERENCES

1. Holzhauser, Curt A., and Martin, Robert K.: The Use of Leading-Edge Area Suction to Increase the Maximum Lift Coefficient of a  $35^\circ$  Swept-Back Wing. NACA RM A52G17, 1952.
2. Maki, Ralph L.: Full-Scale Wind-Tunnel Investigation of the Effects of Wing Modifications and Horizontal-Tail Location on the Low-Speed Static Longitudinal Characteristics of a  $35^\circ$  Swept-Wing Airplane. NACA RM A52B05, 1952.
3. Cook, Woodrow L., and Kelly, Mark W.: The Use of Area Suction for the Purpose of Delaying Separation of Air Flow at the Leading Edge of a  $63^\circ$  Swept-Back Wing - Effects of Controlling the Chordwise Distribution of Suction Air Velocities. NACA RM A51J24, 1952.
4. Kelly, Mark W.: Low-Speed Aerodynamic Characteristics of a Large-Scale  $60^\circ$  Swept-Back Wing With High Lift Devices. NACA RM A52A14a, 1952.
5. James, Harry A., and Dew, Joseph K.: Effects of Double-Slotted Flaps and Leading-Edge Modifications on the Low-Speed Characteristics of a Large-Scale  $45^\circ$  Swept-Back Wing With and Without Camber and Twist. NACA RM A51D13, 1951.
6. Graham, David, and Koenig, David G.: Tests in the Ames 40- by 80-Foot Wind Tunnel of an Airplane Configuration With an Aspect Ratio 2 Triangular Wing and an All-Movable Horizontal Tail - Longitudinal Characteristics. NACA RM A51B21, 1951.
7. Franks, Ralph W.: Tests in the Ames 40- by 80-Foot Wind Tunnel of an Airplane Model With an Aspect Ratio 4 Triangular Wing and an All-Movable Horizontal Tail - High-Lift Devices and Lateral Controls. NACA RM A52K13, 1953.
8. Razak, Virgil K., Razak, Kenneth, and Bondie, R. J. Jr.: Wind-Tunnel Investigation of a Method of Boundary-Layer Control as applied to a Reflection-Plane Model at Full-Scale Reynolds No. Engineering Report 032, Univ. of Wichita.
9. Regenscheit, B.: Tests on a Suction Wing NACA 23015 With and Without Curved Nose. Trans. from ZWB, Berlin, FB1312 Aerodynamische Versuchsanstalt Göttingen E. V., Institut für Wendkanäle, Bericht, 40/14/46, 1948.



10. Stuper, Josef: Flight Experiences and Tests on Two Airplanes with Suction Slots. NACA TM 1232, 1950.
11. Rebuffet, P., and Poisson-Quinton, Ph.: Investigations of the Boundary-Layer Control on a Full Scale Swept Wing with Air Bled Off From the Turbojet. NACA TM 1331, 1952.
12. Nunemaker, John J., and Fisher, Jack W.: Two-Dimensional Wind Tunnel Investigation of Boundary-Layer Control by Blowing on an NACA 23015 Airfoil. Univ. of Wichita Eng. Rept. 023, 1950.
13. DeYoung, John: Theoretical Symmetric Span Loading Due to Flap Deflection for Wings of Arbitrary Plan Form at Subsonic Speeds. NACA Rep. 1071, 1952.
14. Cook, Woodrow L., Griffin, Roy N., Jr., and McCormack, Gerald M.: The Use of Area Suction for the Purpose of Delaying Separation of Air Flow at the Leading Edge of a  $63^\circ$  Swept-Back Wing. NACA RM A50H09, 1950.
15. Dannenberg, Robert E., and Weiberg, James A.: Section Characteristics of a 10.5-Percent-Thick Airfoil With Area Suction as Affected by Chordwise Distribution of Permeability. NACA TN 2847, 1952.
16. Anderson, Seth B., Matteson, Fredrick H., and Van Dyke, Rudolph D., Jr.: A Flight Investigation of the Effect of Leading-Edge Camber on the Aerodynamic Characteristics of a Swept-Wing Airplane. NACA RM A52L16a, 1953.

TABLE I.- COORDINATES OF THE WING AIRFOIL SECTIONS NORMAL  
TO THE WING QUARTER-CHORD LINE AT TWO SPAN STATIONS  
[Dimensions given in inches]

Section at 0.467 semispan			Section at 0.857 semispan		
x	z		x	z	
	Upper surface	Lower surface		Upper surface	Lower surface
0	0.231	- - -	0	-0.098	- - -
.119	.738	-0.307	.089	.278	-0.464
.239	.943	-.516	.177	.420	-.605
.398	1.127	-.698	.295	.562	-.739
.597	1.320	-.895	.443	.701	-.879
.996	1.607	-1.196	.738	.908	-1.089
1.992	2.104	-1.703	1.476	1.273	-1.437
3.984	2.715	-2.358	2.952	1.730	-1.878
5.976	3.121	-2.811	4.428	2.046	-2.176
7.968	3.428	-3.161	5.903	2.290	-2.401
11.952	3.863	-3.687	8.855	2.648	-2.722
15.936	4.157	-4.064	11.806	2.911	-2.944
19.920	4.357	-4.364	14.758	3.104	-3.102
23.904	4.480	-4.573	17.710	3.244	-3.200
27.888	4.533	-4.719	20.661	3.333	-3.250
31.872	4.525	-4.800	23.613	3.380	-3.256
35.856	4.444	-4.812	26.564	3.373	-3.213
39.840	4.299	-4.758	29.516	3.322	-3.126
43.825	4.081	-4.638	32.467	3.219	-2.989
47.809	3.808	-4.452	35.419	3.074	-2.803
51.793	3.470	-4.202	38.370	2.885	-2.574
55.777	3.066	-3.891	41.322	2.650	-2.302
59.761	2.603	-3.521	44.273	2.374	-1.986
<sup>a</sup> 63.745	2.079	-3.089	<sup>a</sup> 47.225	2.054	-1.625
83.681	-.740	- - -	63.031	.321	- - -
L.E. radius: 1.202, center at 1.201, 0.216			L.E. radius: 0.822, center at 0.822, -0.093		

<sup>a</sup> Straight lines to trailing edge





TABLE II.- SUMMARY OF EXTENT AND POSITIONS OF POROUS SURFACE TESTED  
ON SUCTION FLAP, DIMENSIONS NORMAL TO HINGE REFERENCE LINE  
[Dimensions in inches]

Flap deflection, 55°			Flap deflection, 70°		
Config- uration no.	Extent of chordwise opening	Position of for- ward edge (aft of ref.line)	Config- uration no.	Extent of chordwise opening	Position of for- ward edge (aft of ref.line)
1	0.5	2.5	16	2.12	1.87
2	1.0	2.5	17	2.62	1.87
3	1.5	2.5	18	3.12	1.87
4	2.5	2.5	19	3.62	1.87
5	3.5	2.5	20	4.12	1.87
6	5.5	2.5	21	5.12	1.87
7	1.5	0.5	22	3.62	2.12
8	1.5	1.5	23	3.62	2.32
9	1.5	3.5	24	3.62	2.62
10	1.5	4.5	25	3.62	3.12
11	1.5	5.5	26	3.62	3.62
12	1.5	6.5	27	3.62	4.12
13	2.5	3.5			
14	2.5	4.5			
15	2.5	5.5			



TABLE III.- SUMMARY OF LEADING EDGES TESTED

Configuration	Leading edge tested
A	F-86A leading edge, slats closed, slits sealed
B	Porous leading edge with porous surface taped with a nonporous tape - unmodified F-86A leading-edge contour
C	F-86A leading edge, slats open, slits unsealed (fig. 7)
D	Modified leading edge (forward camber and increased leading-edge radius, fig. 7)
B-B	Full-span extent of porous area, 0.11 to 0.96 span (fig. 8)
C-B	Partial-span extent of porous area 0.25 to 0.96 span (fig. 8)
D-B	Partial-span extent of porous area 0.35 to 0.96 span (fig. 8)
E-B	Partial-span extent of porous area 0.35 to 0.96 span (fig. 8)





TABLE IV.- COORDINATES OF THE MODIFIED WING LEADING EDGE AT  
TWO SPAN STATIONS, NORMAL TO THE WING QUARTER-CHORD LINE  
[Dimensions given in inches]

Section at 0.467 semispan			Section at 0.857 semispan		
x	z		x	z	
	Upper surface	Lower surface		Upper surface	Lower surface
-1.692	-1.445	- - -	-1.250	-1.359	- - -
-1.273	-.348	-2.552	-.934	-.495	-2.192
-.855	.222	-2.898	-.619	-.099	-2.454
-.436	.629	-3.114	-.304	.197	-2.609
-.018	.969	-3.272	.011	.456	-2.701
.400	1.266	-3.391	.326	.675	-2.769
.819	1.527	-3.473	.641	.867	-2.796
1.237	1.760	-3.523	.956	1.040	-2.813
1.655	1.952	-3.549	1.272	1.189	-2.821
1.992	2.104	- - -	1.476	1.273	- - -
2.074	- - -	-3.552	1.587	- - -	-2.813
2.911	- - -	-3.531	2.217	- - -	-2.787
4.166	- - -	-3.481	3.163	- - -	-2.742
6.258	- - -	-3.472	4.739	- - -	-2.709
8.350	- - -	-3.542	6.314	- - -	-2.712
10.442	- - -	-3.657	7.890	- - -	-2.751
14.626	- - -	-3.956	9.466	- - -	-2.808
15.936	- - -	-4.064	11.042	- - -	-2.885
			11.806	- - -	-2.944
L.E. radius: 1.674, center at -0.018, -1.445			L.E. radius: 1.261, center at 0.011, -1.359		



TABLE V.- LOCATION OF SURFACE PRESSURE ORIFICES  
 [ Position of orifices<sup>1</sup>, chordwise percent ]

Orifice no.	0.25b/2 and 0.45b/2 station		0.65b/2 and 0.85b/2 station	
	Upper surface	Lower surface	Upper surface	Lower surface
1	0	- - -	0	- - -
2	.25	0.25	.25	0.25
3	.5	.5	.5	.15
4	1.0	1.0	1.0	1.0
5	1.5	1.5	1.5	1.5
6	2.0	2.0	2.0	2.0
7	2.5	2.5	2.5	2.5
8	3.5	3.5	3.5	3.5
9	5.0	5.0	5.0	5.0
10	7.5	7.5	7.5	7.5
11	10.0	10.0	10.0	10.0
12	15.0	15.0	15.0	15.0
13	20.0	20.0	20.0	20.0
14	30.0	30.0	30.0	30.0
15	40.0	40.0	40.0	40.0
16	50.0	70.0	50.0	60.0
17	60.0	75.0	60.0	70.0
18	70.0	80.0	70.0	80.0
19	75.0	88.0	80.0	90.0
20	80.0	90.5	90.0	97.5
21	83.3	93.2	97.5	
22	84.0	96.0		
23	84.4	98.0		
24	84.8			
25	85.4			
26	86.5			
27	87.7			
28	91.0			
29	93.0			
30	95.0			
31	97.0			
32	99.0			

<sup>1</sup>Upper surface orifices omitted: Lower surface orifices omitted:  
 Station 0.25b/2, no. 6 Station 0.25b/2, no. 16  
 Station 0.85b/2, nos. 2, 6, & 11 Station 0.65b/2, nos. 6, 7, & 8  
 Station 0.65b/2, no. 7 Station 0.85b/2, no. 10 above  
 12.8°



TABLE VI.- CONFIGURATIONS TESTED, AND TEST CONDITIONS

Fig. no.	Configurations				Test conditions	
	Leading edge (Table III)	Flap		Horiz. Tail	U <sub>0</sub> ft/sec	W/S
		Suction (Table II)	Deflection deg			
10(a)	A	4	55	on	145 and 183	variable
10(a)	B	no suction	55	on	145	variable
10(a)	B	no suction	70	on	145	variable
10(a)	B	1 through 15	55	on	145 and 183	variable
10(a)	B	16 through 27	70	on	145 and 183	variable
10(b)	B	no suction	55	off	112	variable
10(b)	B	4	55	off	112	variable
20(a)	C	4	55	on	varied	40 and 60
20(a)	D	4	55	on	varied	40 and 60
20(a)	B-B	4	55	on	varied	40 and 60
20(b)	B-B	4	55	off	112	variable
21	C-B	4	55	on	varied	40
21	D-B	4	55	on	112	40
21	E-B	4	55	on	varied	40



TABLE VII.- SUMMARY OF DUCT LOSSES AND PUMP LOSSES FOR  
AREA SUCTION APPLIED AT THE WING LEADING EDGE

Extent of suction B-B								
Wing loading, 40 lb/sq ft					Wing loading, 60 lb/sq ft			
$C_L$	$U_o$ ft/sec	$P_{d_L}$	Duct loss hp	Pump loss hp	$U_o$ ft/sec	$P_{d_L}$	Duct loss hp	Pump loss hp
1.6	145	-11.6	2.0	4.4	179.5	-12.5	3.7	10.9
1.82	136	-17.6	2.5	10.2	166.5	-18.3	6.0	28.9
1.95	131.5	-20.8	3.5	12.2	161.0	-22.1	7.2	36.3
2.07	127.5	-26.9	6.1	21.2	153.0	-28.1	16.0	63.0
2.17	124.5	-32.2	16.0	37.2	- - -	- - -	- - -	- - -





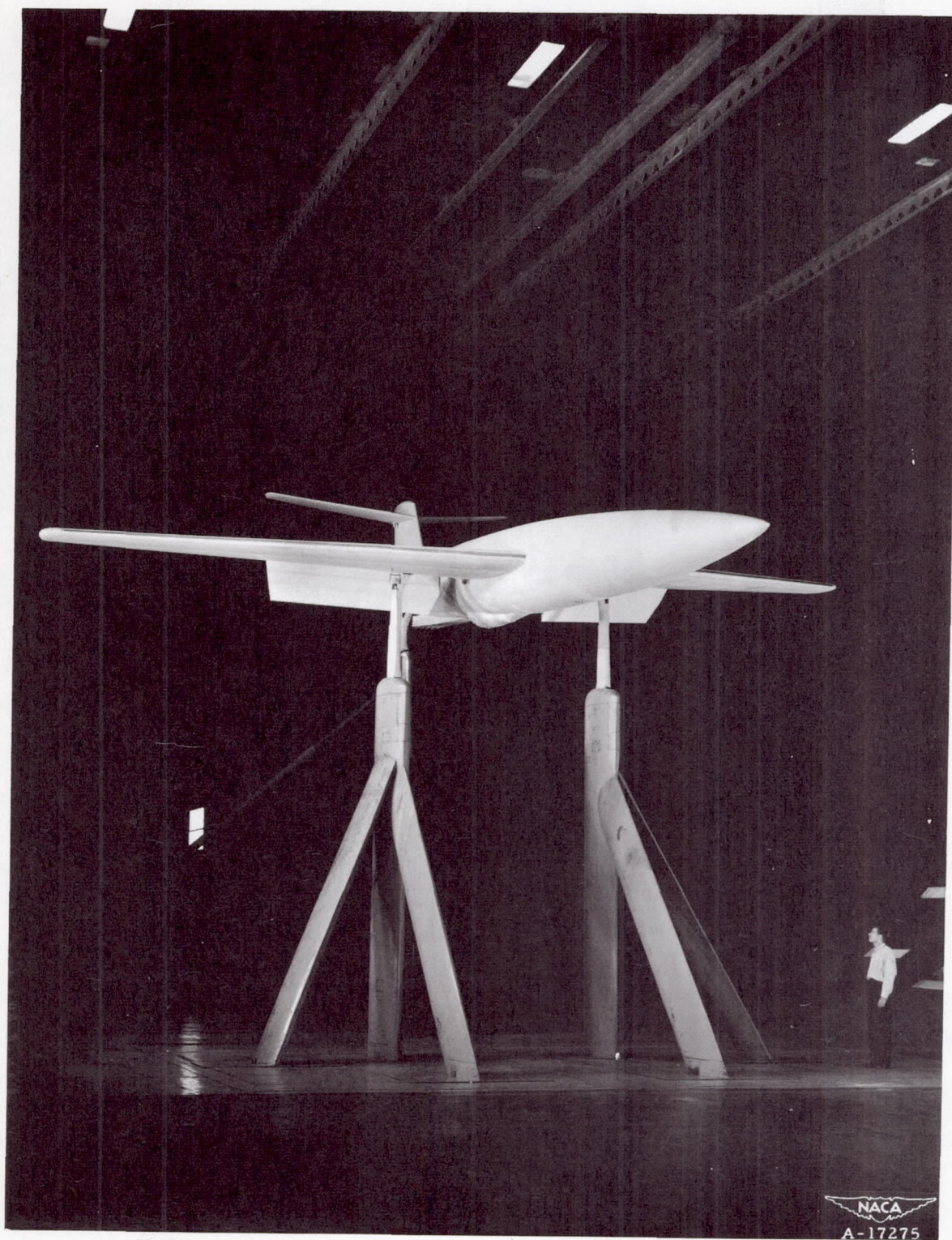


Figure 1.- View of 35° swept-back wing model mounted in the 40- by 80-foot wind tunnel.

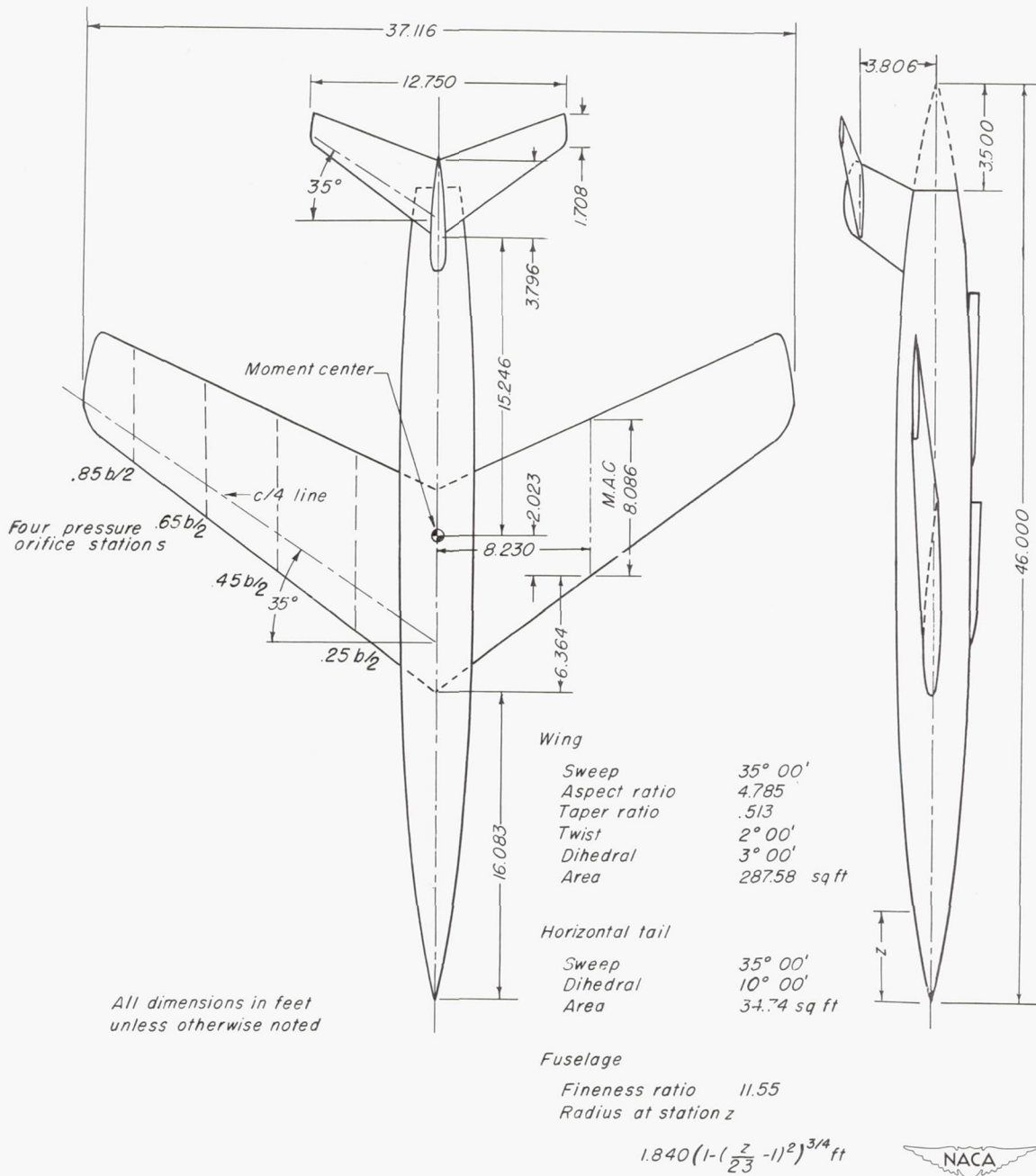
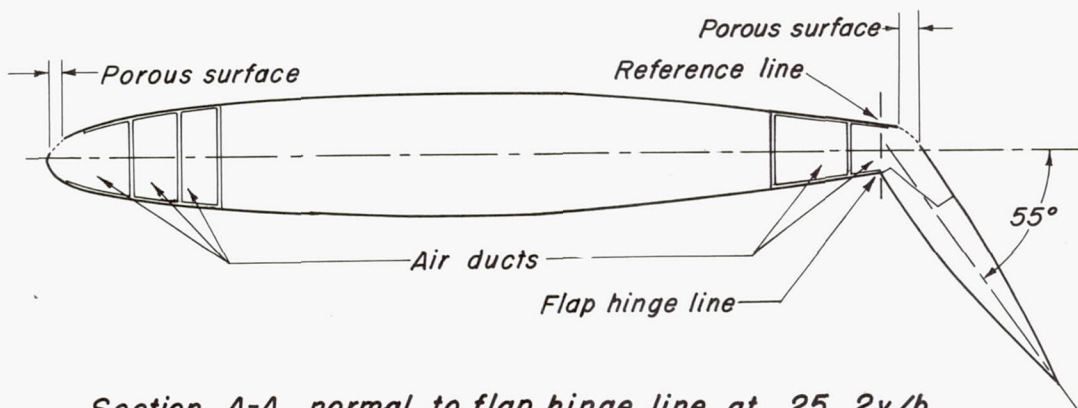


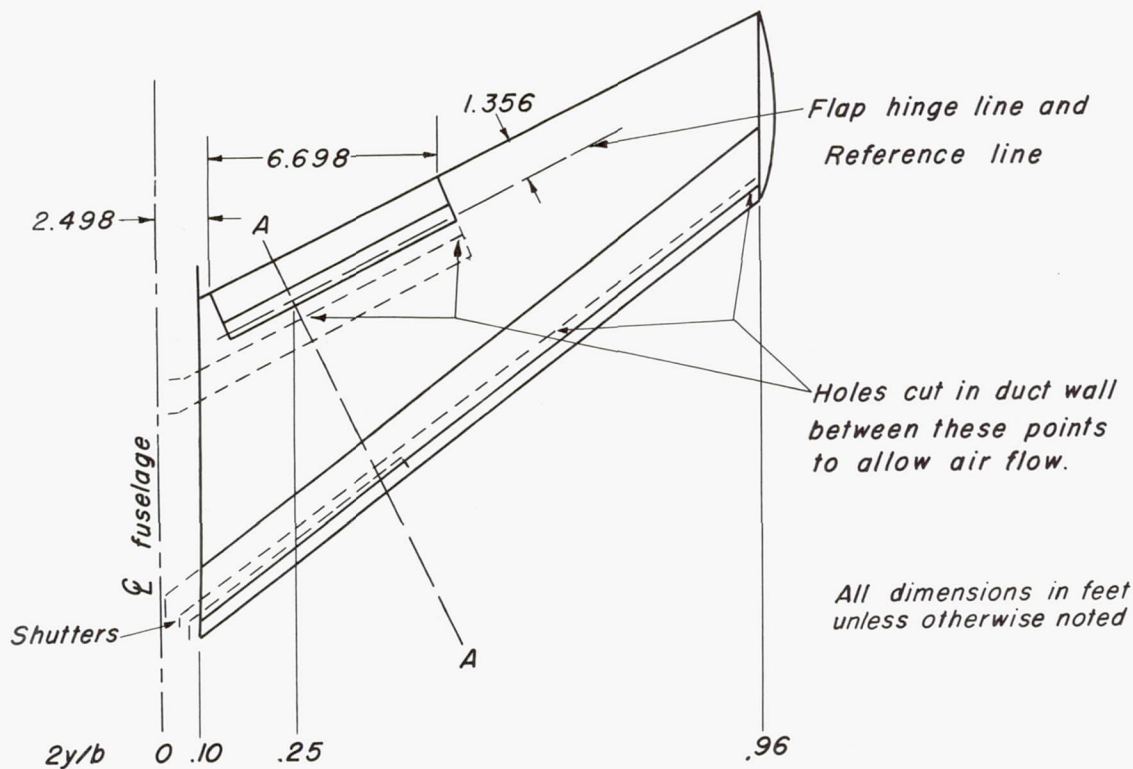
Figure 2.— Geometric characteristics of the 35° swept-wing model.







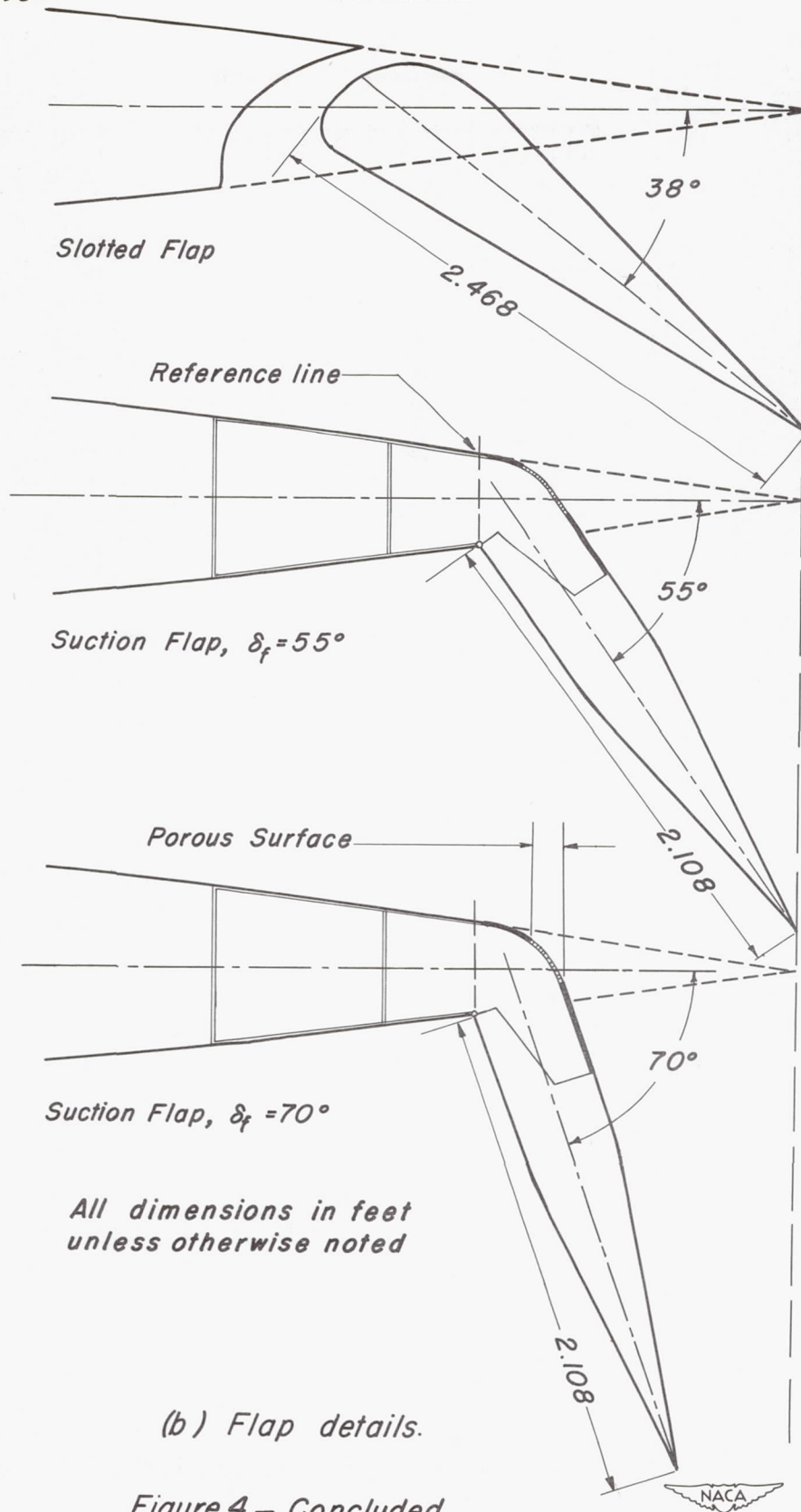
*Section A-A normal to flap hinge line at .25  $2y/b$*



*(a) Wing details.*

*Figure 4.— Schematic diagram showing ducting and flaps.*





All dimensions in feet  
unless otherwise noted

(b) Flap details.

Figure 4.— Concluded.

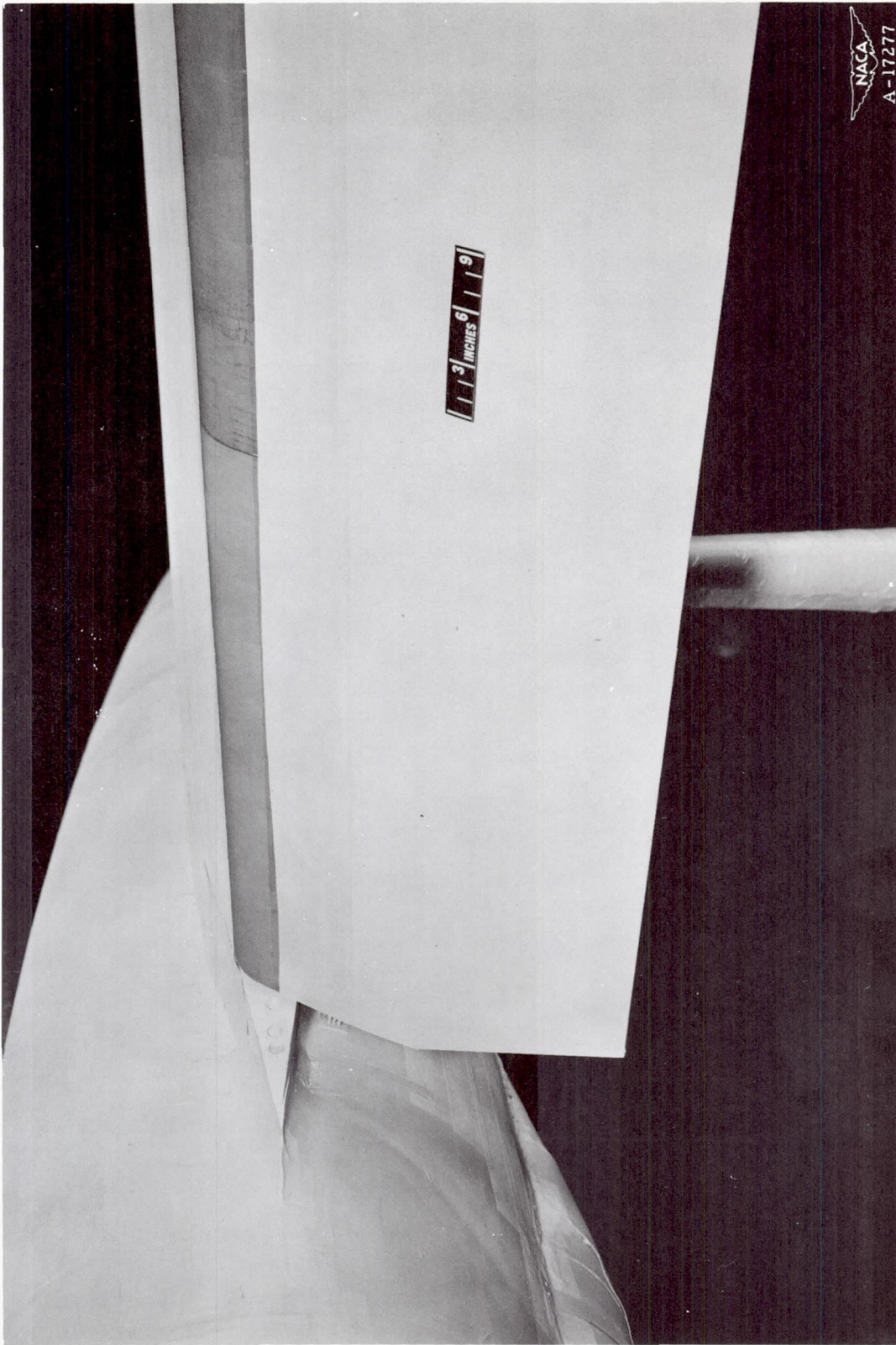


Figure 5.- Close-up view of suction flap deflected 55°.



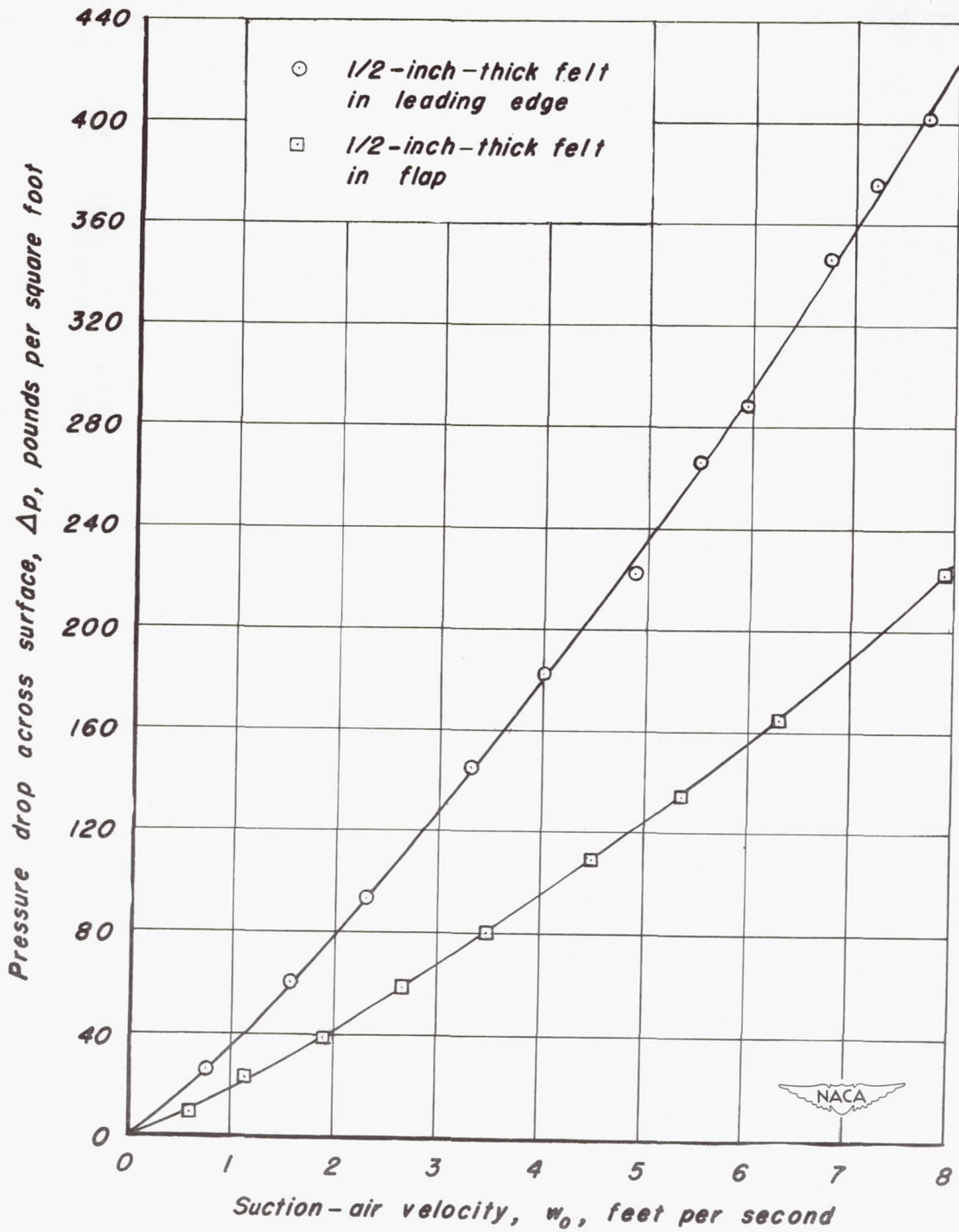
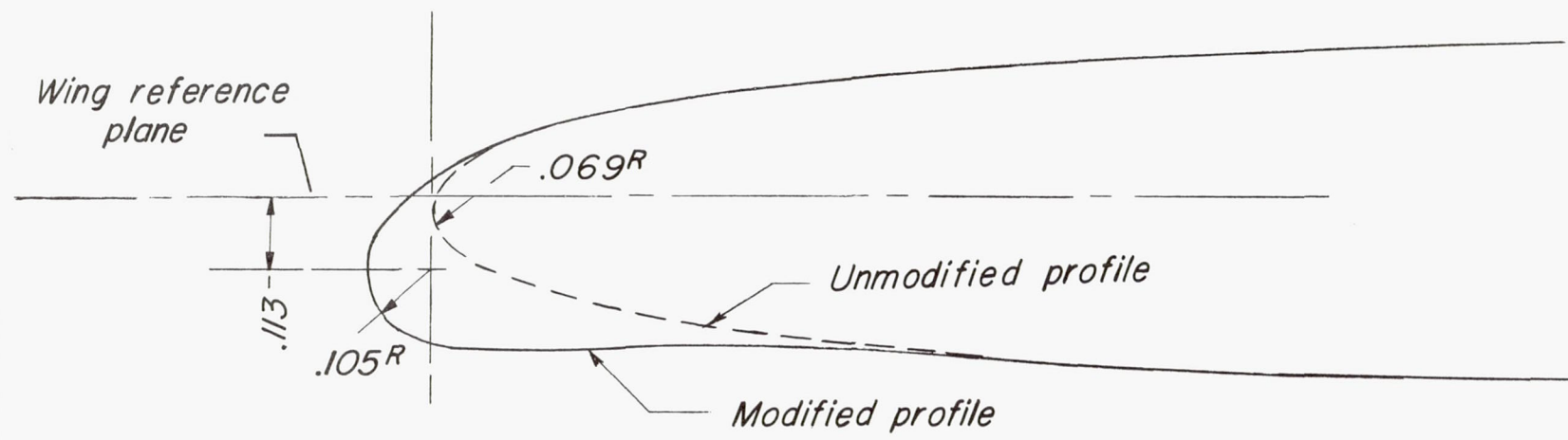


Figure 6.— Calibration of suction-air velocities for the porous mesh sheet backed with one-half inch wool felt material.

Dimensions in feet  
unless otherwise noted



CONFIDENTIAL

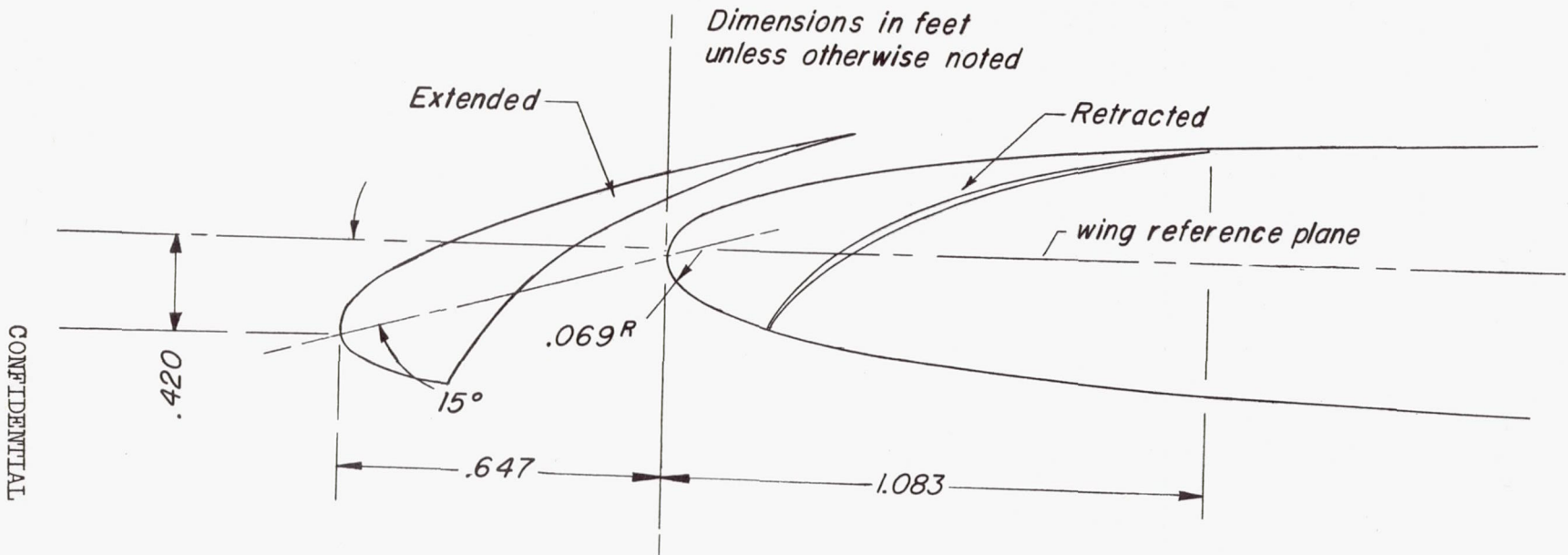
CONFIDENTIAL

(a) Modified leading edge.



Figure 7.—Details of the wing airfoil sections at 0.857 semispan, taken normal to the wing quarter-chord line.





CONFIDENTIAL

(b) Unmodified section showing slat extended and retracted.



Figure 7.— concluded.

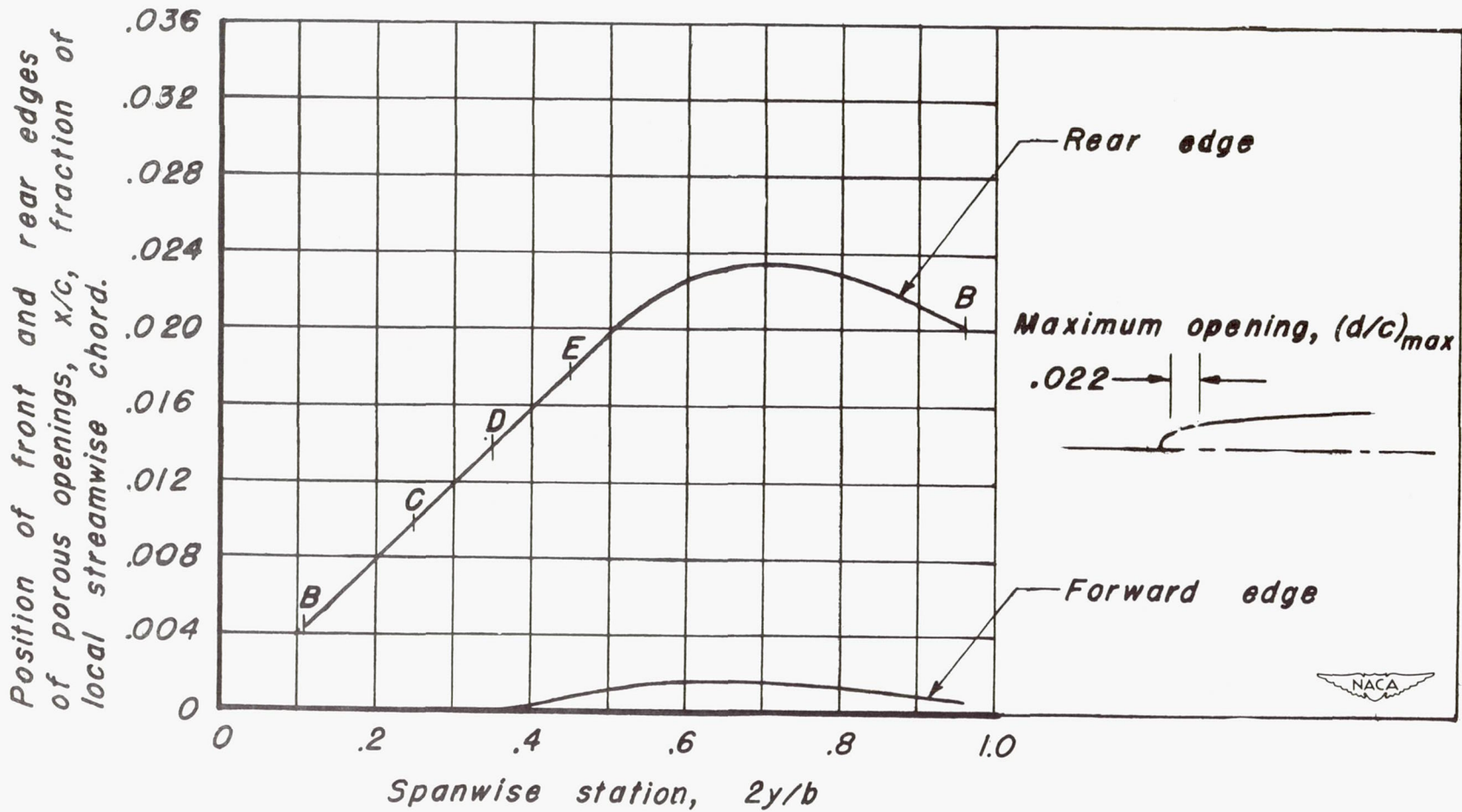


Figure 8.— Chordwise extent of porous surface at wing leading edge for several spanwise extents of area suction.

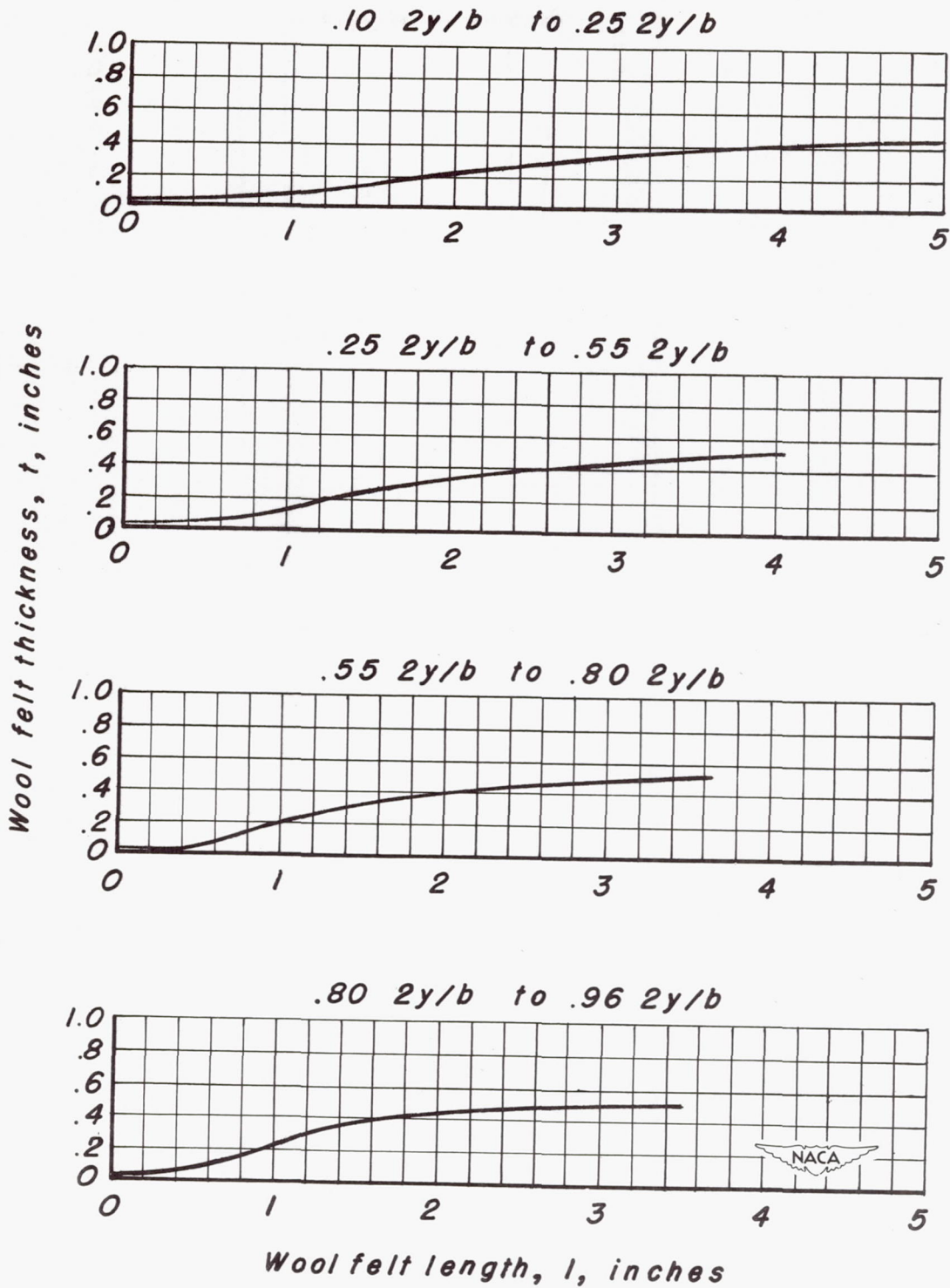
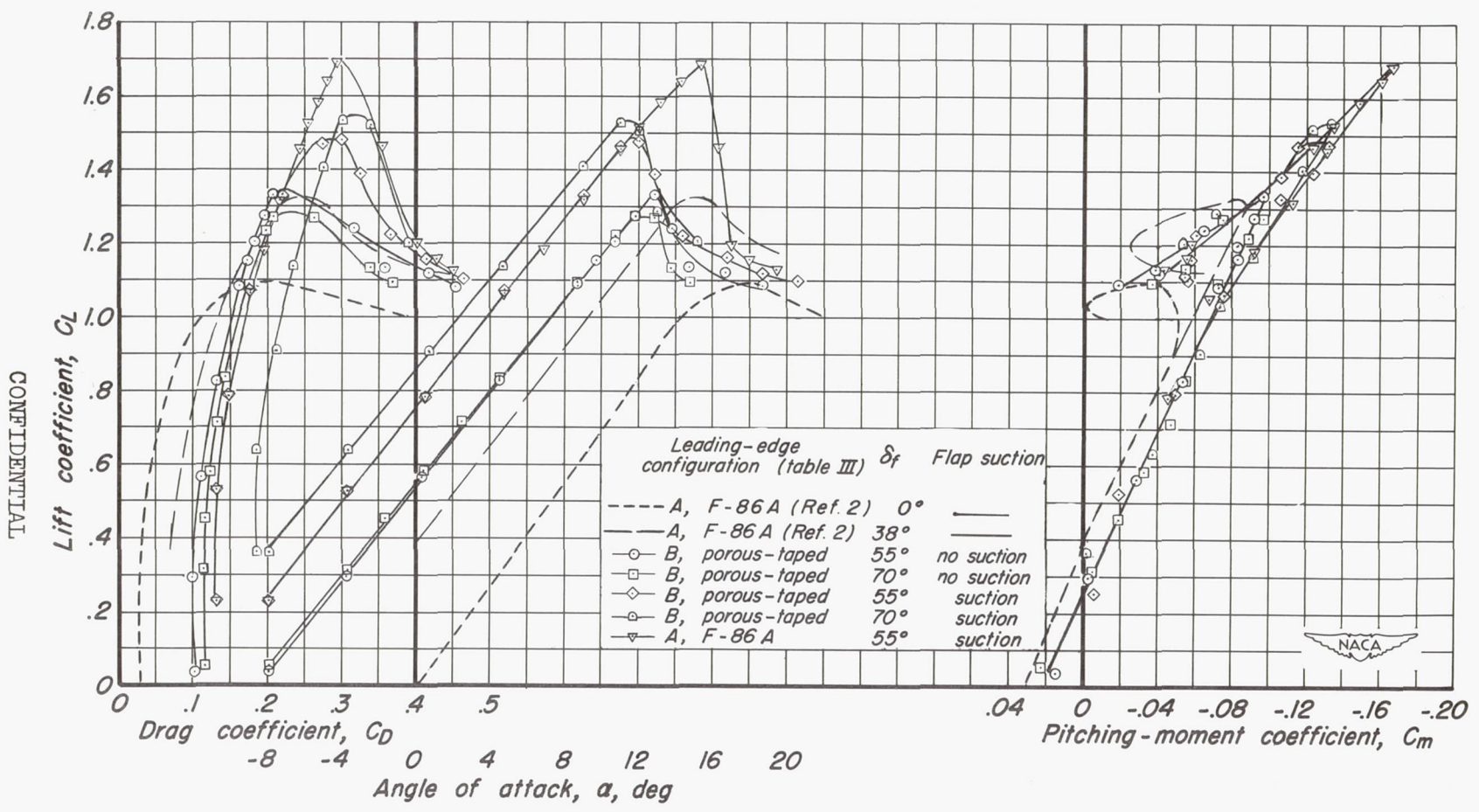


Figure 9.— Thickness variations of the felt backing used in the wing.

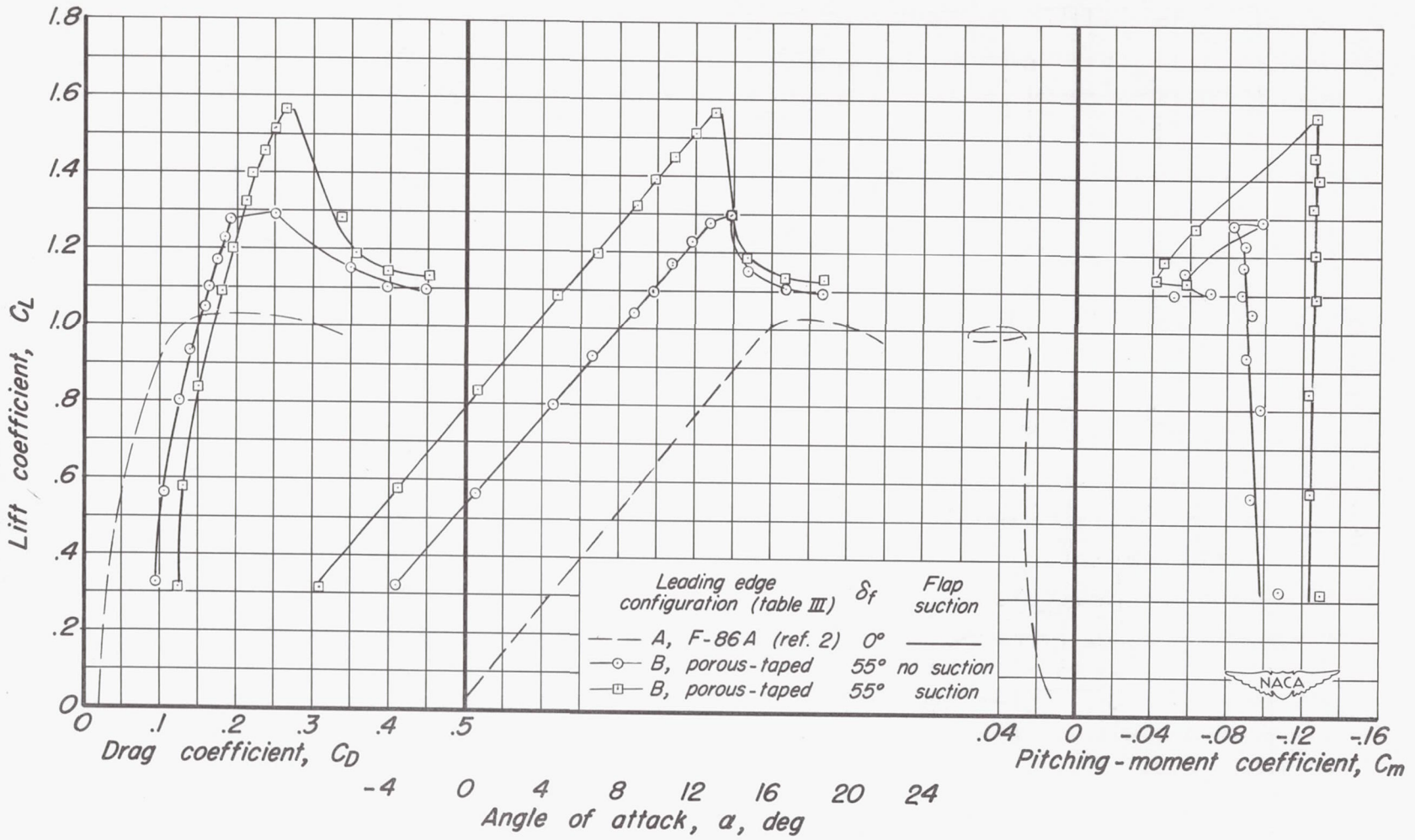




(a) Horizontal tail on.

Figure 10.— Aerodynamic characteristics of the 35° swept-back wing with the suction flap deflected 55° and 70° with and without suction.

CONFIDENTIAL



(b) Horizontal tail off.  
Figure 10.- Concluded.

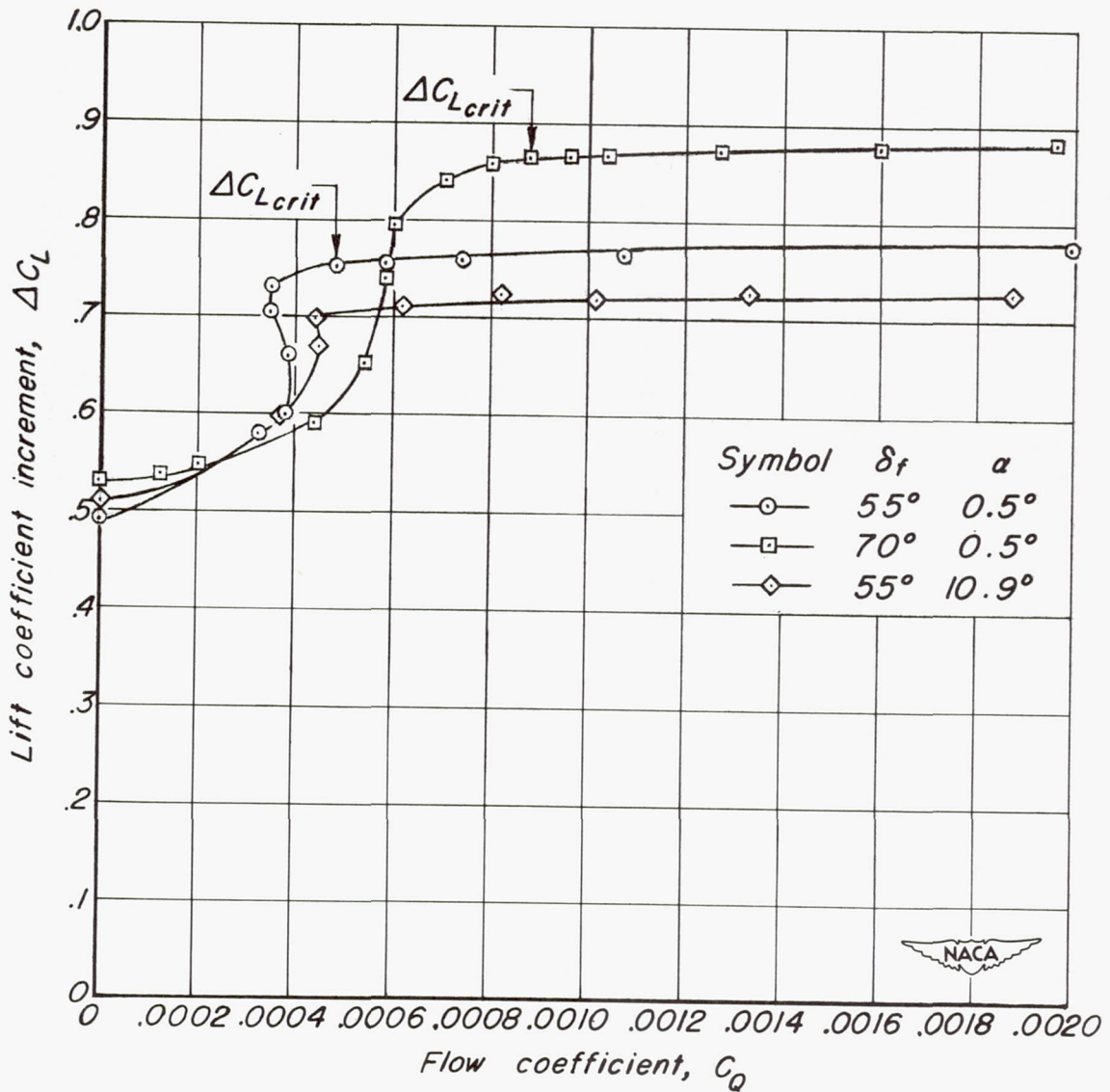
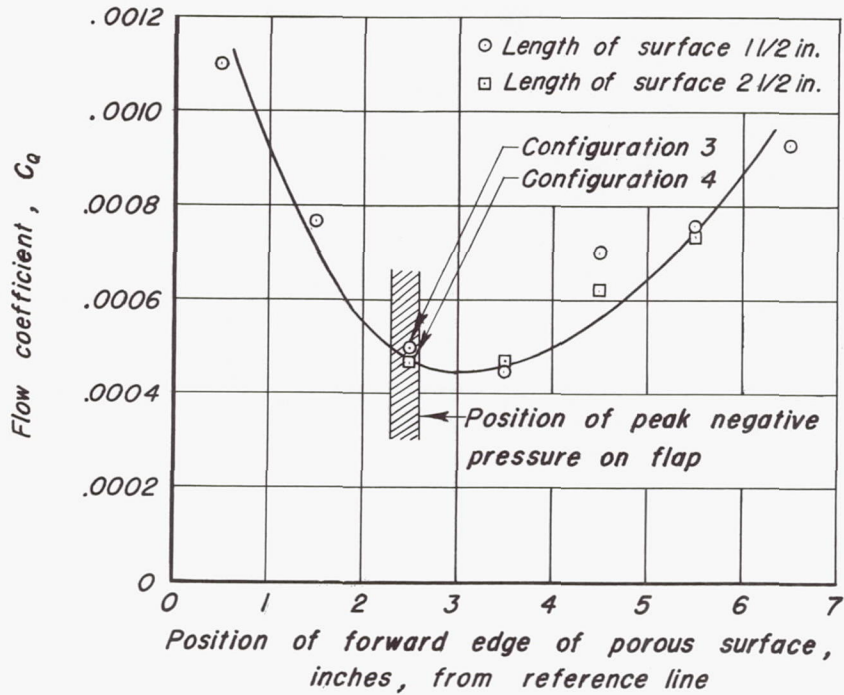
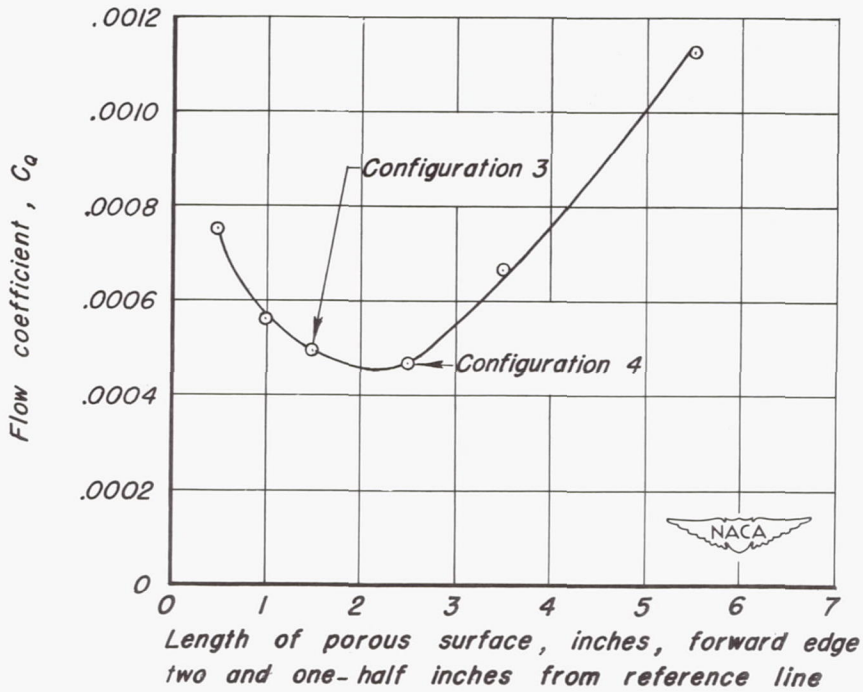


Figure 11.— Variation of increment of flap lift coefficient with suction flow coefficient for 55° and 70° of flap deflection.  $U_0 = 145$  ft/sec.



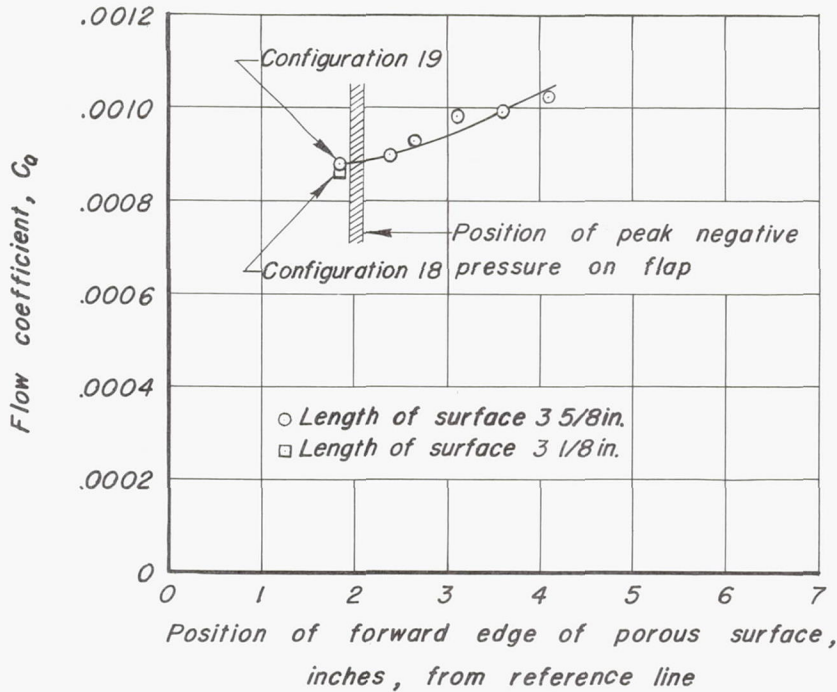


(a) Porous-surface position.

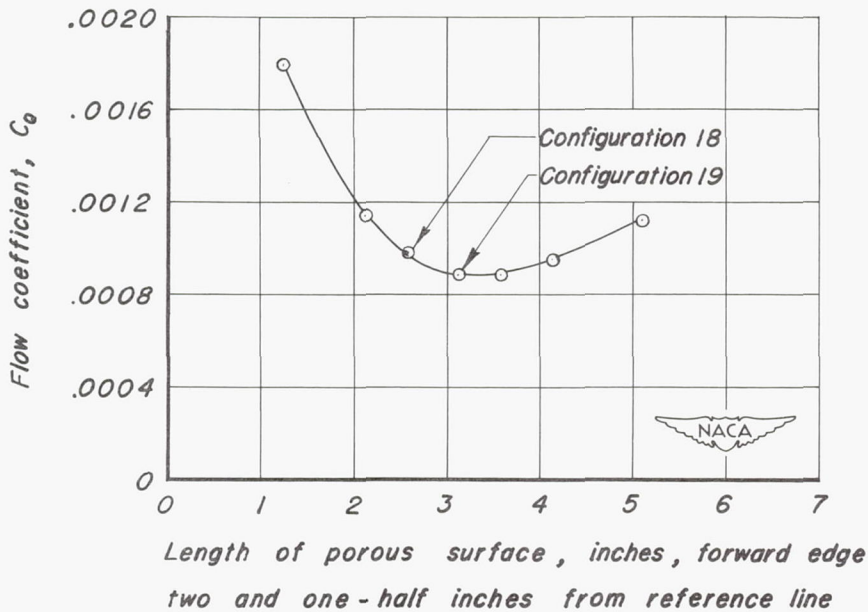


(b) Porous-surface extent.

Figure 12.- Variation of flow coefficient with extent and position of area suction on the flap deflected  $55^\circ$ .  $\Delta C_L = 0.78$ . Free-stream velocity = 145 feet per second.



(a) Porous - surface position.



(b) Porous - surface extent.

Figure 13.- Variation of flow coefficient with position and extent of area suction on the flap deflected 70°.  $\Delta C_L = 0.87$ . Free-stream velocity = 145 feet per second.

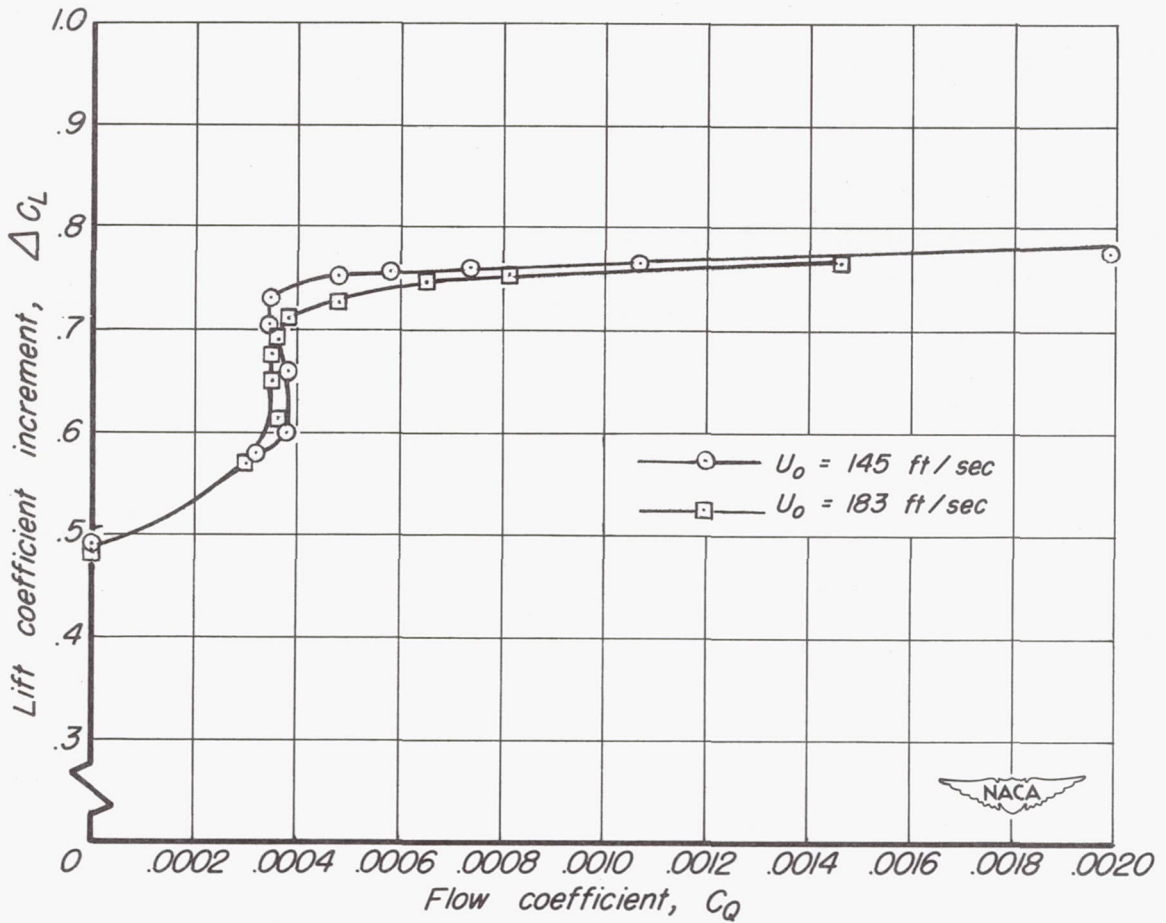


Figure 14.— Variation of flap increment of lift coefficient with flow coefficient for two free-stream velocities.  $\delta_f = 55^\circ$ . Configuration 4.  $\alpha = 0.5^\circ$ .



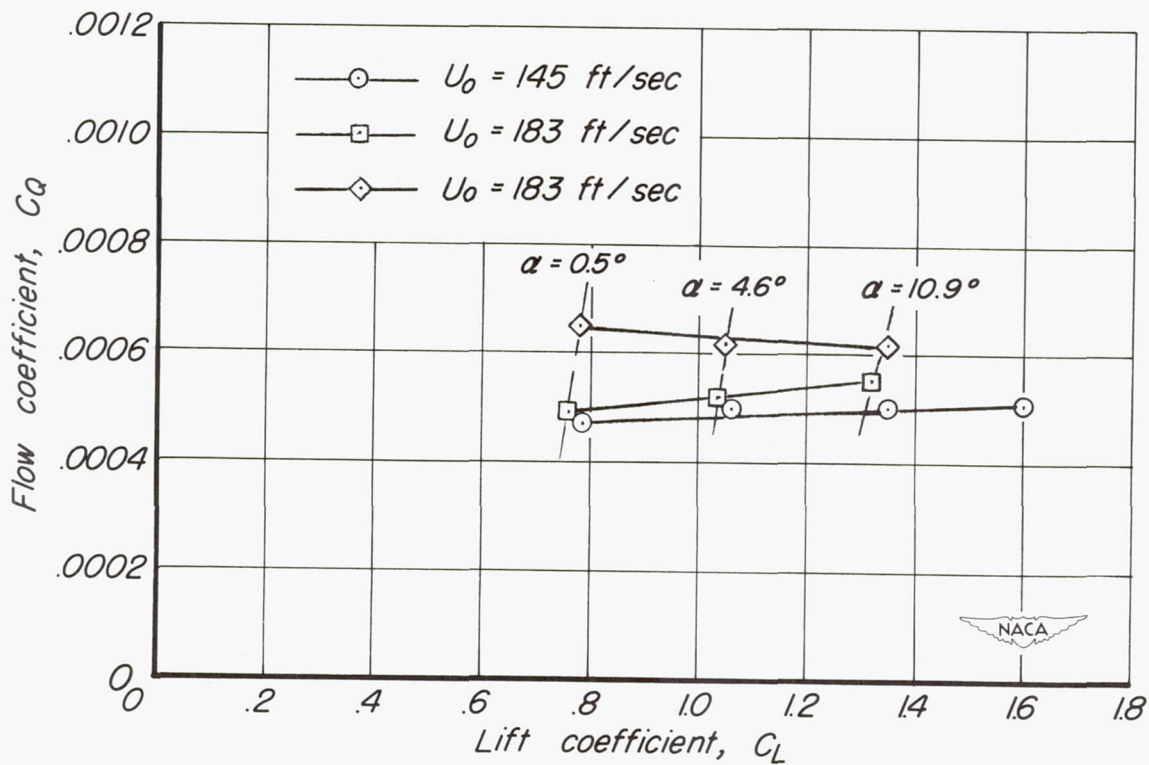


Figure 15.— Variation of flow coefficient required for suction flap with wing lift coefficient for two free-stream velocities.  $\delta_f = 55^\circ$ . Configuration 4.

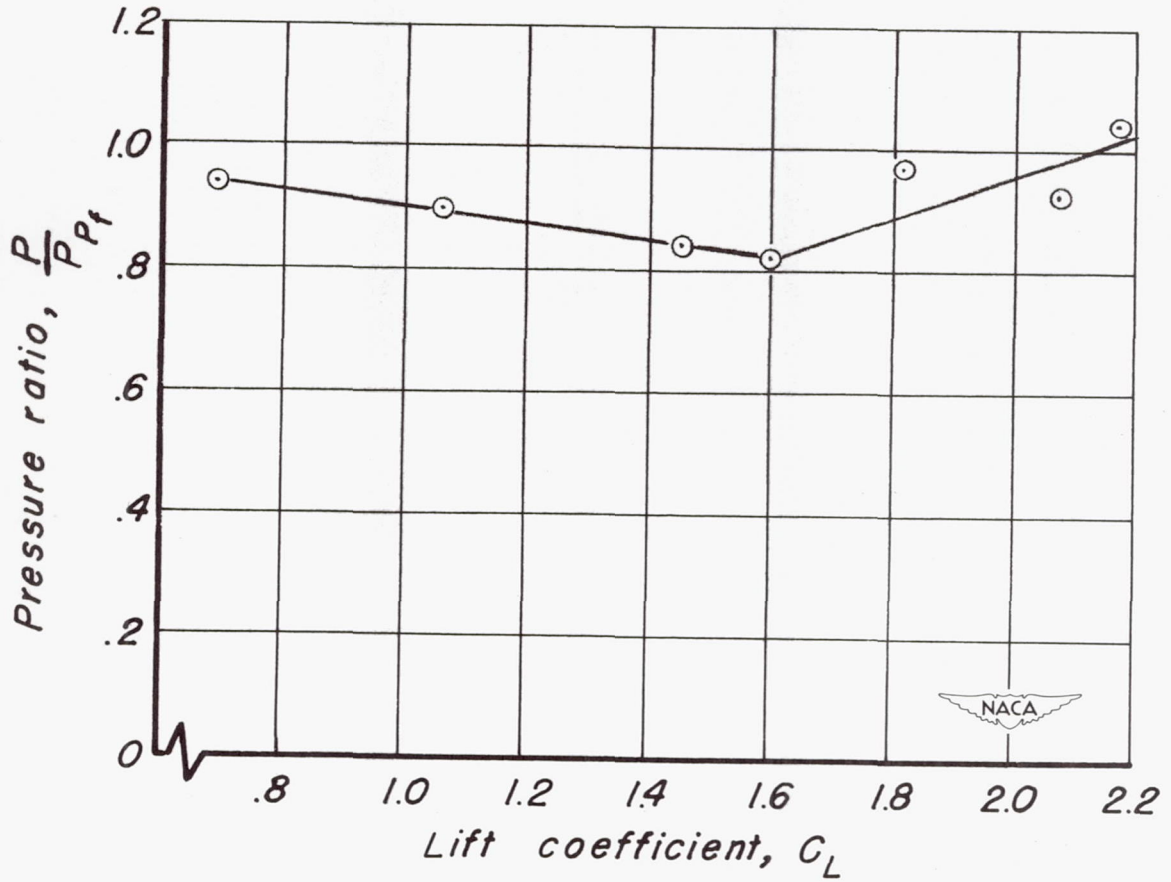


Figure 16.- Variation of pressure ratio at flap with wing lift coefficient.  $\delta_f = 55^\circ$

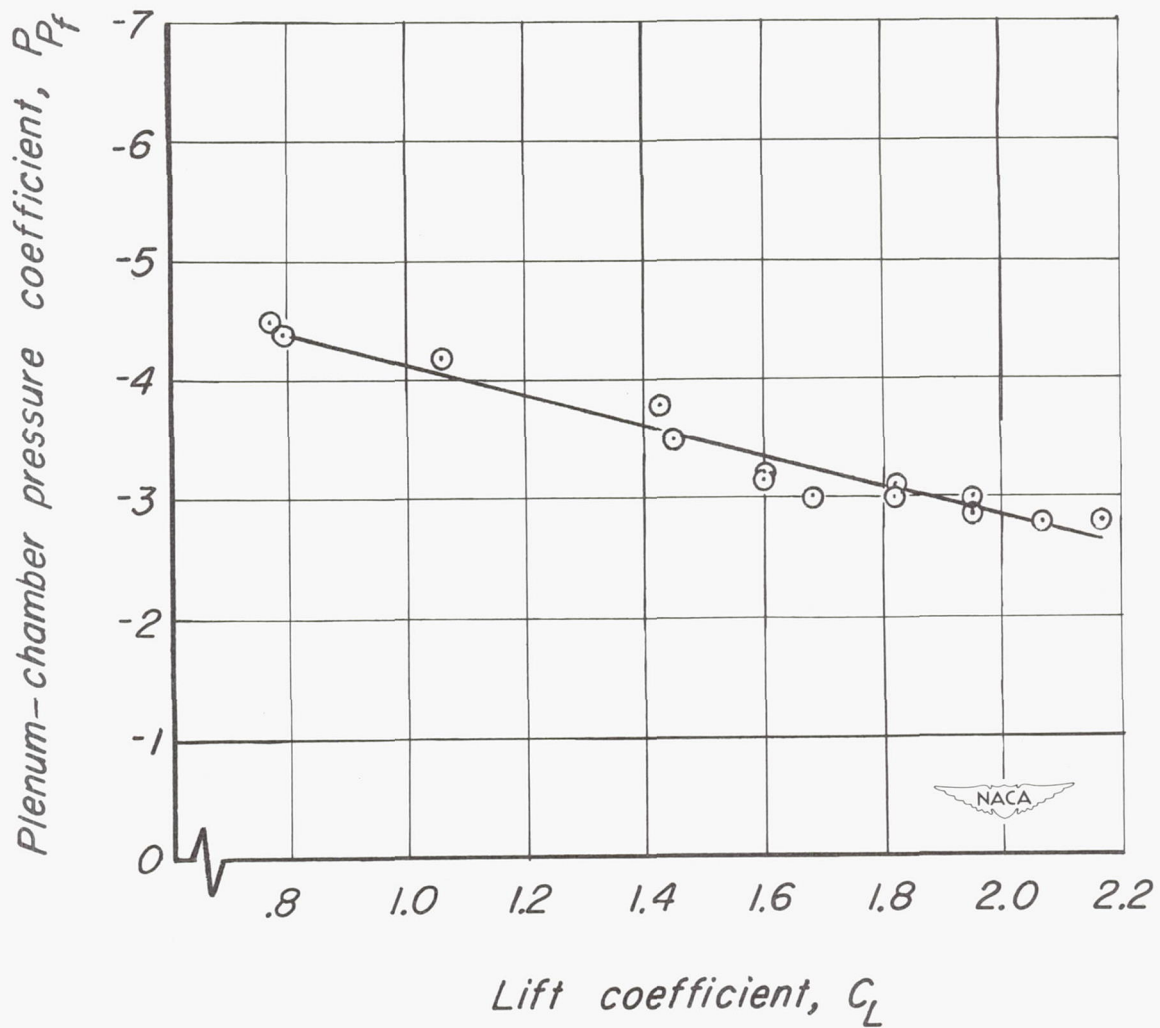


Figure 17.— Variation of plenum-chamber pressure coefficient with lift coefficient.  $\delta_f = 55^\circ$ .



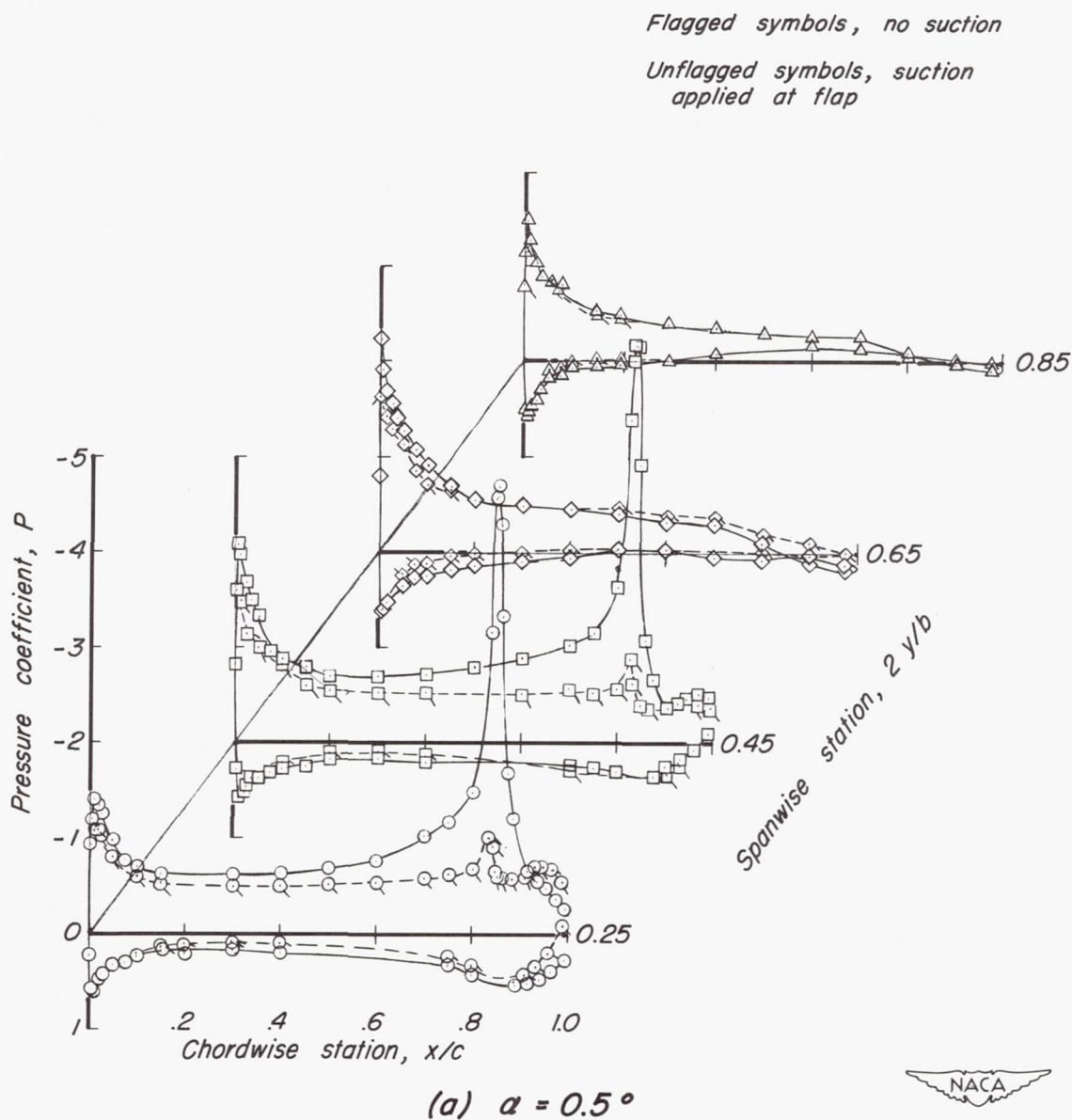
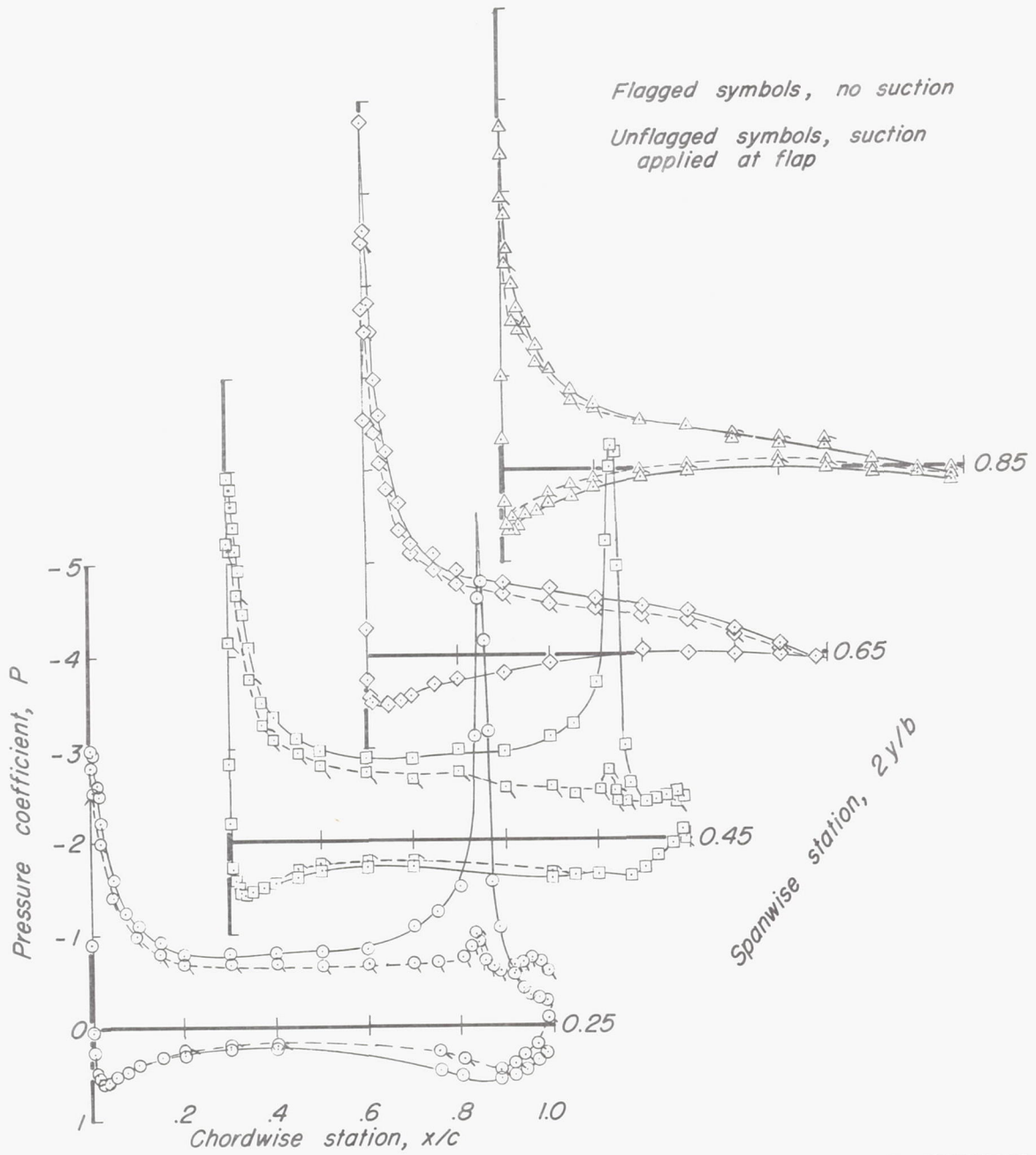


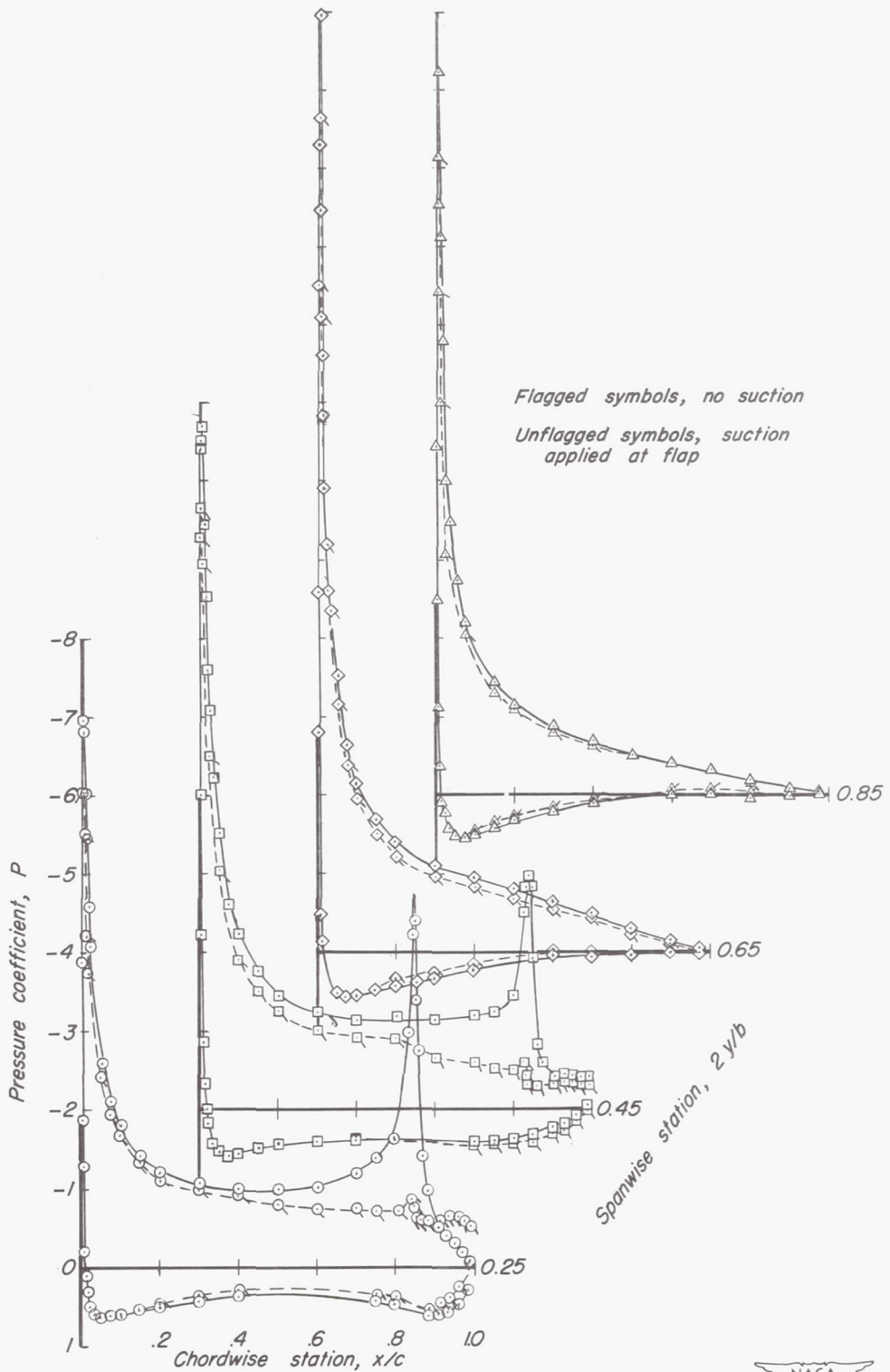
Figure 18.— Chordwise pressure distributions of the  $35^\circ$  swept-back wing with and without area suction applied to the flap deflected  $55^\circ$ .



(b)  $\alpha = 4.7^\circ$

Figure 18.— Continued.



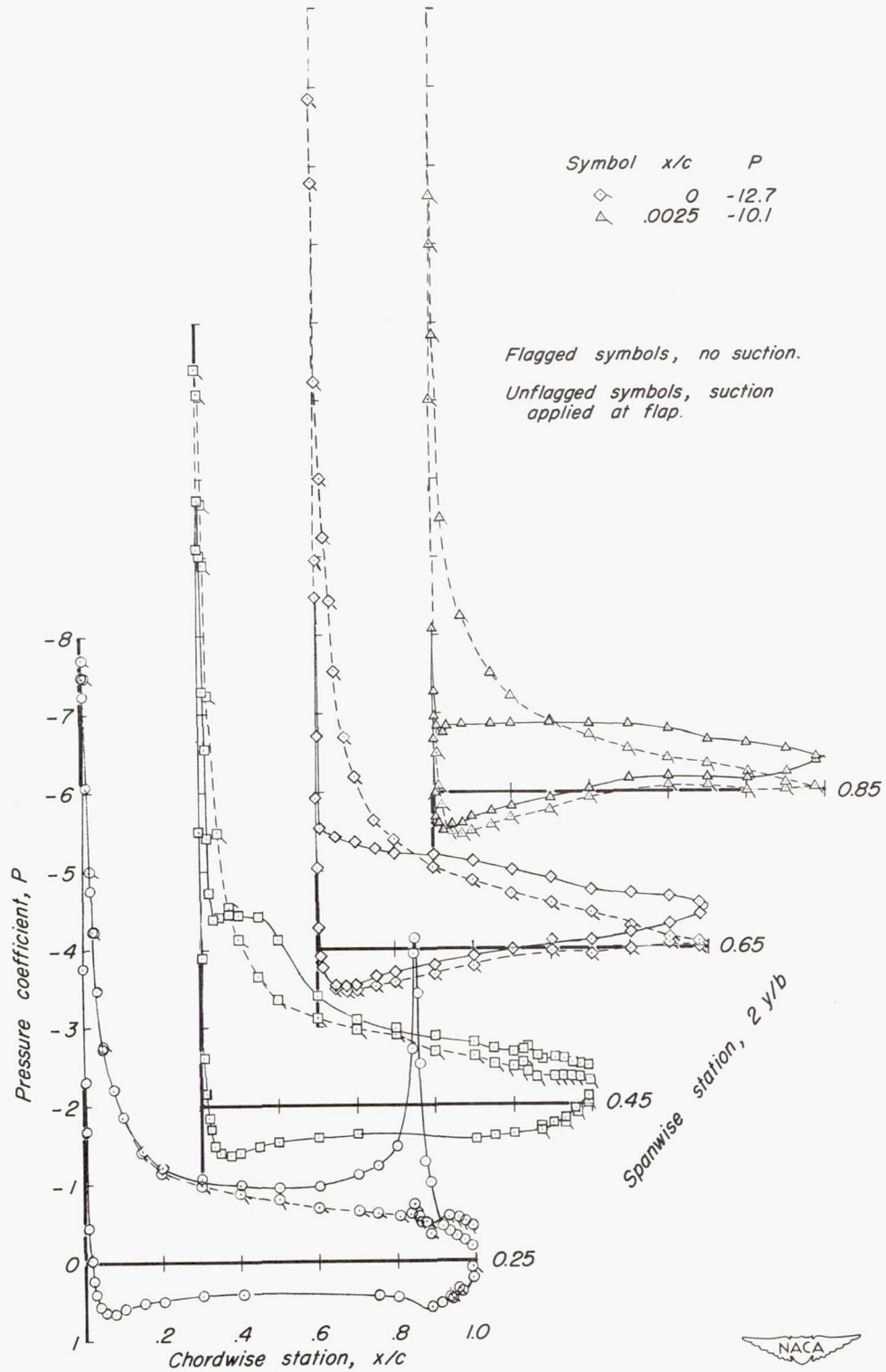


(c)  $\alpha = 10.9^\circ$

Figure 18.— Continued.







(d)  $\alpha = 12.8^\circ$

Figure 18.— Concluded.



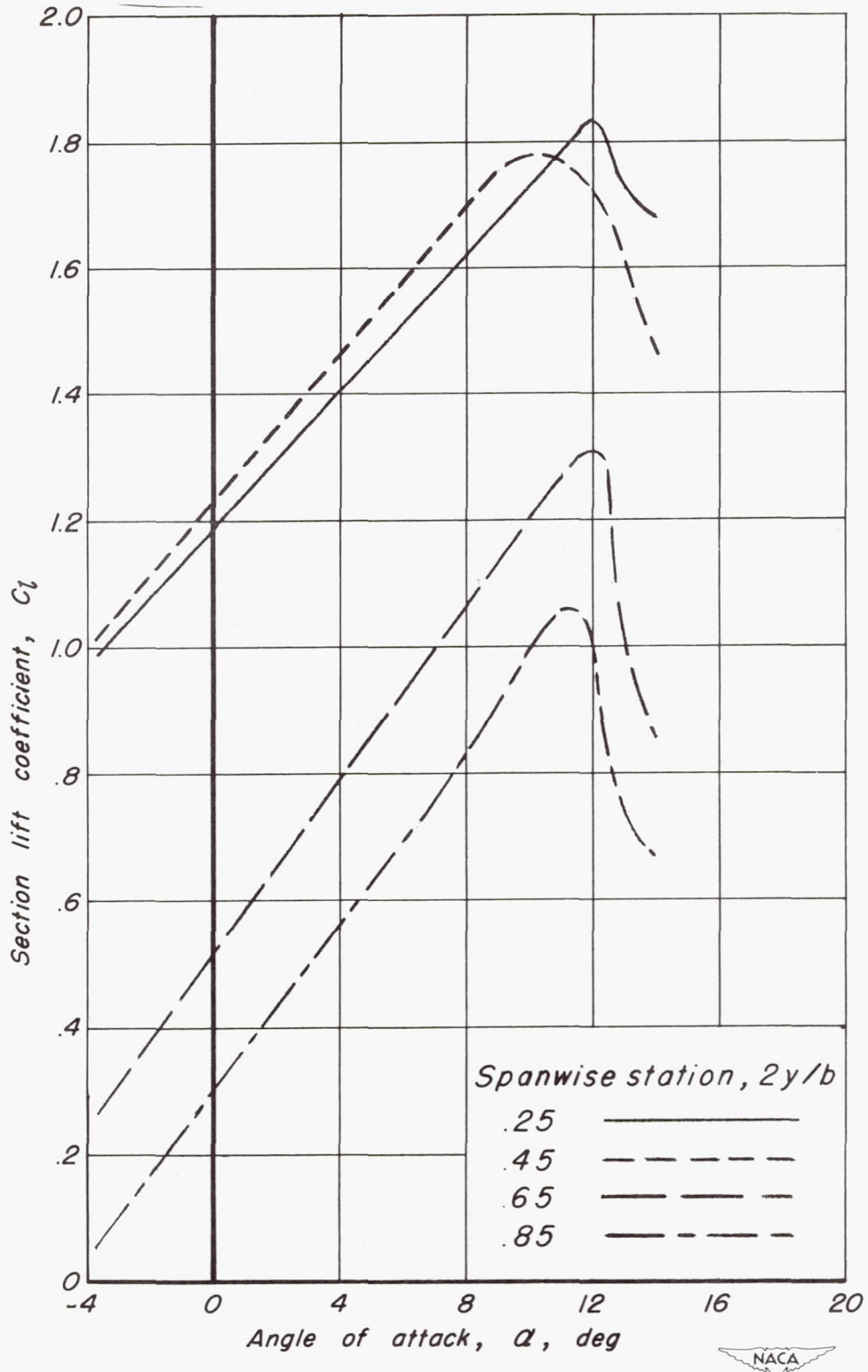
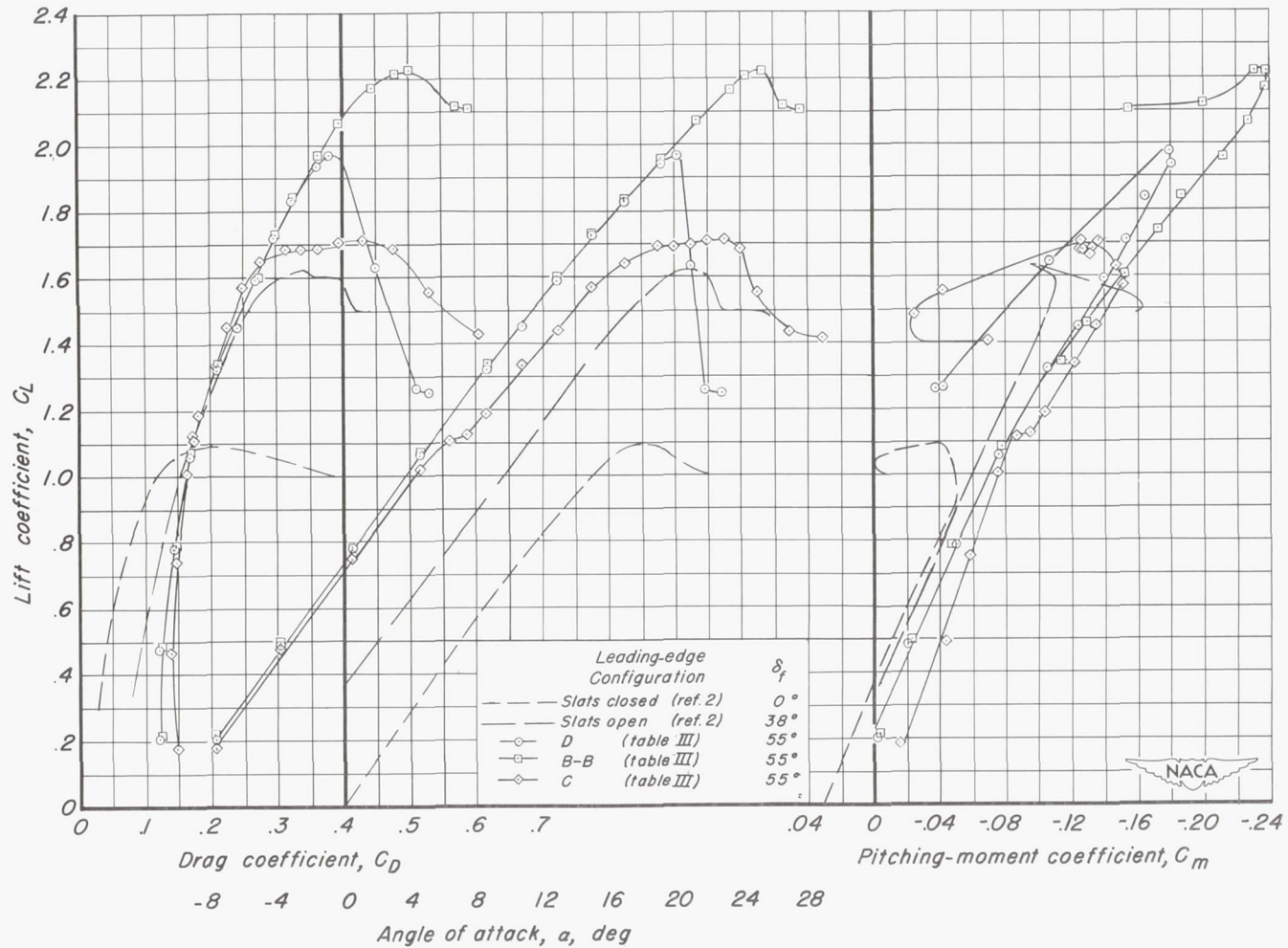


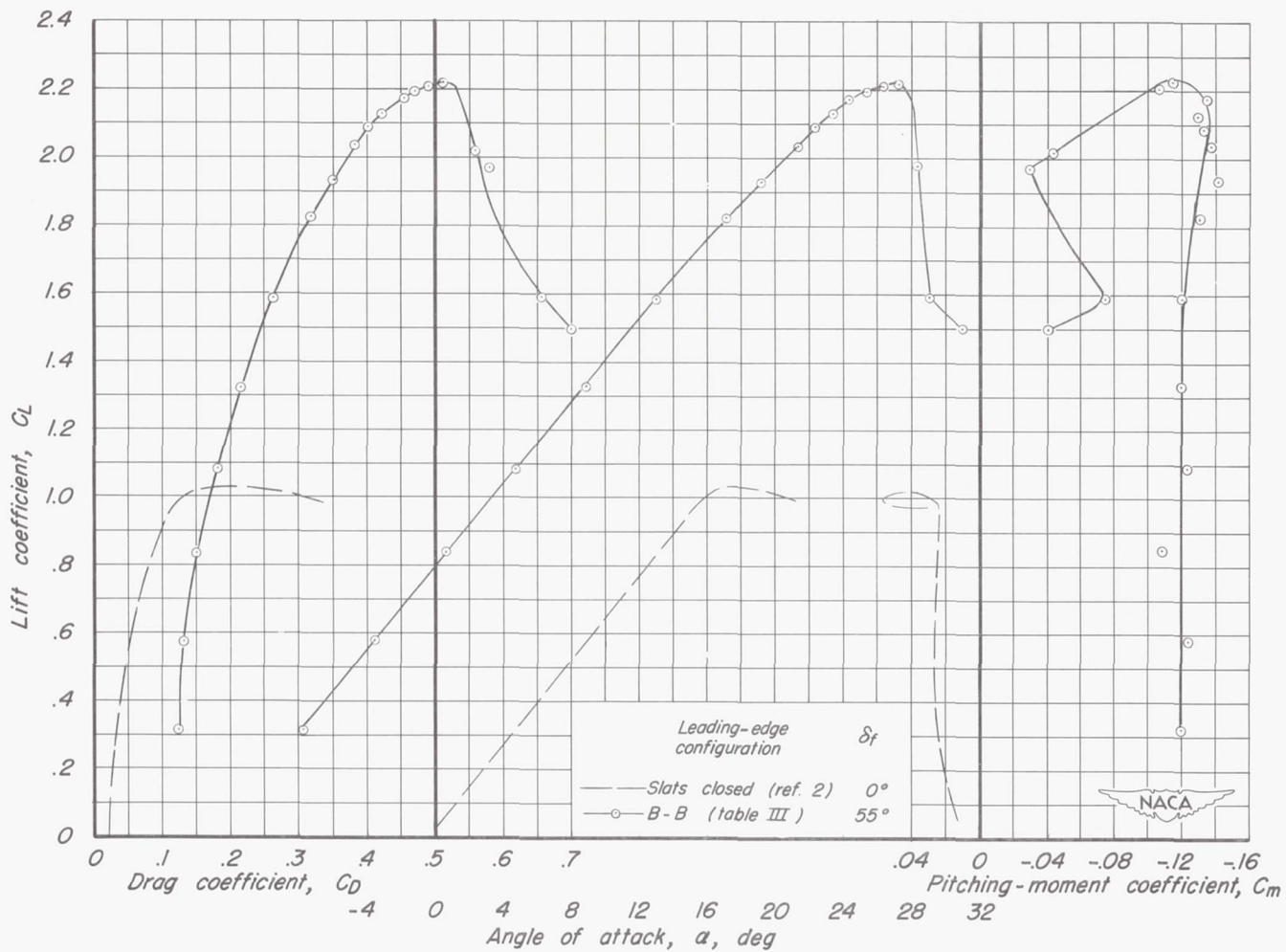
Figure 19.— Section lift curves for the 35° swept-back wing with suction flap deflected 55°.



(a) Horizontal tail on.

Figure 20.— Aerodynamic characteristics of the 35° swept-back wing with area suction applied to the 55° suction flap and with various leading-edge devices.





(b) Horizontal tail off.  
Figure 20.- Concluded.

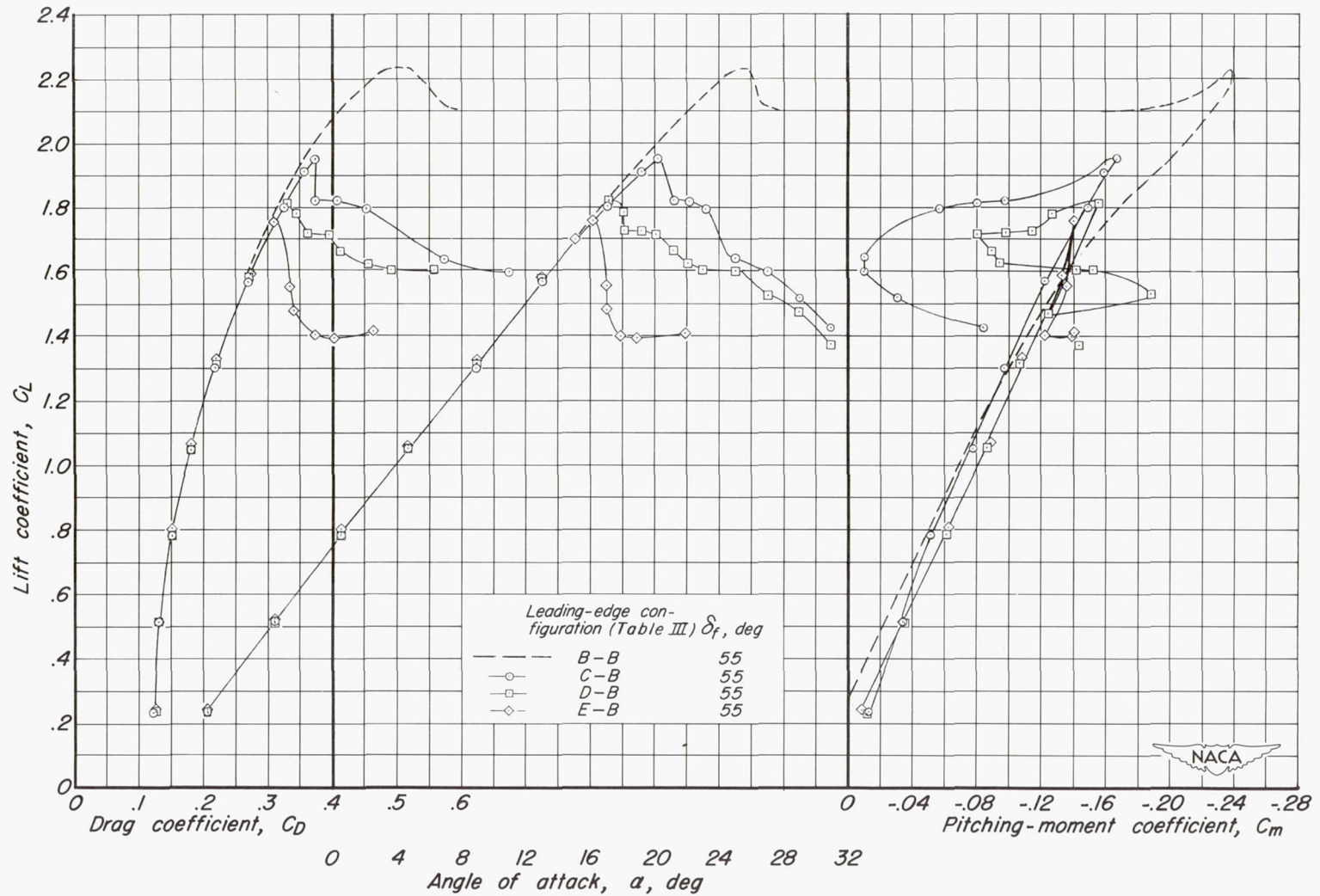
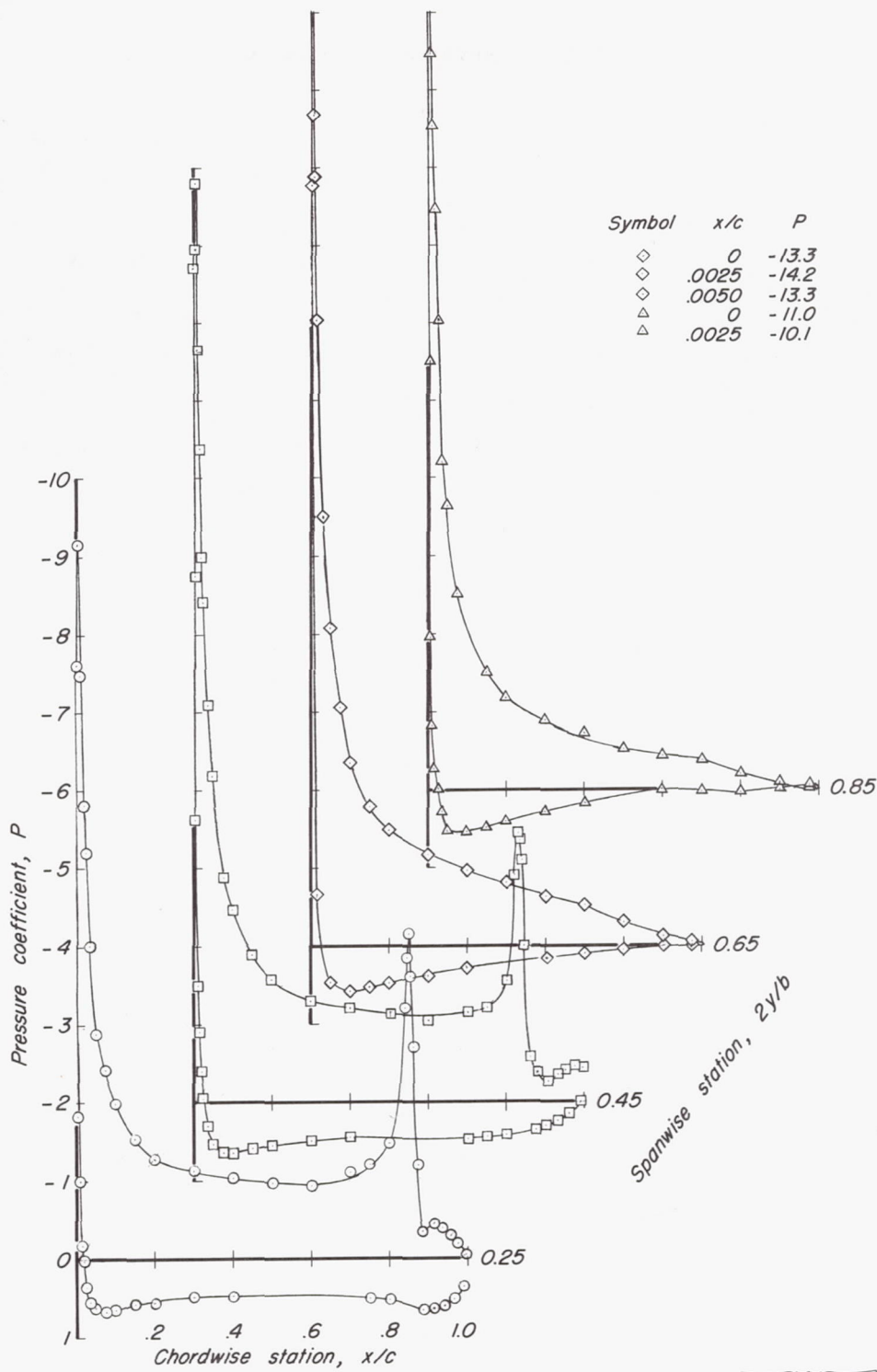


Figure 21.— Aerodynamic characteristics of the 35° swept-back wing with the suction flap deflected 55° and with various spanwise extents of leading edge area suction.

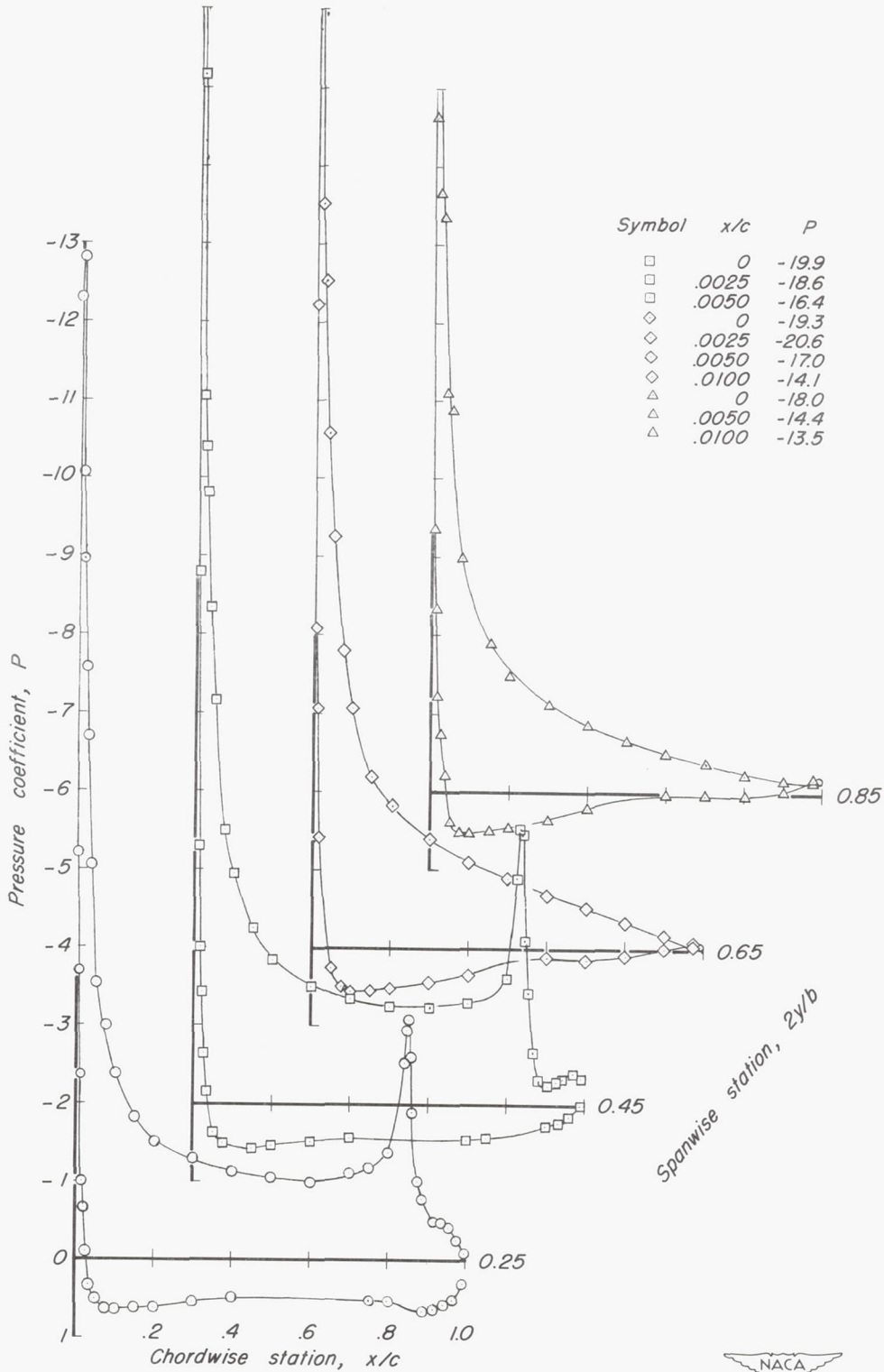


(a)  $\alpha = 13.0^\circ$



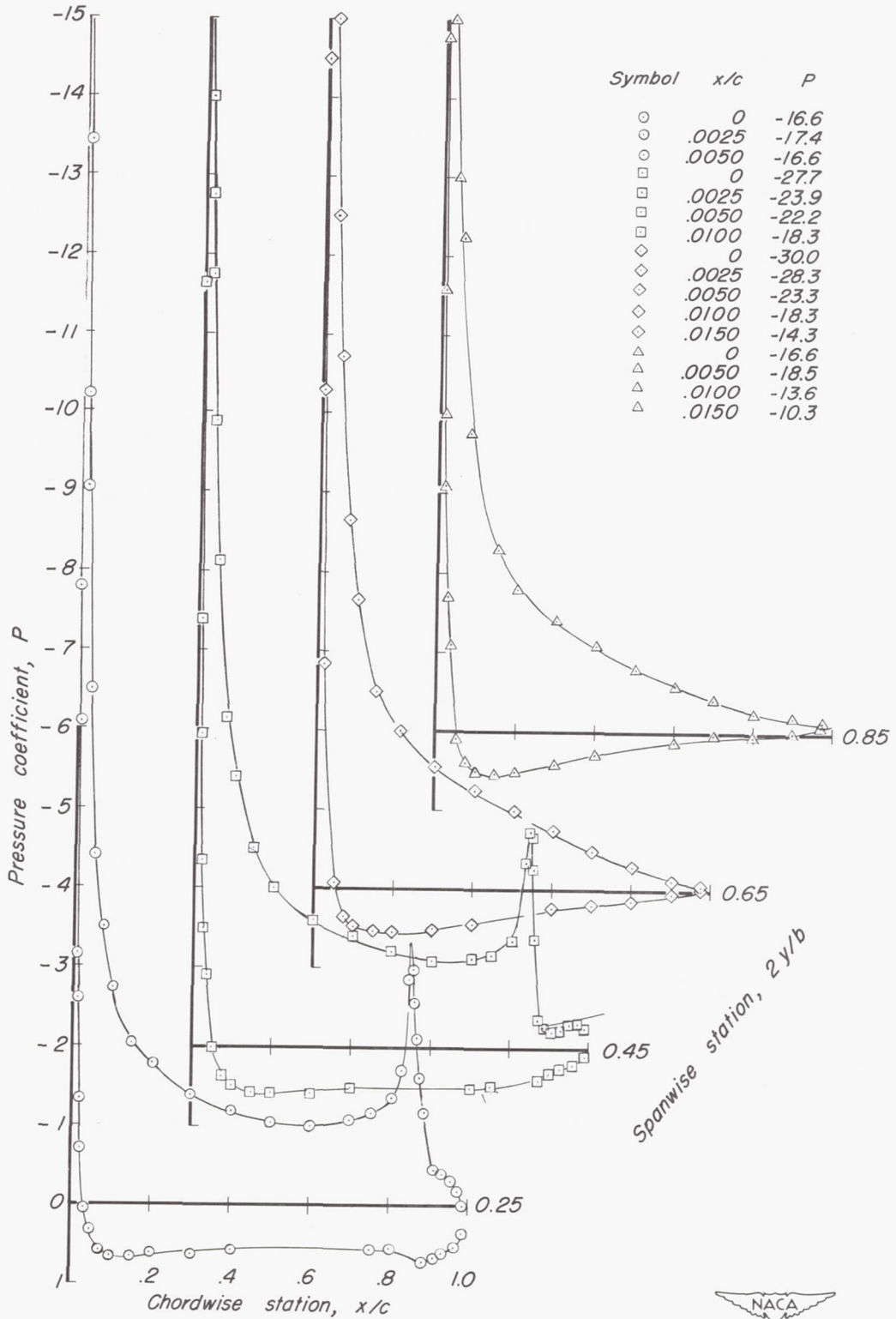
Figure 22.— Chordwise pressure distributions of the 35° swept-back wing with the suction flap deflected 55° and with area suction applied to the leading edge. Configuration B-B.





(b)  $\alpha = 17.2^\circ$

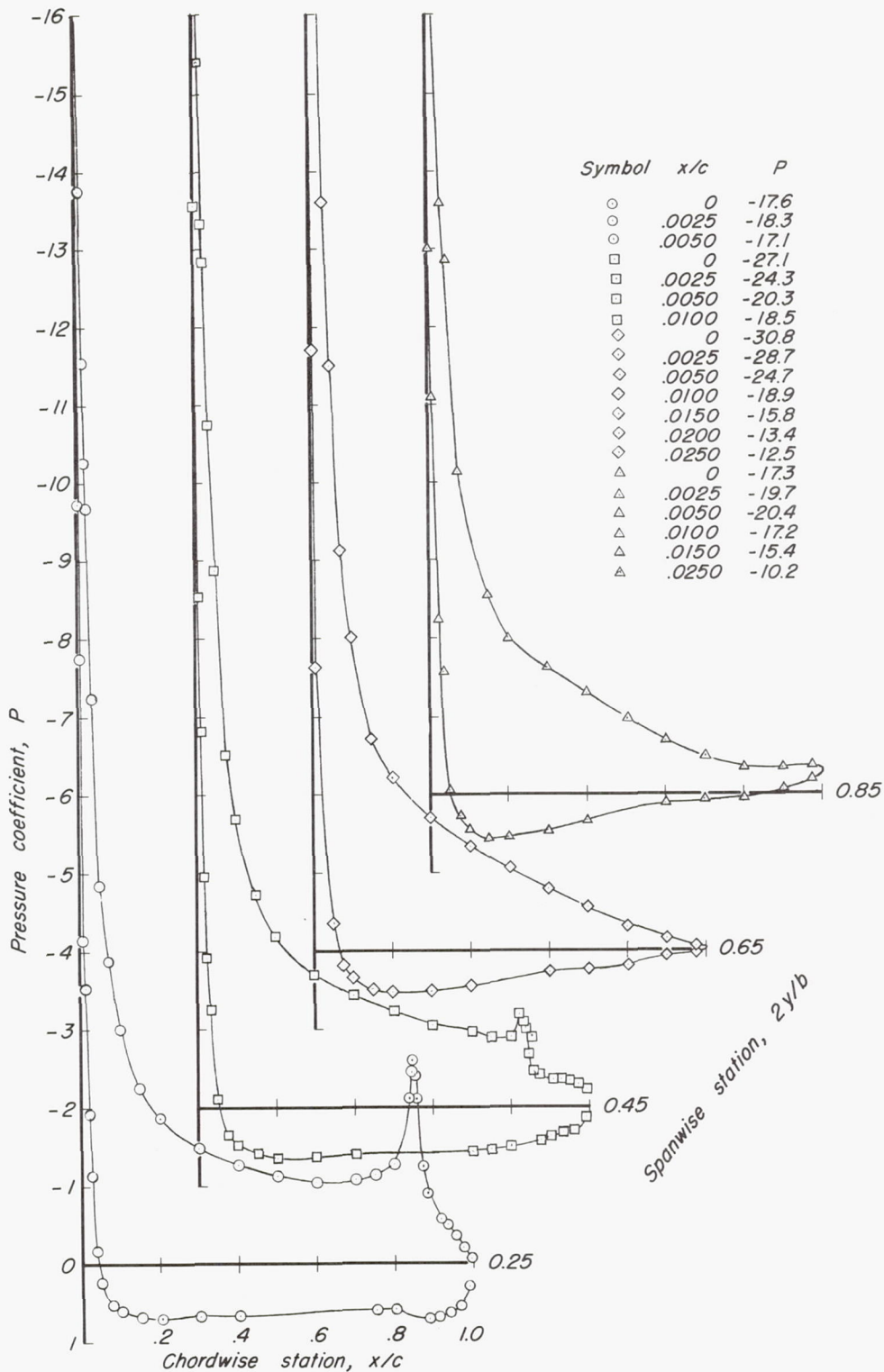
Figure 22.— Continued.



(c)  $\alpha = 21.3^\circ$

Figure 22.— Continued.





(d)  $\alpha = 23.4^\circ$

Figure 22.— Concluded.





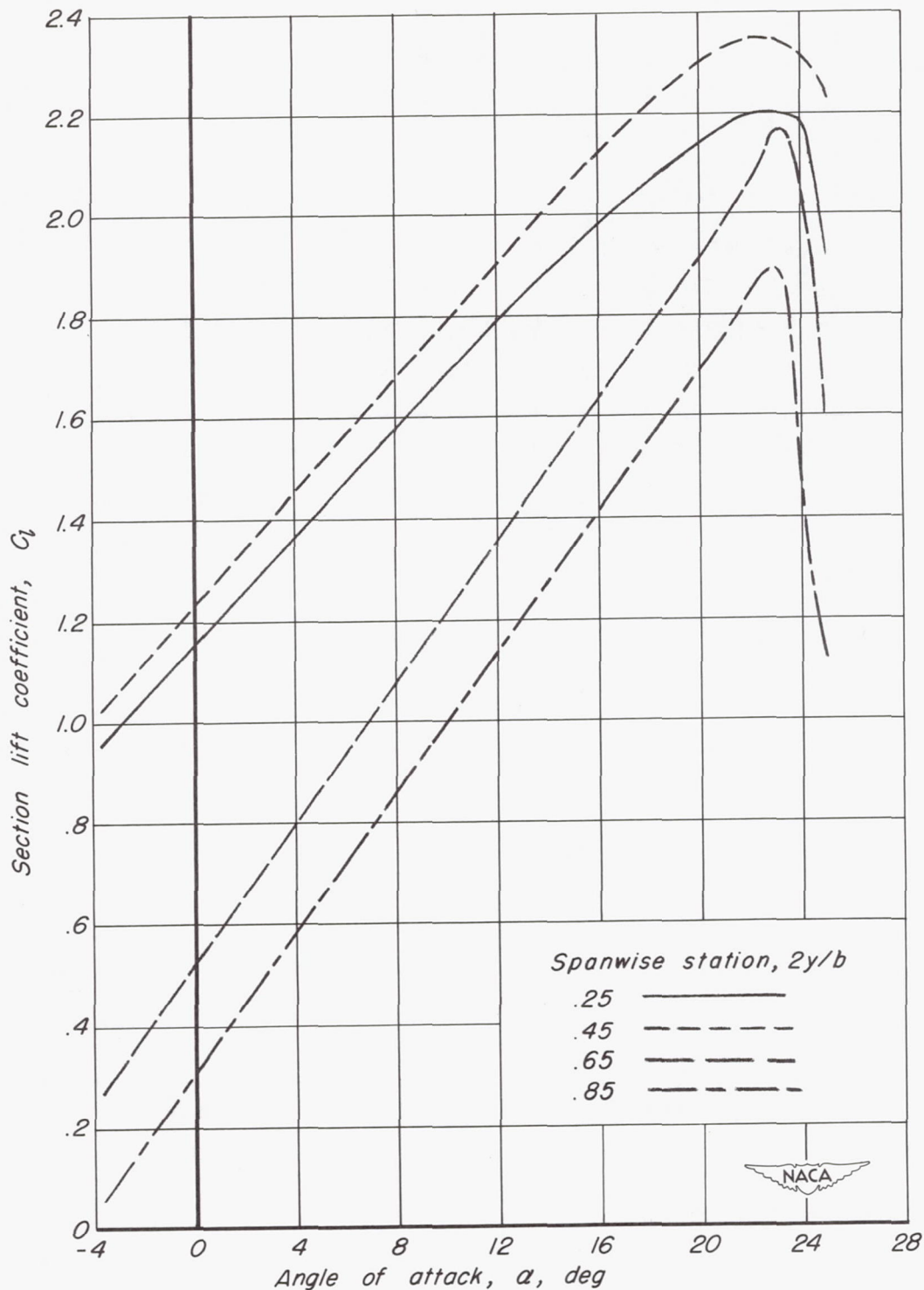


Figure 23.— Section lift curves for the  $35^\circ$  swept-back wing with suction flap deflected  $55^\circ$  and area suction applied to the leading edge.

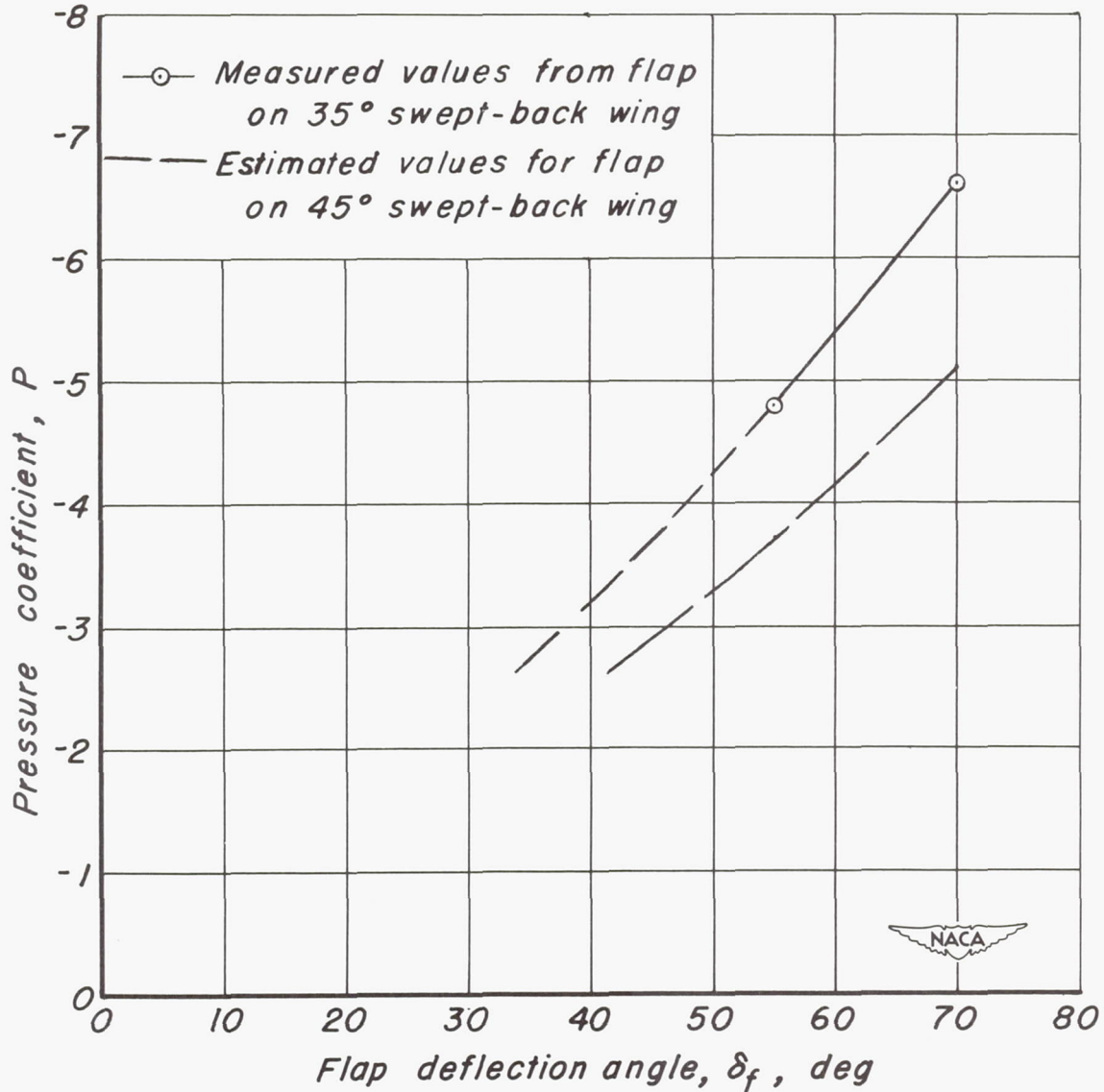


Figure 24.—Variation of peak negative pressure coefficient over flap radius of curvature with flap deflection angle.

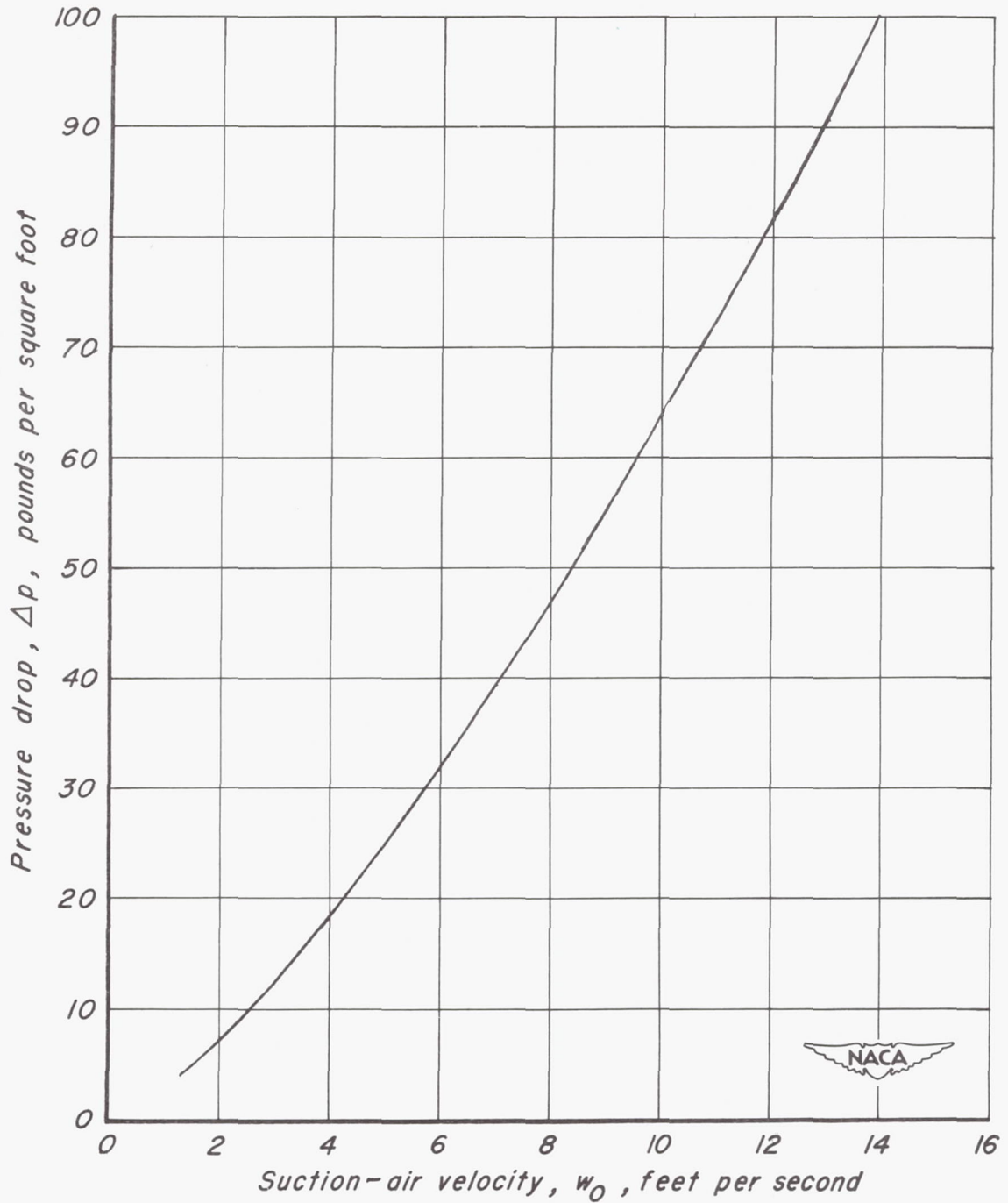


Figure 25.— Flow characteristics of 1/16-inch-thick porous stainless steel



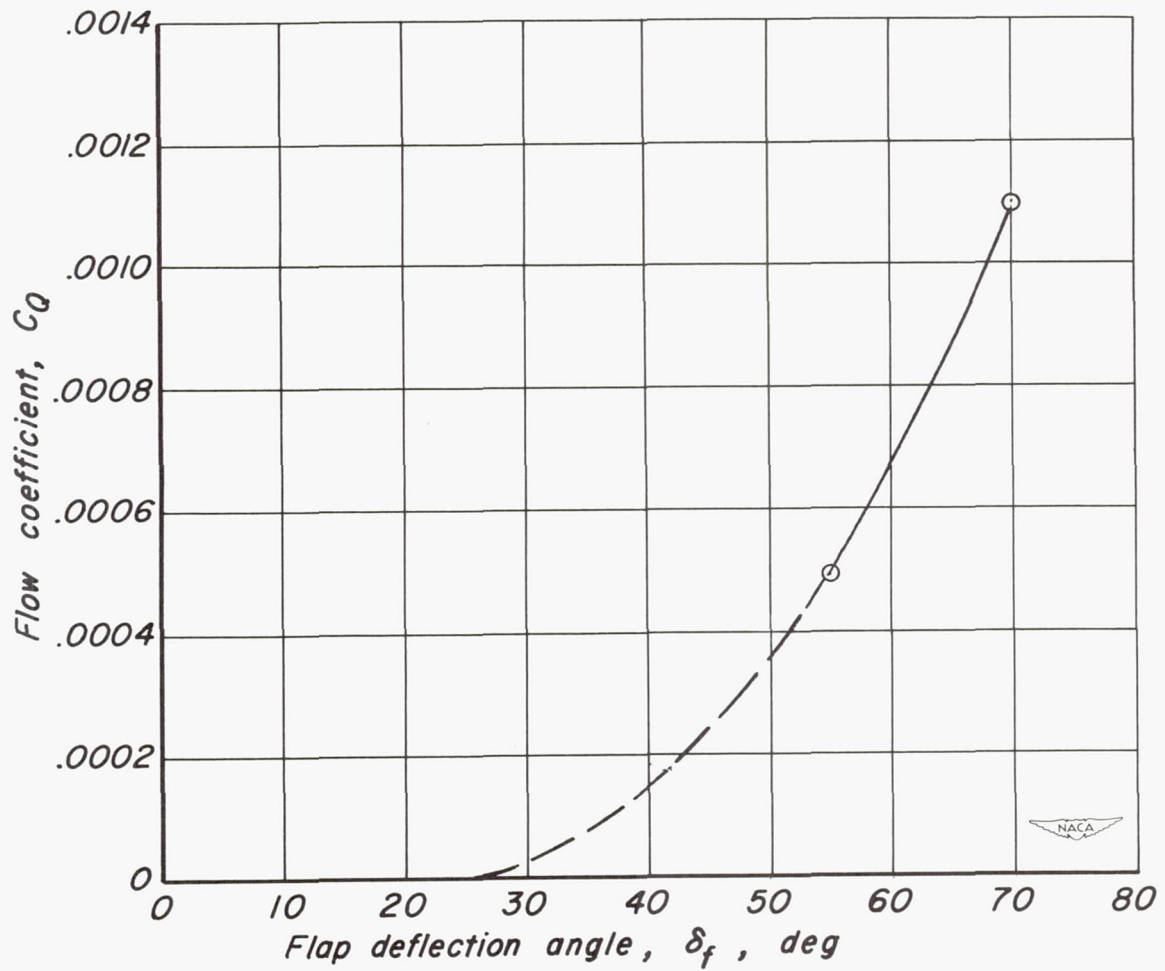


Figure 26.— Variation of flow coefficient with flap deflection angle.  $U_o = 183$  ft per sec.

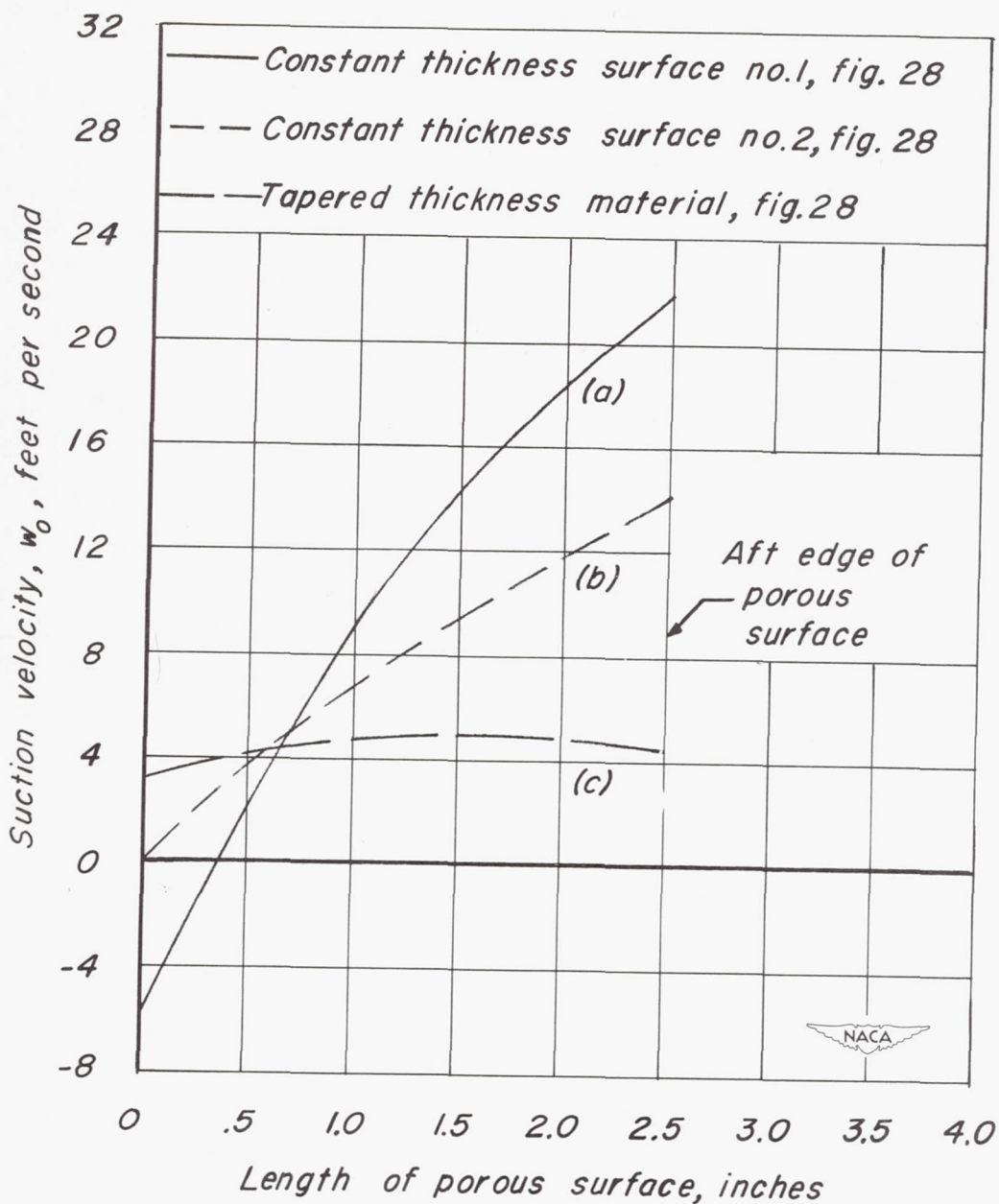
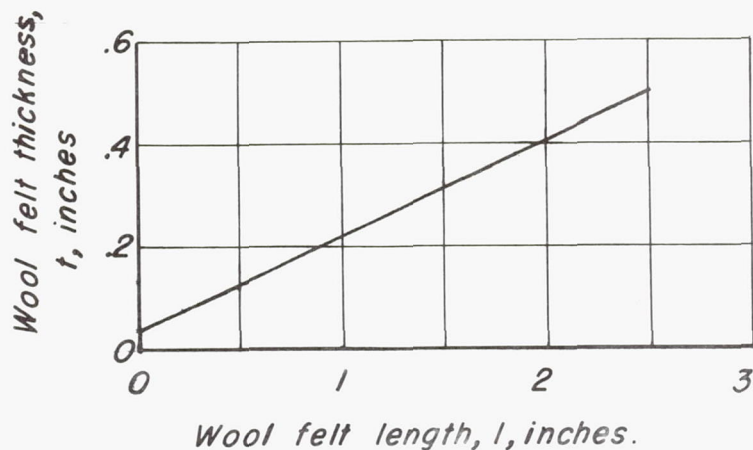
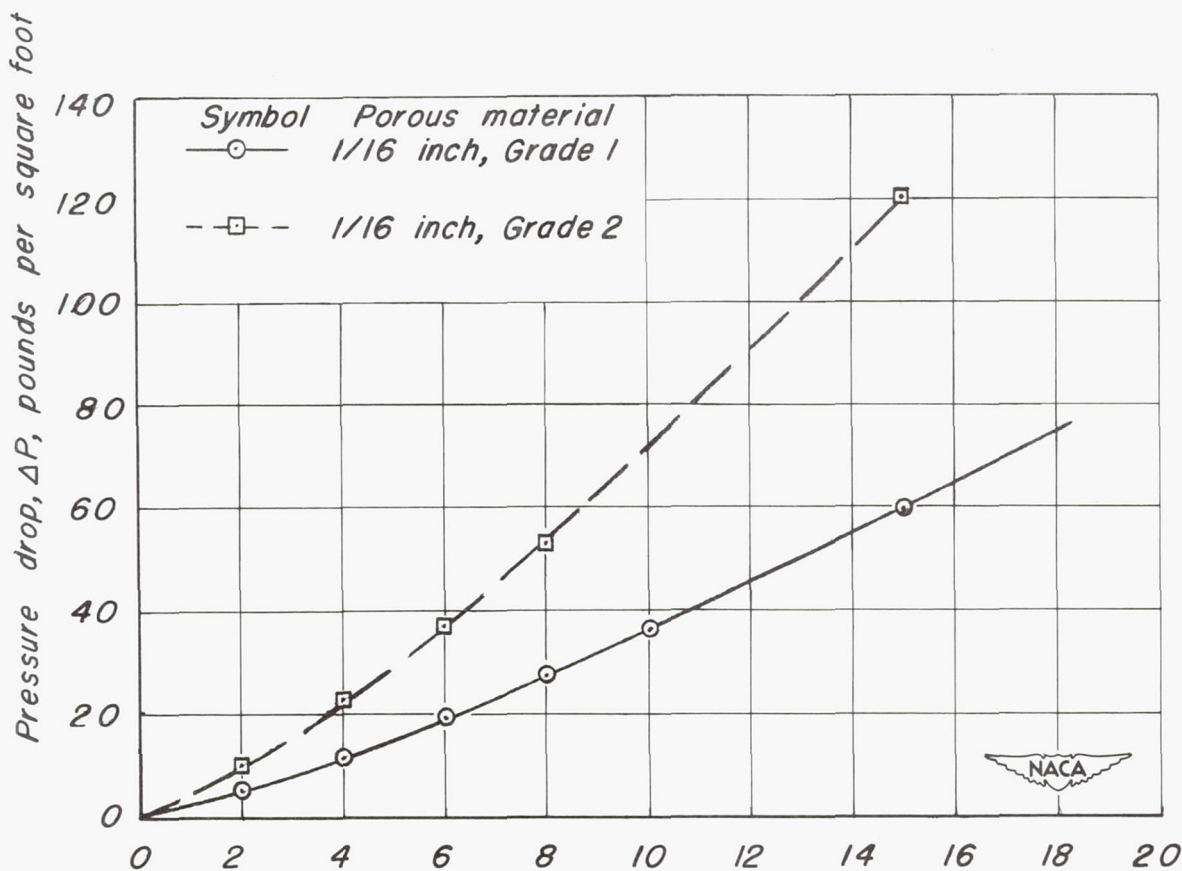


Figure 27.—Measured chordwise distribution of suction-air velocities for three types of porous materials.  $\delta_f = 55^\circ$ ;  $U_0 = 183$  feet per second.



(a) Chordwise distribution of thickness for tapered felt in flaps. Grade 1 felt.



(b) Flow characteristics of two grades of 1/16-inch-thick wool felt.

Figure 28.— Chordwise distribution of felt thickness and flow characteristics of two grades of wool felt material.



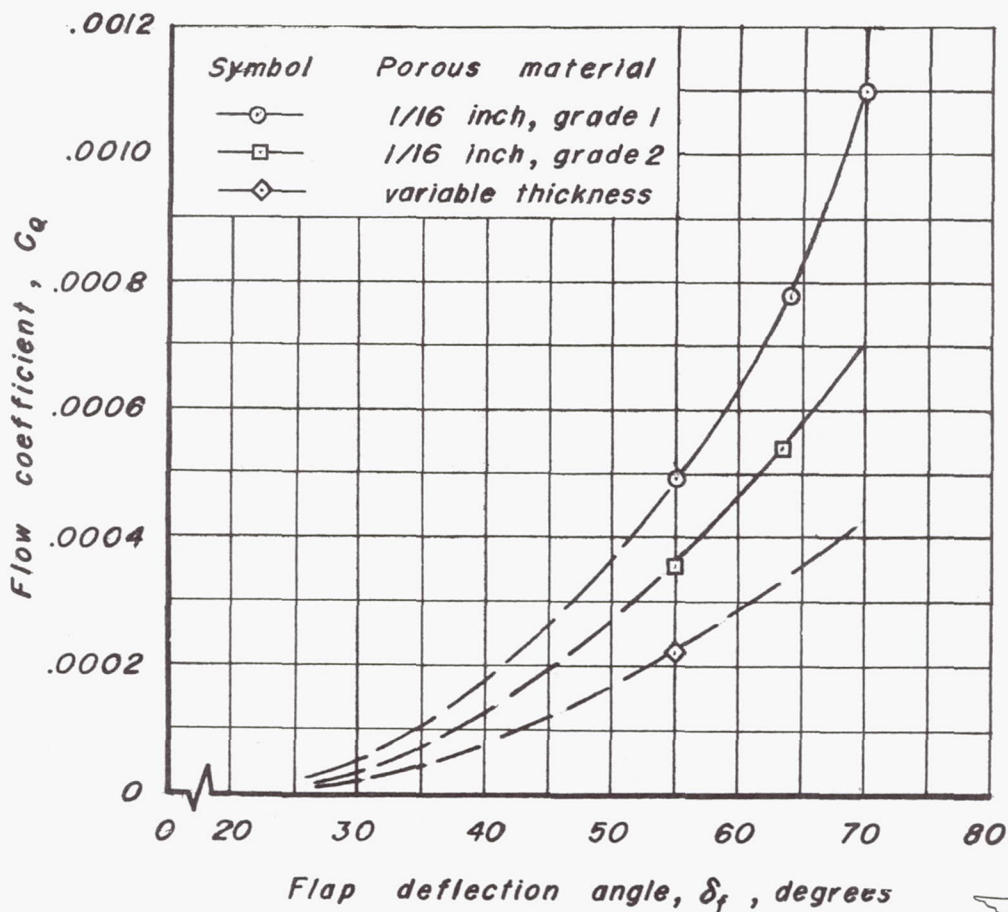


Figure 29.— Variation of flow coefficient with flap deflection angle for three types of porous materials.

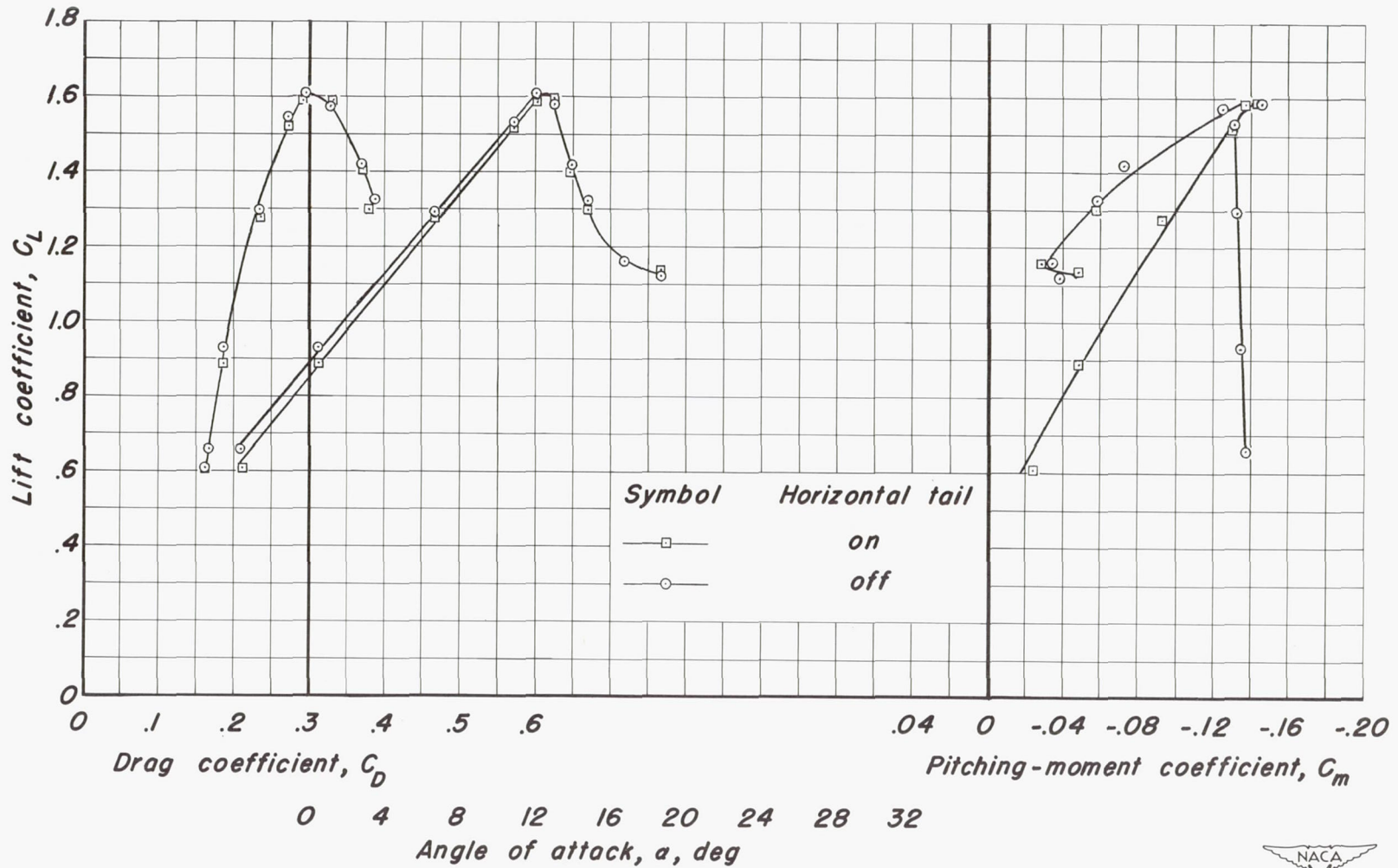


Figure 30.— Aerodynamic characteristics of the 35° swept-back wing with the suction flap deflected 64°. Unmodified leading edge.



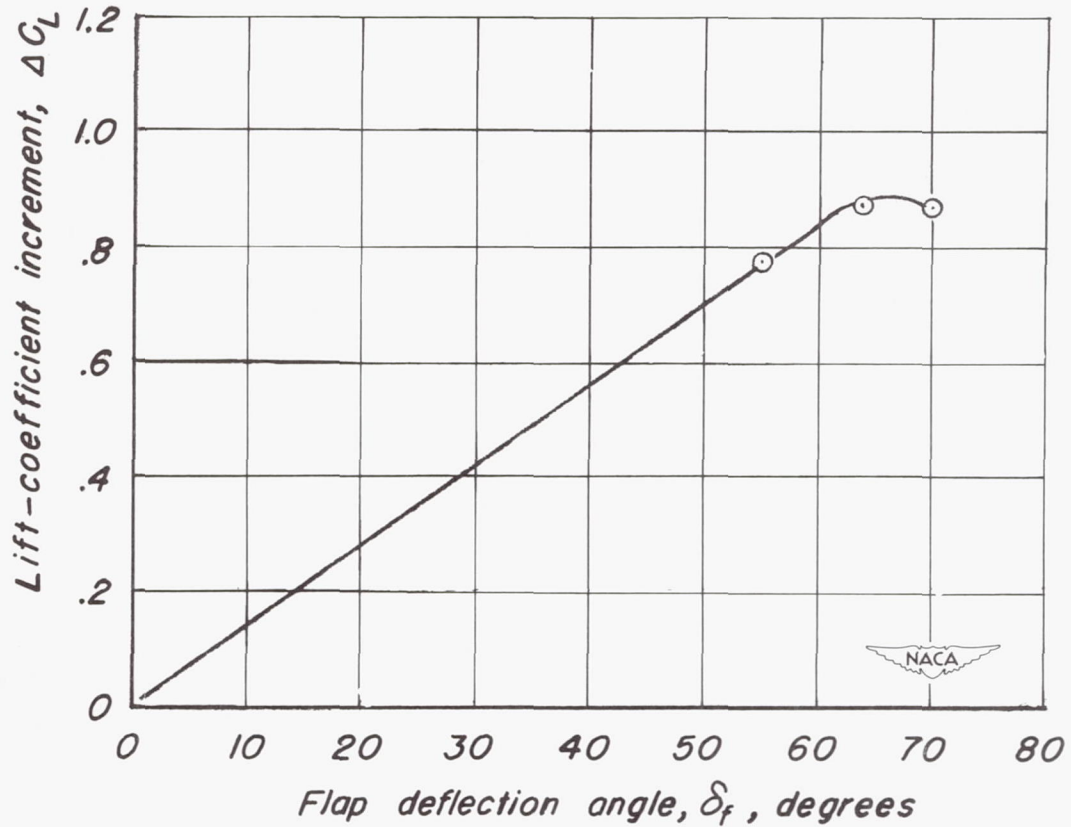


Figure 31.— Variation of increment of flap lift coefficient with flap deflection angle. Horizontal tail off.



SECURITY INFORMATION

CONFIDENTIAL

CONFIDENTIAL